



# HABIT-2025



## International Conference on

### Health and Agricultural Biotechnology: Interdisciplinary Trends

Feb. 28  
to  
Mar. 02  
**2025**

#### Editors

Dr. Ashutosh Mani

•

Dr. Radha Rani

•

Dr. Joyabrata Mal

•

Dr. Rupika Sinha

•

Dr. Harinder Singh

•

Dr. Dushyant Kumar Singh

#### Organized by

#### Department of Biotechnology

Motilal Nehru National Institute of Technology Allahabad,  
Prayagraj-211004, India

**ISBN : 978-81-963268-6-9**

**First Impression : 2025**

©

Motilal Nehru National Institute of Technology Allahabad,  
Prayagraj – 211004, India

No part of this publication may be reproduced or transmitted in any form by any means, electronic or mechanical, including photocopy, recording, or any information storage and retrieval system, without permission in writing from the copyright owners.

#### **DISCLAIMER**

The authors are solely responsible for the contents of the papers compiled in the any manner. Errors, if any, are purely unintentional and readers are requested to communicate such errors to the editors or publishers to avoid discrepancies in future.

Published by:  
**Mohan Enterprises**  
55/14, Motilal Nehru Road  
Prayagraj- 211002  
E-mail: mohanenterprises2003@gmail.com

## Our Sponsors



अनुसंधान नेशनल रिसर्च फाउंडेशन  
Anusandhan National Research Foundation



## **Organizing Committee**

Patron

**Prof. Rama Shanker Verma**

Director

MNNIT Allahabad, Prayagraj

•

Chairperson

**Prof. Manisha Sachan**

Head

BTD, MNNIT Allahabad, Prayagraj

•

Convener

**Dr. Ashutosh Mani**

BTD, MNNIT Allahabad, Prayagraj

•

Treasurer

**Dr. Joyabrata Mal**

BTD, MNNIT Allahabad, Prayagraj

•

Organizing Secretaries

**Dr. Radha Rani**

**Dr. Rupika Sinha**

**Dr. Dushyant Kumar (CSED)**

**Dr. Harinder Singh (CHED)**

## CONTENT

1. Elucidating potential role of WRKY gene family in conferring blast tolerance in finger millet  
Varsha Rani and Dinesh Yadav ... 06-16
2. Untapped potential of microalgae in industrial effluent treatment and bio-diesel production supporting circular bio-economy.  
Tribhuwan Kumar & Monika Prakash Rai ... 17-21
3. Discovery of novel inhibitors of Aminodeoxychorismate lyase enzyme from Plasmodium falciparum: A Comparative binding analytics  
Shruti Shukla, Ashutosh Mani ... 22-26
4. Green Synthesis of Silver Nanoparticles using Algae and their Applications  
Preeti Maurya and Sanjay Singh ... 27-33
5. Exploring Conserved Motifs and Novel Functional Elements in Human Olfactory Receptors: A Phylogenetic and Domain-Based Analysis  
Nidhi Dubey, Imlimaong Aier, Prabhat Tripathi, Ankish Arya, Amaresh Kumar Sahoo, Pritish Kumar Varadwaj ... 34-38
6. Screening of Fresh Water Algal Extracts for their Antioxidant Potential  
Khushaboo Soni, and Sanjay Singh ... 39-45
7. Genetic Determinants of Helicobacter pylori Adaptation and Survival mechanism: Prospects for Therapeutic Targeting  
Meghna Agrawal, Diksha Singh, Ashutosh Mani ... 46-50
8. Molecular Cloning and Expression of a Recombinant Laccase Gene in Escherichia coli  
Manasee Wadgaonkar, Vidya Tale, Shamim Shaikh, Shraddha Jaiswal ... 51-54
9. Characteristics of Thermal Power Plant Ash in Slurry form using Treated Waste Water from STP  
Sapna Gautam , Anubhav Rawat , Nekram Rawal ... 55-59
10. Computational Design and virtual screening of designed short peptides as potential BACE1 inhibitors for Alzheimer's disease  
Kavita Patel, Ashutosh Mani ... 60-66
11. Exploring the Gut Resistome: Insights into Antimicrobial Resistance Genes in the Indian Population  
Ankish Arya, Sankalp Patil, Prabhat Tripathi, Imlimaong Aier, Nidhi Dubey, Pritish Kumar Varadwaj ... 67-70
12. Title: Metagenomics in the era of deep learning: Addressing the limitations of traditional analysis methods  
Diksha Singh, Dr. Ashutosh Mani ... 71-77

## Elucidating potential role of WRKY gene family in conferring blast tolerance in finger millet

Varsha Rani<sup>1</sup> and Dinesh Yadav<sup>2\*\*\*</sup>

<sup>1</sup> Department of Biotechnology  
School of Engineering and Technology, Sandip University,  
Nashik-422213 (Maharashtra)-INDIA

<sup>2</sup> Department of Biotechnology,  
Deen Dayal Upadhyaya Gorakhpur University,  
Gorakhpur-273009 (Uttar Pradesh)-INDIA

\*Email id of corresponding author: dinesh.biotech@ddugu.ac.in

---

### Abstract

The WRKY transcription factor family plays a crucial role in regulating growth, phytochrome signalling, and tolerance to biotic and abiotic stresses across plant species. This study presents a genome-wide analysis of the WRKY transcription factor (TF) family in finger millet (*Eleusine coracana* L.), a drought-tolerant crop well-suited for subsistence farming in dry and semi-arid regions. A total of 13 EcWRKY genes were identified and categorized based on their conserved zinc-finger motifs and WRKY DNA-binding domains. Cis-regulatory elements, including MYB, MYC, and W-box motifs, were detected in the finger millet promoter regions, suggesting their potential involvement in stress tolerance. Expression profiling identified EcWRKY5 as a candidate gene exhibiting high transcript abundance in response to *Magnaporthe oryzae* inoculation, indicating its potential role as a negative regulator of blast tolerance. This study provides the first comprehensive insight into the regulatory mechanisms and functional characterization of the WRKY gene family in finger millet, offering a foundation for further in-depth analysis of these genes in this resilient yet underutilized crop.

---

Keywords: Biotic stress, finger millet, RNA seq, WRKY Transcription factor

## Introduction

Finger millet (*Eleusine coracana* L. Gaertn), is a well-adapted crop in Africa and South-East Asia. It is one of the cheapest and most easily available sources of food for millions of poor residing in the semi-arid regions and drylands of the world and also provides nutritious fodder to livestock (Sood et al. 2022). By its adaptation to harsh and low input marginal agroecology, it is regarded as a resilient crop to several abiotic stresses including moisture stress, high soil pH, and elevated temperature (Wright and Devos 2024). In general, grains of finger millet are free from storage pests and can be stored for several years, making it particularly valuable in areas suffering from high rates of famine (Sood et al. 2022). Aside from being able to grow under adverse environmental conditions, finger millet grains are nutritionally dense compared to major cereals in terms of essential micronutrients and other trace elements (Maharajan et al. 2022). Considering these characteristics, finger millet production is being boosted worldwide to combat climate change, food insecurity, and malnutrition. Moisture and salinity stress are the most important abiotic stresses accounting for more than 50 percent loss in agricultural production (Chawala et al. 2020). Millets are highly flexible and stress-tolerant, as compared to most other major crops such as rice and wheat. Thousands of transcription factors (TFs) and associated gene networks govern response to abiotic stresses in plants (Rani et al. 2023). However, these mechanisms are poorly explored and documented in finger millet. As an important member of stress-related transcription factor families, the WRKY TF family plays an important role in the regulation of biotic and abiotic stress responses and plant development (Agarwal et al. 2011). Structurally, WRKY TFs are identified by the signature sequence WRKYGQK at the N-terminal, as well as Cys-Cys-His-Cys (C2HC) or Cys-Cys-His (C2H2) zinc finger motif at the C-terminus (Eulgem et al. 2000; Rushton et al. 2010). Based on the number of domains, WRKY family members are classified into three groups. The first group typically contains two WRKY domains and a C2H2-type zinc finger motif. Groups II and III are characterized by only one WRKY domain. However, the III group differs from the II as it is characterized by the C2HC zinc finger motif instead of the C2H2 motif (Zhang and Wang 2005a).

WRKY TFs play an important role in coping with drought, heat, salt, and cold (Agarwal et al. 2011; Dabi et al. 2020). Apart from this, they are also associated with growth and development in plants, such as seed development and trichome initiation (Ülker and Somssich 2004; Rushton et al. 2010; Agarwal et al. 2011). Therefore, it has been highly sought after to study WRKY TF as a possible candidate for genetic enhancement of crop plants (Qiu et al. 2004; Wei et al. 2012; Jiang et al. 2017; Satapathy et al. 2018; Chawala et al. 2020). Despite this, efforts have not been made to decipher the WRKY TFs of finger millet and its potential role in stress tolerance. In addition, there are only a limited number of TFs reported in finger millet, such as DoF (Gupta et al. 2018), NAC (Rahman et al. 2016), MYB (Jadhav, 2018) and NF-Y (Rani et al. 2024a, b). With the recent availability of a well-assembled reference genome (Devos et

al. 2023), finger millet has emerged as a valuable “millet model” for the identification and functional characterization of several TFs and genes that respond to biotic and abiotic stresses.

Considering this research gap, the present study aims to identify a WRKY gene in the finger millet genome that can be targeted for Overexpression or knockout to potentially enhance tolerance to *Magnaporthe oryzae*. Notably, homologs of OsWRKY70, a known positive regulator against herbivores and a negative regulator against *M. oryzae* (Li et al. 2024), are of particular interest. Knocking out the homolog of OsWRKY70 in finger millet using the CRISPR/Cas9 system may lead to enhanced resistance to *M. oryzae* in this crop.

A total of thirteen WRKY genes (EcWRKYS) of finger millet were identified at the genome level and checked for their expression under *M. oryzae* infection stress. The role of WRKY TFs in imparting tolerance against blast pathogen in finger millet has been investigated in the present study because blast is the most important biotic constraint that severely affects finger millet production across the world (Mbinda and Masaki 2021). Microarray data for finger millet were utilized to profile tissue-specific gene expression patterns for EcWRKY genes in response to blast pathogen. The study performed will assist in understanding the mechanisms that explain finger millet's natural adaptation to blast pathogens and identify the candidate genes that can be targeted to enhance tolerance against blast infection.

## Materials and Methods

### **Mining for WRKY proteins from finger millet**

To identify the putative WRKY proteins responsive to biotic stress we searched Phytozome v.13 (Goodstein et al. 2012) for finger millet genome sequences by using the OsWRKY70, OsWRKY7, OsWRKY62, OsWRKY64 and OsWRKY 74 as a query sequence (Li et al. 2024) to find out the putative homolog in the finger millet genome. The obtained non-redundant sequences were checked for the presence of the conserved WRKY domain by using the PFM database, specific to the PFAM domain (PF03106).

### **Evolutionary, physical property and CRE estimation**

Based on default parameters, the finger millet and rice WRKY protein sequences specially OsWRKY70, OsWRKY7, OsWRKY62, OsWRKY64 and OsWRKY 74, a potential candidate genes for resistance to panicle blast were aligned using MUSCLE in MEGA v.11 (Edgar 2004; Tamura et al. 2021). An evolutionary tree is then constructed by using bootstrap testing of 1000 replications, Further analysis of finger millet WRKY protein sequences was conducted by using the ExPASy ProtParam program to determine physicochemical property (Gasteiger et al. 2005). A cis regulatory element (CRE) was estimated by using PlantCare in the 2KB upstream of the promoter region of the mined WRKY gene of finger millet.

### **Expression profiling**

For identification of WRKY genes in response to blast pathogen (*M. Oryzae*), the microarray data set (GSE48500) (Chujo et al. 2014) was retrieved from the NCBI GEO database (<https://www.ncbi.nlm.nih.gov/geo/geo2r/?acc=GSE48500>; accession numbers GSM1179995-GSM1179998, GSM1180003-GSM118006, GSM1180011-GSM1180014, GSM1180019-GSM1180022, GSM1180027-GSM1180030). The transcript data were obtained from four resistance lines infected with a 6-day inoculation with blast pathogen (*M. oryzae*). The GEO2R program was used for the mining of differentially expressed genes (DEGs) in the finger millet genome. The log2 fold change of each EcWRKY gene, a rice ortholog was used to generate a heat map by using TBtools software.

## Results

### Identification of the finger millet WRKY family

We identified thirteen EcWRKY genes in the finger millet, which show the highest similarity to rice OsWRKY70, OsWRKY7, OsWRKY62, OsWRKY64, and OsWRKY74 genes known for responding to BLAST infection. Based on our previous research (Data under publication), finger millet WRKY genes were differentiated according to the nomenclature system for EcWRKYS (*Eleusine coracana* WRKYS). Finger millet subgenomes A and B contained these thirteen putative WRKY genes. The physical properties, together with the gene structure of these EcWRKY genes, are shown in Table 1.

### Characterization of EcWRKYS and evolutionary study

The domain analysis of EcWRKY genes revealed the presence of both group-I and group-II members, shown in Table 1. For further evolutionary analysis, 13 members of EcWRKY proteins, mapped with overexpressed rice sequences for blast tolerance, depicted in Fig. 1. The phylogenetic tree revealed five clades, designated as clades I, II, III, IV, and V (Fig. 1). Most of the OsWRKY genes were clustered with EcWRKY genes in clades I, I, I, and III. EcWRKY58 of clade I is closely clustered with WRKY7 of Rice, which showed expression in the resistant genotype against the virulent strain, suggesting EcWRKY58 might also be associated with positive regulation for immune response in blast infection (Sureshkumar et al. 2019). Similarly, in clade III, WRKY62 and WRKY76 are closely clustered together and distantly clustered with finger millet EcWRKY99 (Fig.1). WRKY62 and WRKY76 of rice were potential candidate genes for resistance to panicle blast (Sureshkumar et al. 2019). Downregulation of these WRKY genes of rice severely reduced the tolerance level for the blast pathogen. Hence, the expression profiling and functional characterization of EcWRKY99 and EcWRKY58 would help us to understand the further relationship between these two homologs and the actual contribution toward blast tolerance. The clade II of the phylogenetic tree contains most of the EcWRKY genes of group I category, consisting of two WRKYGQK domains. Among these clade-II members, EcWRKY5 is closely clustered with OsWRKY70, suggesting a perfect homolog, a negative regulator of the blast tolerance (Li et al. 2024).

### cis-regulatory element analysis

The analysis of the 2kb upstream region of the promoter sequence of thirteen EcWRKY proteins for identification of cis-regulatory element (CRE), reveals the possible functions of EcWRKY genes in response to hormones, stress, light responsiveness, and plant growth and development (Fig. 2). The highest proportion of CRE was in the growth and development category (48%), followed by stress-responsive elements (20%), light-responsive elements (16%), and hormone-responsive elements (14%). Stress-responsive elements majorly include MYB, MYC and W boxes; hormone-responsive elements include majorly contain ABRE followed by MeJA responsive elements; light-responsive cis-elements majorly includes G-Boxes followed by GT1-motifs; growth and development related Cis elements majorly include CAAT-boxes.

### Expression Analysis of EcWRKY genes blast infection

By using the standard transcriptome analysis procedure on NCBI GEO dataset GSE48500, the expression patterns of thirteen differentially expressed genes (DEGs) were analysed for blast resistance. The FPKM value > 1 and log2FC > 1, is considered as upregulated DEGs, whereas FPKM value=0 represents non-expressed genes.

The differential expression analysis revealed distinct transcriptional responses among the EcWRKY genes under *M. oryzae* treatment conditions. Most EcWRKY members, including EcWRKY111, EcWRKY35, EcWRKY116, EcWRKY82, EcWRKY64, EcWRKY16, and EcWRKY120, exhibited significant downregulation, indicating a strong transcriptional repression in response to the imposed stress (Fig. 3). In contrast, a few genes, namely EcWRKY58, EcWRKY99, EcWRKY63, EcWRKY19, EcWRKY5 significantly induced by these strains positive regulatory role under the given treatment. Notably, EcWRKY5 showed the most pronounced upregulation (~5 fold change), highlighting it as a potentially key negative regulator in the stress-response network. Therefore, EcWRKY5 exhibits the strongest responses to *M. oryzae* infecting line (Fig. 3), indicating that these genes may play a significant role in finger millet's biotic stress.

## Discussion

Finger millet is cultivated worldwide in harsh, low-input marginal agroecosystems. Despite its ability to thrive well in harsh environmental conditions, genomic resources, such as TFs are not well studied (Rani et al. 2023). The WRKY TF family represents one of the largest families associated with several stresses reported in several plants (Agarwal et al. 2011). Owing to its status as a “climate resilient” and “future smart crop” efforts have been made to decipher the WRKY TFs in finger millet. This could be probably the first report on the identification and characterization of EcWRKY TFs in finger millet for blast infection.

A total of thirteen EcWRKYS were identified by a comprehensive genome screening of finger millet. Further, these were classified into several groups and subgroups, based on the conserved WRKY domain and zinc finger motif. It has been observed that variation in the C2HC or C2H2 sequence of N-terminal contributes to the evolution of new isoforms of WRKYS (Wei et al. 2016). Such signature variation motifs have been reported in rice (Qiu et al. 2004), wheat (Satapathy et al. 2018), maize (Wei et al. 2012), foxtail millet (Zhang et al. 2017), and pearl millet (Chanwala et al. 2020). This type of WRKY motif variant has the potential to change DNA binding activity and eventually lead to functional diversity of the WRKY gene family (Zhang and Wang 2005b).

The promoter analysis of EcWRKYS suggests its role in a variety of biological processes related to plant development and growth (Goel et al. 2016). In the promoter region of identified EcWRKYS, several cis-regulatory elements are specific to abiotic stress (Fig. 9a-b) that may contribute to natural tolerance to salinity stress, drought, heat, and *M. Oryzae* infection. Additionally, the presence of phytohormone-specific cis-elements (ABA, MeJA, and SA) indicates that they are involved in hormonal signaling and biotic and abiotic stress management. Apart from cis-regulatory elements, it was also observed that, in most cases, EcWRKY proteins were very similar to WRKY proteins from different plant species relating to biotic and abiotic stress (Agarwal et al. 2011). Based on this hypothesis, we analysed DEGs of finger millet (EcWRKY) proteins, that may play a role in promoting tolerance against blast infection. In this study, 13 EcWRKY genes were analyzed using a whole genome microarray dataset after six days of the inoculation of *M. oryzae* in 4 contrasting resistance cell lines of rice in comparison with the control (Chujo et al. 2014). Based on the variation in transcript abundance level after six days of infection with *M. oryzae* compared to control and in between four contrasting resistance lines, we selected 13 EcWRKY genes orthologous to rice OSWRKY. Based on homology study, selected EcWRKY genes (EcWRKY58, EcWRKY99, EcWRKY111, EcWRKY35, EcWRKY116, EcWRKY82, EcWRKY63, EcWRKY5, EcWRKY16, EcWRKY63, EcWRKY8 and EcWRKY120) showed the highest similarity with rice-related WRKY genes associated with biotic stress, and EcWRKY5 genes showed highest transcript abundance (> 4 fold change) after blast infection by *M. oryzae* inoculation (Fig. 3), which is the perfect homolog of OsWRKY70. The functional characterization of OsWRKY70 suggested that it negatively regulates the fungal

immunity in rice. Hence the knock out of OsWRKY70 mutants enhanced resistance against *M. oryzae* (Li et al. 2024). The phylogenetic relation and digital expression profiling of EcWRKY5 suggest that it may be strongly involved in the negative regulation of the fungal immunity in finger millet which further validation and functional characterization. It will help to identify the specific role of WRKY genes in finger millet and other cereals. Altogether, it provides information for future functional analyses on WRKY TF and improve blast tolerance in finger millet and other cereals.

## Conclusion

The genome mining of finger millet identified 13 EcWRKY genes. Cis-regulatory element analyses revealed the presence of W-boxes, CAATs, ABREs, and MeJAs, which may play a significant role in hormonal and stress signaling pathways. In response to Magnaporthe oryzae infection, EcWRKY5 was identified as a candidate gene exhibiting high transcript abundance, suggesting its potential negative contribution to blast resistance and potential positive contribution to abiotic stress tolerance. These findings provide a foundation for further wet-lab validation and provide a strategic roadmap for breeding finger millet with enhanced tolerance to the blast pathogen. Through gene editing, molecular breeding, or genomics-assisted breeding approaches, extensive functional validation of EcWRKY genes could be leveraged for crop improvement.

## References

- Agarwal P, Reddy MP, Chikara J (2011) WRKY: Its structure, evolutionary relationship, DNA-binding selectivity, role in stress tolerance and development of plants. Mol Biol Rep 38:3883–3896. <https://doi.org/10.1007/s11033-010-0504-5>
- Chanwala J, Satpati S, Dixit A, et al (2020) Genome-wide identification and expression analysis of WRKY transcription factors in pearl millet ( *Pennisetum glaucum* ) under dehydration and salinity stress. BMC Genomics 1–16
- Chujo T, Miyamoto K, Ogawa S, et al (2014) Overexpression of Phosphomimic Mutated OsWRKY53 Leads to Enhanced Blast Resistance in Rice. 9:. <https://doi.org/10.1371/journal.pone.0098737>
- Dabi M, Agarwal P, Agarwal PK (2020) Overexpression of JcWRKY2 confers increased resistance towards Macrophomina phaseolina in transgenic tobacco. 3 Biotech 10:1–10. <https://doi.org/10.1007/s13205-020-02490-0>
- Devos KM, Qi P, Bahri BA, et al (2023) Genome analyses reveal population structure and a purple stigma color gene candidate in finger millet. <https://doi.org/10.1038/s41467-023-38915-6>
- Edgar RC (2004) MUSCLE: Multiple sequence alignment with high accuracy and high throughput. Nucleic Acids Res 32:1792–1797. <https://doi.org/10.1093/nar/gkh340>
- Eulgem T, Rushton PJ, Robatzek S, Somssich IE (2000) The WRKY superfamily of plant transcription factors. Trends Plant Sci 5:199–206. [https://doi.org/10.1016/S1360-1385\(00\)01600-9](https://doi.org/10.1016/S1360-1385(00)01600-9)
- Gasteiger E, Hoogland C, Gattiker A, et al (2005) Protein Identification and Analysis Tools on the ExPASy Server BT - The Proteomics Protocols Handbook. In: Walker JM (ed). Humana Press, Totowa, NJ, pp 571–607

- Goel R, Pandey A, Trivedi PK, Asif MH (2016) Genome-wide analysis of the *musa* WRKY gene family: Evolution and differential expression during development and stress. *Front Plant Sci* 7:1–13. <https://doi.org/10.3389/fpls.2016.00299>
- Goodstein DM, Shu S, Howson R, et al (2012) Phytozome: a comparative platform for green plant genomics. *Nucleic Acids Res* 40:D1178–86. <https://doi.org/10.1093/nar/gkr944>
- Gupta S, Pathak RK, Gupta SM, et al (2018) Identification and molecular characterization of Dof transcription factor gene family preferentially expressed in developing spikes of *Eleusine coracana* L. *3 Biotech* 8:1–13. <https://doi.org/10.1007/s13205-017-1068-z>
- Jadhav, P (2018) Expression of ECMYB Transcription Factor Gene Under Different Abiotic Stress Conditions in *Eleusine coracana*. *Int J Agric Environ Biotechnol* 11:30954. <https://doi.org/10.30954/0974-1712.10.2018.12>
- Jiang J, Ma S, Ye N, et al (2017) WRKY transcription factors in plant responses to stresses. *J Integr Plant Biol* 59:86–101. <https://doi.org/10.1111/jipb.12513>
- Li J, Chen Y, Zhang R, et al (2024) OsWRKY70 Plays Opposite Roles in Blast Resistance and Cold Stress Tolerance in Rice. *Rice* 17:. <https://doi.org/10.1186/s12284-024-00741-9>
- Maharajan T, Ceasar SA, Ajeesh Krishna TP (2022) Finger Millet (*Eleusine coracana* (L.) Gaertn): Nutritional Importance and Nutrient Transporters. *CRC Crit Rev Plant Sci* 41:1–31. <https://doi.org/10.1080/07352689.2022.2037834>
- Mbinda W, Masaki H (2021) Breeding Strategies and Challenges in the Improvement of Blast Disease Resistance in Finger Millet. A Current Review. *Front Plant Sci* 11:1–12. <https://doi.org/10.3389/fpls.2020.602882>
- Qiu Y, Jing S, Fu J, et al (2004) Cloning and analysis of expression profile of 13 WRKY genes in rice. *Chinese Sci Bull* 49:2159–2168. <https://doi.org/10.1360/982004-183>
- Rahman H, Ramanathan V, Nallathambi J, et al (2016) Over-expression of a NAC 67 transcription factor from finger millet (*Eleusine coracana* L.) confers tolerance against salinity and drought stress in rice. *BMC Biotechnol* 16:. <https://doi.org/10.1186/s12896-016-0261-1>
- Rani V, Joshi DC, Joshi P, et al (2023) “Millet Models” for harnessing nuclear factor-Y transcription factors to engineer stress tolerance in plants: current knowledge and emerging paradigms. *Planta* 258:. <https://doi.org/10.1007/s00425-023-04186-0>
- Rani V, Rana S, Muthamilarasan M, et al (2024a) Expression profiling of Nuclear Factor-Y (NF-Y) transcription factors during dehydration and salt stress in finger millet reveals potential candidate genes for multiple stress tolerance. *Planta* 259:136. <https://doi.org/10.1007/s00425-024-04417-y>
- Rani V, Singh VK, Joshi DC, et al (2024b) Genome-Wide Identification of Nuclear Factor -Y (NF-Y) Transcription Factors Family in Finger Millet Reveals Structural and Functional Diversity. *Helion* e36370. <https://doi.org/10.1016/j.heliyon.2024.e36370>
- Rushton PJ, Somssich IE, Ringler P, Shen QJ (2010) WRKY transcription factors. *Trends Plant Sci* 15:247–258. <https://doi.org/10.1016/j.tplants.2010.02.006>

- Satapathy L, Kumar D, Kumar M, Mukhopadhyay K (2018) Functional and DNA–protein binding studies of WRKY transcription factors and their expression analysis in response to biotic and abiotic stress in wheat (*Triticum aestivum* L.). *3 Biotech* 8:. <https://doi.org/10.1007/s13205-017-1064-3>
- Sood S, Babu BK, Joshi D (2022) History, Botanical and Taxonomic Description, Domestication, and Spread BT - The Finger Millet Genome. In: Kumar A, Sood S, Babu BK, et al. (eds). Springer International Publishing, Cham, pp 1–12
- Sureshkumar V, Dutta B, Kumar V, et al (2019) RiceMetaSysB: A database of blast and bacterial blight responsive genes in rice and its utilization in identifying key blast-resistant WRKY genes. *Database* 2019:1–13. <https://doi.org/10.1093/database/baz015>
- Tamura K, Stecher G, Kumar S (2021) MEGA11: Molecular Evolutionary Genetics Analysis Version 11. *Mol Biol Evol* 38:3022–3027. <https://doi.org/10.1093/molbev/msab120>
- Ülker B, Somssich IE (2004) WRKY transcription factors: from DNA binding towards biological function. *Curr Opin Plant Biol* 7:491–498. [https://doi.org/https://doi.org/10.1016/j.pbi.2004.07.012](https://doi.org/10.1016/j.pbi.2004.07.012)
- Wei K-F, Chen J, Chen Y-F, et al (2012) Molecular Phylogenetic and Expression Analysis of the Complete WRKY Transcription Factor Family in Maize. *DNA Res* 19:153–164. <https://doi.org/10.1093/dnares/dsr048>
- Wei Y, Shi H, Xia Z, et al (2016) Genome- wide identification and expression analysis of the WRKY gene family in cassava. *Front Plant Sci* 7:1–18. <https://doi.org/10.3389/fpls.2016.00025>
- Wright H, Devos KM (2024) Finger millet: a hero in the making to combat food insecurity. *Theor Appl Genet* 137:1–13. <https://doi.org/10.1007/s00122-024-04637-6>
- Zhang L, Shu H, Zhang AY, et al (2017) Foxtail millet WRKY genes and drought stress. *J Agric Sci* 155:777–790. <https://doi.org/10.1017/S0021859616000873>
- Zhang Y, Wang L (2005a) The WRKY transcription factor superfamily: Its origin in eukaryotes and expansion in plants. *BMC Evol Biol* 5:1–12. <https://doi.org/10.1186/1471-2148-5-1>
- Zhang Y, Wang L (2005b) The WRKY transcription factor superfamily: its origin in eukaryotes and expansion in plants. *BMC Evol Biol* 5:1. <https://doi.org/10.1186/1471-2148-5-1>

Table 1 Gene structure, physical properties and group of EcWRKY proteins of finger millet responsive for blast infection.

S.N	Gene Name	Gene Accession number	Gene Start (bp)	Gene End (bp)	Strand	Chromosome Name	length of CDS	AA	molecular Weight (kDa)	pI	GRAVY	Instability Index	Aliphatic Index	Group
1.	EcWRKY5	ELECO_07_5BG0424350	11070724	11072751	-1	5B	1755	584	62.97851	9.19	-0.794	56.55	54.42	1
2.	EcWRKY8	ELECO_07_8BG0653220	20869217	20874683	-1	8B	1821	606	65.06562	5.89	-0.694	49.77	60.73	1
3.	EcWRKY16	ELECO_07_5AG0369350	5887140	5889474	-1	5A	1725	574	60.79804	6.76	-0.55	52.95	53.97	1
4.	EcWRKY19	ELECO_07_7BG0606110	53712181	53717566	-1	7B	1845	614	65.96498	6.3	-0.806	50.29	52.44	1
5.	EcWRKY35	ELECO_07_5BG0410120	604646	606059	1	5B	876	291	31.78504	6.39	-0.882	53.56	51.99	1
6.	EcWRKY58	ELECO_07_1AG0012660	10204493	10205205	-1	1A	621	206	22.55615	6.7	-0.632	46.36	44.61	2
7.	EcWRKY63	ELECO_07_4BG0339610	6938255	6942851	1	4B	705	234	25.51801	8.74	-0.512	43.91	60.94	2
8.	EcWRKY64	ELECO_07_4BG0335780	4430794	4431940	-1	4B	924	307	32.35511	10.18	-0.334	55.3	71.34	2
9.	EcWRKY82	ELECO_07_3AG0216800	6458998	6460928	-1	3A	1161	386	41.56344	9.85	-0.533	51.21	68.78	2
10.	EcWRKY99	ELECO_07_5AG0362810	1571090	1573529	-1	5A	1695	564	59.14505	6.58	-0.47	51.93	64.38	2
11.	EcWRKY111	ELECO_07_1BG0072390	49923331	49923723	1	1B	288	95	11.00256	9.82	-1.146	59.45	47.05	2
12.	EcWRKY116	ELECO_07_4AG0323730	27022604	27023981	1	4A	1164	387	41.77713	9.61	-0.549	48.92	61.06	2
13.	EcWRKY120	ELECO_07_7BG0583030	109672	111961	-1	7B	984	327	34.08317	6.34	-0.276	50.95	61.99	2

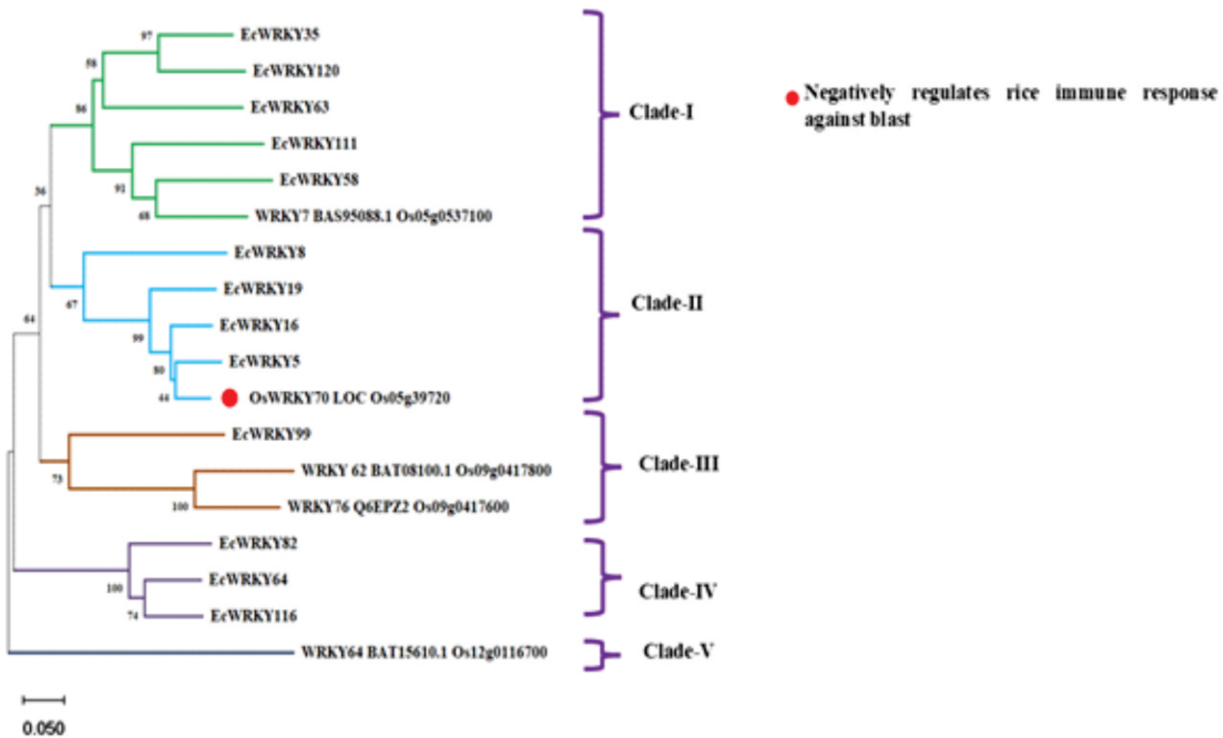


Fig. 1: Phylogenetic analysis of EcWRKY proteins with rice WRKYs, showing five distinct clades. The red marker highlights OsWRKY70, a known negative regulator of rice blast immunity.

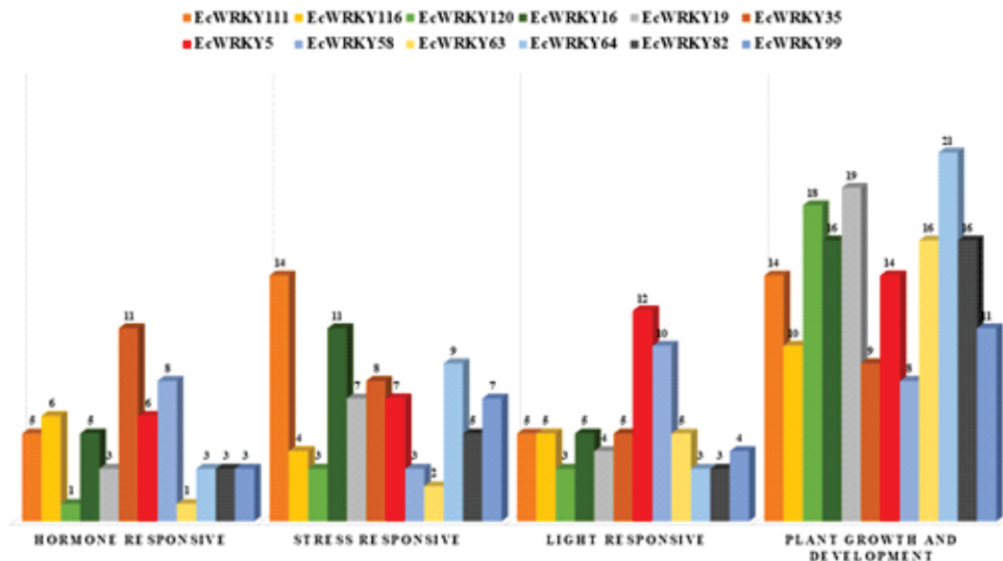


Fig. 2: Distribution of *cis*-regulatory elements in selected EcWRKY genes related to hormone responsiveness, stress responsiveness, light responsiveness, and plant growth and development.

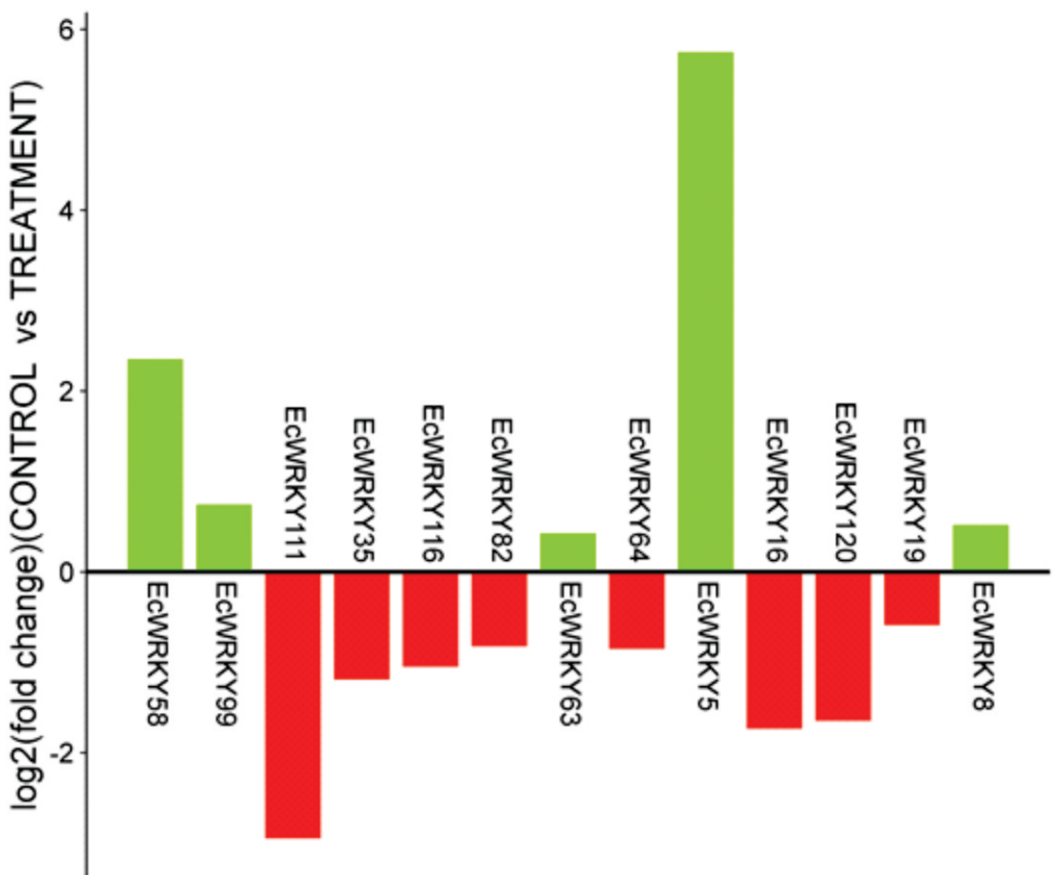


Fig. 3: Differential expression profile of ECWRKY genes under treatment, showing significant downregulation (red) and upregulation (green) based on log<sub>2</sub> fold change (Control vs Treatment).

## Untapped potential of microalgae in industrial effluent treatment and bio-diesel production supporting circular bio-economy.

Tribhuwan Kumar<sup>1,2\*</sup> & Monika Prakash Rai<sup>1\*</sup>

<sup>1</sup>Bioenergy & Biorefinery Laboratory Department of Bio- Technology, Motilal Nehru National Institute of Technology, Allahabad, Prayagraj, 211004. <sup>2</sup>Department of Molecular Biology & Genetic Engineering, Bihar Agricultural University, Sabour, 813210

\*Presenting Author: [tribhuwan.2024rbt14@mnnit.ac.in](mailto:tribhuwan.2024rbt14@mnnit.ac.in)

\*Corresponding Author Email: [mprai@mnnit.ac.in](mailto:mprai@mnnit.ac.in)

---

### Abstract

The escalated industrialization and urbanization has resulted in release of harmful effluents day by day. Many methods of remediation of industrial effluent and wastewater are available but suffer from efficiency problem and economic non feasibility. Microalgae have exhibited good potential in the treatment of wastewater and industrial effluents such as of fertilizer, pulp, thermal power, textile, dye, tannery, brewery, oil drilling, pharmaceutical industries and others. It has enormous potential to remove pollutants like excess carbon, nitrogen, phosphorous, sulfur, potassium, heavy metals, and other xenobiotic compounds. The algal biomass resulting from treatments of wastewater and industrial effluents are renewable source of bio-fuel. Algal biomass is used to produce biodiesel, which reduce the emission of greenhouse gas and dependency on fossil fuels as well. Now a day, biodiesel is blended with diesel with permissible proportions. Efforts are being made to make the algal biodiesel more compatible with higher blending percentage in newly launched vehicles with integration to cutting edge automobile technology. Screening and improvement of algal strain encompassing huge biodiesel production is required to make it more productive and economic. Microalgae such as *Chlorella sp.*, *Scenedesmus sp.*, *Coelastrella sp.*, *Nannochloropsis sp.*, possess high quantity of lipids that produce fatty acid methyl esters (Bio-diesel) and also being exploited for improved qualitative production of biodiesel. More over the de-oiled microalgal biomass comprise plenty of potential to generate by-products in various ways such as feed, bio-fertilizer, bio-ethanol, chemicals, biomaterials, bio-sorbent etc. Algal based biodiesel production has emerged as a savior technology to meet the worldwide demands of sustainable and eco-friendly approach of renewable energy generation. Algal biodiesel production is the most preferred and accepted approach as it capitalizes the treatments of industrial effluent, the major global concern. In addition, the uses of de-oiled algal biomass as mentioned above support and streamline the most needed circular economy system in India.

---

**Keywords:** Microalgae, Wastewater, Biodiesel, Pollution, circular bioeconomy

## Introduction

Waste water contains high value of chemical oxygen demand, biological oxygen demand, dissolved and suspended inorganic compounds such as carbonates, bicarbonates, chlorides, nitrates, nitrites phosphates etc. Heavy metals, such as arsenic, cadmium, nickel, and titanium are more common in industrial effluents that may result in health complications by biological magnification (Grace Pavithra et al. 2020). The use of macroalgae in the treatment of the wastewater was first applied by Oswald in 1960s and it is known as an economic and sustainable approach for wastewater treatment. Lipids are the major substrate for biodiesel production. Transesterification is the substitution and replacement of glycerol using methanol and conversion of triglycerides to biodiesel and glycerol. It is the most commercially applied biorefinery process leading to algal mass culture and biodiesel production. Defatted algal biomass also has the potential to be derived in value-added bioproducts without exploiting environmental sustenance and generating economic benefits (Kothari et al., 2021)

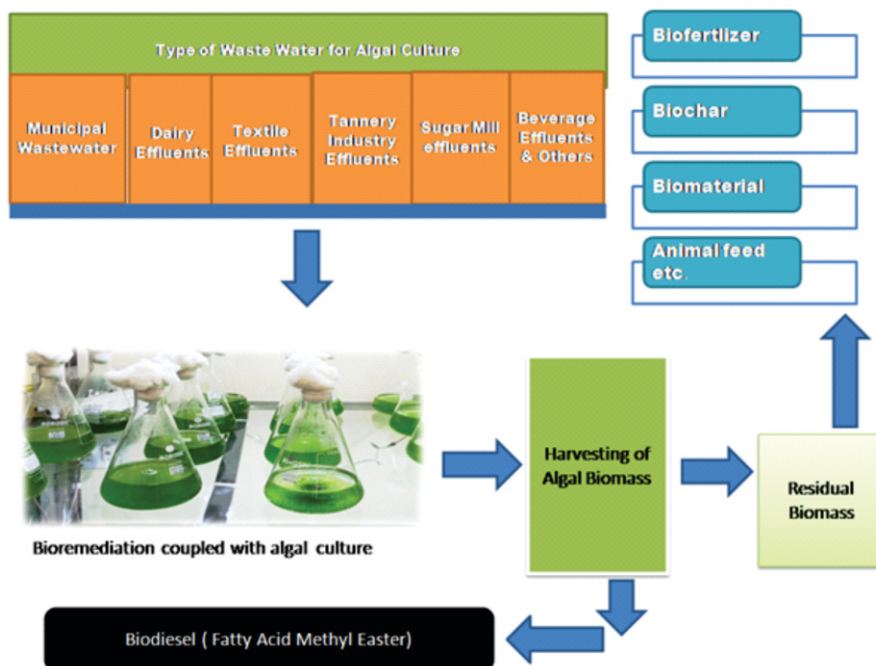


*Fig1: Diagrammatic representation of Biodiesel production coupled with waste water treatment and supporting circular bio economy.*

**Lipid Accumulation coupled with waste water treatment:** The good association of lipid accumulation and waste water treatment has been exhibited by the experiments conducted in the past (Table 1).

S. No.	Microalgae	Type of waste water	Quantity of Lipid/ Biodiesel	Process	Reference
1	Chlorella zofinginensis	Piggery wastewater	9.19 % of dry weight	Continuous Photo bioreactor	Zhu et al., 2013
2	Scenedesmus obliquus, Micractinium pisillum, Dictyosiphon pulchellum & Coleastrum Sp.	Municipal waste water	70.9% of algal oil	Cultivated in high rate algal pond	Doma et al., 2016
3	<i>C. vulgaris</i>	Aquaculture and pulp	9.07 (Lipid)	Flask Scale	Daneshwar et al., 2018
4	<i>S. obliquus</i>	Brewery effluent	64 (bio-oil)	Cylindrical bubble column bioreactor	Ferreira et al., 2019
5	<i>S. obliquus</i>	Primary & Secondary Settling tank	0.38 g L <sup>-1</sup> & 0.33 g L <sup>-1</sup> Biodiesel	Flask Culture	Wei Han et al., 2021
6	<i>S. obliquus</i>	Domestic wastewater	25.67 (lipid)	Erlenmeyer Flask Culture	Satheesh et al., 2023
7	<i>C. pyrenoidosa</i>	Domestic wastewater	25.34 Lipid)	Erlenmeyer Flask Culture	Satheesh et al., 2023
8	<i>C. sorokiniana</i>	Domestic wastewater	26.23 (Lipid)	Erlenmeyer Flask Culture	Satheesh et al., 2023

This approach not only enriches the biomass for the lipid and biodiesel extraction but also gives a technology to clean the water released from the industry or municipality. Like other sources of Biodiesel, micro algae grown on the waste water does not use arable land and special effort to grow feedstock reducing the overall cost of biodiesel production. In this direction research is going on to capitalize this technology and to introduce this technology in effluent or waste water treatment system.

**Methods of Biodiesel Production:** The production of Biodiesel from microalgae involves four different steps: production of micro algal biomass, its harvesting, disruption of microalgae, isolation and purification of lipid and conversion of lipid into biodiesel. There are many ways to harvest microalgae and it includes biological, chemical and physical with respective advantage and disadvantage. The use of these methods is specific to species of microalgae and depends on conditions of culture. It first requires involves breaking of microalgae cells to gain access to components inside the cell including lipids and other macromolecules. Now lipid extraction from the complex mixture of macromolecules requires many steps such as [solvent-solvent extraction](#) and concentration. For solvent extraction organic solvents such as chloroform, hexane and methyl alcohol are common to use. The extracted lipids are further purified and concentrated through processes like distillation, chromatography or evaporation (Vasistha et al., 2021). The purity of the biodiesel relies on the quality of the microalgae and the use of extraction & purification steps of lipids and their efficiency. Eventually transesterification decides the quality and quantity of biodiesel production by converting simple lipid to fatty acid methyl ester and Glycerol as a by product with the help of NaOH or KOH (Gaurav et al., 2024).

**Challenges in the Production of Biodiesel:** The production of Biodiesel from the microalgae is a sustainable energy solution as microalgae are renewable source. However, each step involved in biodiesel production has to face challenges such as consumption of high electricity, requirement of toxic chemicals and non economic processes. These challenges address an extensive research to devise a techno feasible process for efficient and economic biodiesel production (Pandey et al., 2024).

**Potential application of deoiled biomass supporting circular economy:** Defatted algal biomass after extraction of biodiesel also has various uses including animal feed and bio fertilizers in addition biofuel (biogas, ethanol, biohydrogen) and other useful materials. De-oiled algae contain valuable protein and carbohydrate; therefore, it is an important source for animal feed and also reduces dependency on other fodder crops. Microalgae have shown its effect on animal growth and on the quality of meat when it was included in livestock diets. De-oiled algal biomasses are rich in nutrients like nitrogen, phosphorus, and potassium and it make an ideal biofertilizer. Moreover it improves the structure of soil structure, water retention ability, and microbial activity for enhanced plant growth and yields. Algae-based biofertilizers exhibit consistent and precise release of nutrients, as per plant uptake. This wastewater treatment coupled with enrichment of biomass of algae, extraction of biodiesel and use of deoiled biomass of algae as animal feed, biofertilizer etc. in combination generate a circular bioeconomy model, promoting sustainable energy production (Betancourt-Lozano, 2025).

**Conclusion & Future Perspective:** The algal based biodiesel production involves benefits at each level right from bioremediation coupled with biomass culture to diverse use of deoiled biomass of algae. This approach not only support circular economy but also sustainable process of biofuel production mitigating water pollution. However, the future of biodiesel production from microalgae lies in minimising cost and enhancing efficiency. Research and development in this direction are on the way to optimize cultivation, harvesting, and conversion processes to enhance the cost benefit ratio.

**Acknowledgement:** Authors acknowledge MNNIT, Allahabad for providing research facilities and support.

**Reference:**

- Betancourt-Lozano, M., & Luna-Avelar, K. D. (2025). Microalgal Biorefineries: Advances and Techno-Economic Challenges. *Microalgae as Promising Source of Commercial Bioproducts: Advances and Emerging Technologies in Bioactive Compounds, Biofuels, Food and Biorefineries*, 14, 309.
- Daneshvar E, Antikainen L, Koutra E, Kornaros M, Bhatnagar A. (2018) Investigation on the feasibility of Chlorella vulgaris cultivation in a mixture of pulp and aquaculture effluents: Treatment of wastewater and lipid extraction. *Bioresour Technol.* 255:104-110. doi: 10.1016/j.biortech.2018.01.101. Epub 2018 Jan 31. PMID: 29414154.
- Doma, H. S., Abdo, S. M., Mahmoud, R. H., Enin, S. A. El., and Diwani, G. El. (2016). Production and characterization of biodiesel from microalgae cultivated in municipal wastewater treatment plant. *Res. J. Pharm. Biol. Chem. Sci.* 7 (2), 1912–1919.
- Ferreira, A., Ribeiro, B., Ferreira, A. F., Tavares, M. L., Vladic, J., Vidović, S., ... & Gouveia, L. (2019). Scenedesmus obliquus microalga-based biorefinery—from brewery effluent to bioactive compounds, biofuels and biofertilizers—aiming at a circular bioeconomy. *Biofuels, Bioproducts and Biorefining*, 13(5), 1169-1186.
- Gaurav, K., Neeti, K., & Singh, R. (2024). Microalgae-based biodiesel production and its challenges and future opportunities: A review. *Green Technologies and Sustainability*, 2(1), 100060.
- Grace Pavithra, K., Senthil Kumar, P., Jaikumar, V., & SundarRajan, P. (2020). A review on three-dimensional electrochemical systems: analysis of influencing parameters and cleaner approach mechanism for wastewater. *Reviews in Environmental Science and Bio/Technology*, 19(4), 873-896.
- Kothari, Richa & Ahmad, Shamshad & Pathak, Vinayak & Pandey, Arya & Kumar, Ashwani & Shankarayyan, Raju & Black, Paul & Tyagi, Vineet. (2021). Algal-based biofuel generation through flue gas and wastewater utilization: a sustainable prospective approach. *Biomass Conversion and Biorefinery*. 11. 1-24. 10.1007/s13399-019-00533-y.
- Pandey, S., Narayanan, I., Selvaraj, R., Varadavenkatesan, T., & Vinayagam, R. (2024). Biodiesel production from microalgae: a comprehensive review on influential factors, transesterification processes, and challenges. *Fuel*, 367, 131547.
- Satheesh S, Pugazhendi A, Bandar A. Al-Mur, Balasubramani R (2023)Biohydrogen production coupled with wastewater treatment using selected microalgae,Chemosphere,Volume 334,138932,ISSN 0045-6535, <https://doi.org/10.1016/j.chemosphere.2023.138932>.
- Vasistha, S., Khanra, A., Clifford, M., & Rai, M. P. (2021). Current advances in microalgae harvesting and lipid extraction processes for improved biodiesel production: A review. *Renewable and Sustainable Energy Reviews*, 137, 110498.
- Wei Han, Wenbiao Jin, Ze Li, Yubin Wei, Zhongqi He, Chuan Chen, Changlei Qin, Yidi Chen, Renjie Tu, Xu Zhou (2021) Cultivation of microalgae for lipid production using municipal wastewater, *Process Safety and Environmental Protection*, Volume 155,2021, Pages 155-165, ISSN 0957-5820,<https://doi.org/10.1016/j.psep.2021.09.014>.
- Zhu, L., Wang, Z., Takala, J., Hiltunen, E., Qin, L., Xu, Z., ... & Yuan, Z. (2013). Scale-up potential of cultivating Chlorella zofingiensis in piggery wastewater for biodiesel production. *Bioresource technology*, 137, 318-325.

## Discovery of novel inhibitors of Aminodeoxychorismate lyase enzyme from *Plasmodium falciparum*: A Comparative binding analytics

Shruti Shukla, Ashutosh Mani\*

Department of Biotechnology, Motilal Nehru National Institute of Technology,  
Allahabad, Prayagraj, Uttar Pradesh, 211004, India.

Corresponding Author email: amani@mnnit.ac.in

### Abstract

Malaria is a major life-threatening parasitic infection caused by *Plasmodium*. According to the World Malaria Report 2024, there were 263 million malaria cases, which resulted in 59700 deaths in the year 2023 (World malaria report 2024: addressing inequity in the global malaria response n.d.). The increasing emergence of drug-resistant strains necessitates the urgent discovery of novel antimalarial therapeutics. Aminodeoxychorismate lyase is an essential enzyme of the folate biosynthesis in *Plasmodium falciparum*, and plays a crucial role in parasite survival, making it a promising drug target (Hyde 2005; McConkey 1999). In the present study, a computational approach was used to identify potential inhibitors of aminodeoxychorismate lyase, and inhibitors were screened against aminodeoxychorismate lyase. The three-dimensional structure of the enzyme was predicted using Modeller 10.5 (Cosconati et al. 2010), followed by structural validation and active sites predicted. Molecular docking was performed using the Autodock tools 1.5.7, and protein-ligand interactions were further analyzed using the PLIP server. Among the screened-out compounds, DB01078 shows the best results with a binding affinity of -11.4 Kcal/mol with the target enzyme.

---

**Keywords:** Aminodeoxychorismate, Folate biosynthesis pathway, Homology modelling, Molecular Docking.

## Introduction

Folate metabolism is essential for the survival of malaria parasites and has been a target for both treatment and prophylaxis of the disease for over half a century. Aminodeoxychorismate lyase (ADCL) synthesizes Para-aminobenzoate (PABA), a key precursor in the folate biosynthesis pathway of *Plasmodium falciparum*, and plays a crucial role in parasite growth and survival, making it a promising drug target. The increasing emergence of drug-resistant strains necessitates the urgent discovery of novel antimalarial therapeutics.

### **1. Materials and methods**

#### **1.1 Tools and materials**

The current study utilized the DrugBank database, PyRx, Autodock 4, Autodock-Vina, and Modeller 10.5, along with the visualization tools like Chimera, Pymol, and BIOVIA Discovery Studio Visualizer.

#### **1.2 Protein structure prediction and validation**

The aminodeoxychorismate lyase protein has 316 amino acid residues. The homologs were searched for aminodeoxychorismate lyase protein by using the HHpred tool (Soding, Biegert, and Lupas 2005). Since no reported significant homologs for aminodeoxychorismate lyase were available, a modelling approach was considered. The Modeller 10.5 (Eswar et al. 2006) was utilized to generate 3-D models for aminodeoxychorismate lyase. The obtained 3-D structures were further validated through the PROCHECK utility of the UCLA SAVES server (Laskowski et al. 1993). The best-obtained protein model was subjected to energy minimization using Modeller 10.5. Further polar hydrogen bonds were added, missing residues and atoms were checked and repaired, and Kollman charges were added to the modelled protein structure using AutoDock 4 tools(Cosconati et al. 2010).

#### **1.3 Ligand Preparation**

The FDA approved 3758 drugs in the SDF file format. The structural optimization through energy minimization was performed before virtual screening using PyRx(Dallakyan and Olson 2015).

#### **1.4. Determination of binding pockets**

The PrankWeb web server was used to predict the binding pockets of the aminodeoxychorismate lyase protein (Jendele et al. 2019). It provides detailed information about the amino acid residues involved in the active site and their position. It identifies the voids and the pockets along with the volume and area present in the interior of the 3-D protein conformation. The best binding pockets usually have the highest volume and area and contain potential active sites for performing molecular docking studies and analysis.

### 1.5. Molecular Docking

A molecular docking simulation was conducted to elucidate the molecular interactions between the chosen drug bank compounds and the aminodeoxychorismate lyase protein, utilizing the Autodock Vina v1.2.3 (Eberhardt et al. 2021) program through a Perl script. The drugs, after undergoing initial energy minimization, were converted to the PDBQT file format. AutoGrid tools were employed to generate the grid maps in such a way that they could cover the maximum active site region of the protein. The configuration file includes center\_x = 13.403, center\_y = 0.928, and center\_z = 12.988 with dimensions of size\_x = 62, size\_y = 52, and size\_z = 58 and a grid spacing of 0.375 Å. The Lamarckian genetic algorithm was employed to predict the binding mode between the drugs and the target protein, and the results were analyzed based on binding energies. All the other parameters were set to default. All the docked compounds were further ranked based on their binding affinity scores. The drugs that had binding affinity  $\geq 10$  kJ/mol were selected. Thereafter, molecular interaction between aminodeoxychorismate lyase and top-scoring drugs was examined using the PLIP server –(Salentin et al. 2015).

## 2. Results and Discussion

### 2.1. Predicting and validating protein structure

The 3D structure of aminodeoxychorismate lyase derived from the modeller consists of 316 amino acids. The validation of the 3D structure for the modelled aminodeoxychorismate lyase protein using PROCHECK showed percentages of 86%, 10.6%, and 2.3% (355, 29, and 1) in the most favoured, additional allowed, and generously allowed regions of the Ramachandran plot. The disallowed region contained 1% (6) residues, as illustrated in **Figure 1**.

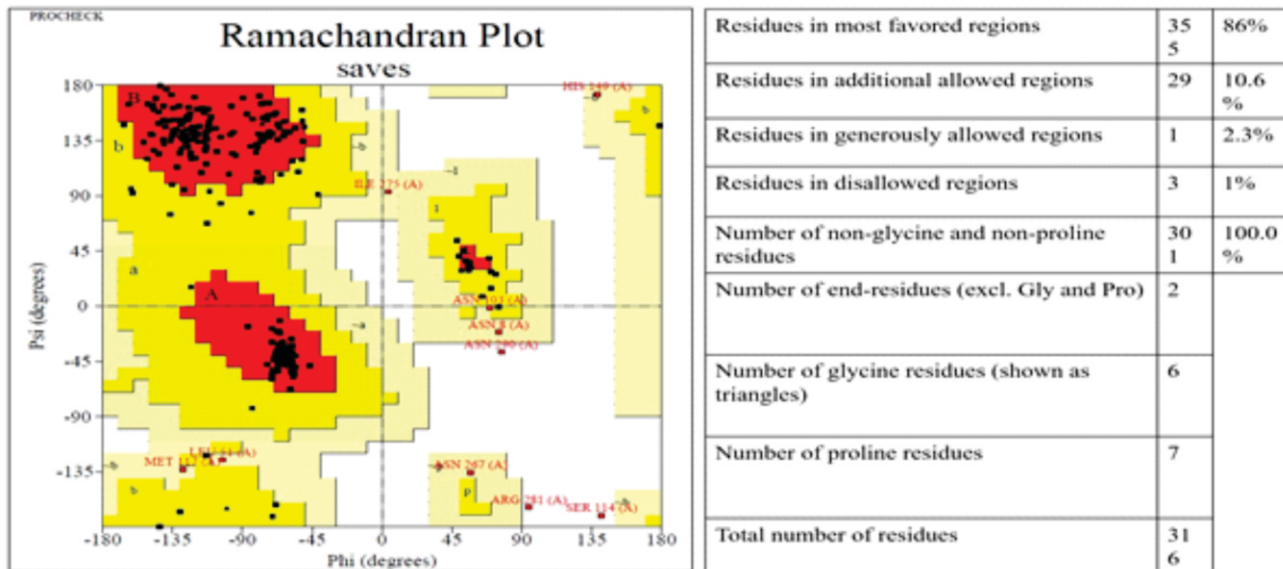


**Figure 1:** Ramachandran plot analysis of the modelled Aminodeoxychorismate lyase protein.

## 2.2. Determination of binding pockets

The identification of binding pockets of a protein is necessary to understand the regions and amino acids available for interaction with drug compounds. The PrankWeb web server had identified one binding pocket, as shown in **Figure 2**. A total of 50 residues are involved in the binding pockets.

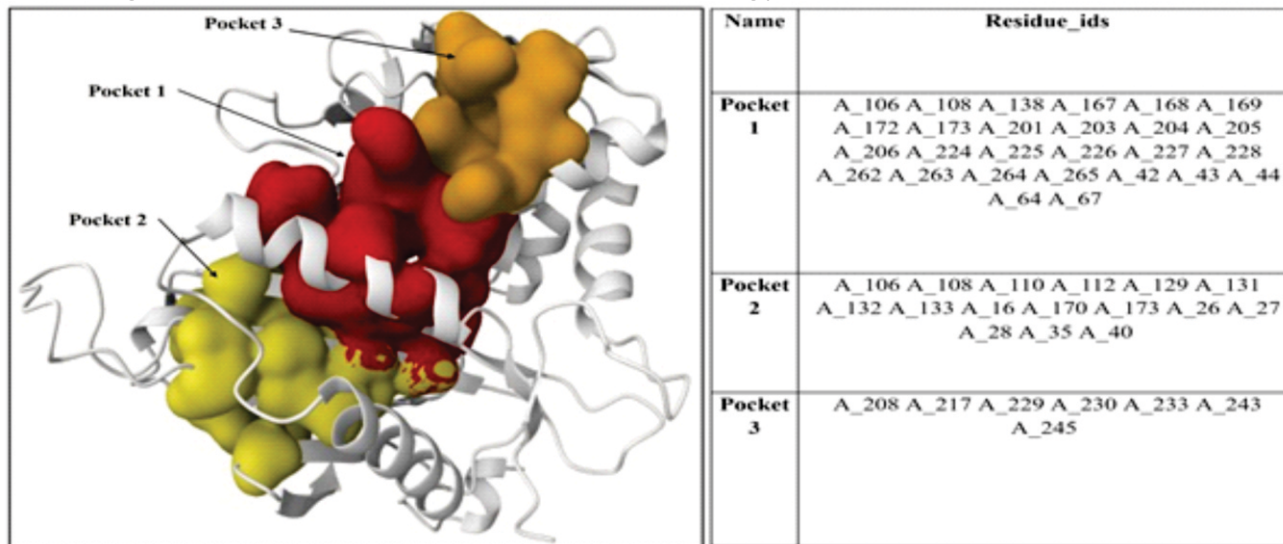


**Figure 2:** Predicted binding pockets of Aminodeoxychorismate lyase protein and corresponding amino acid residues.

## 2.3. Molecular docking analysis

All the FDA-approved drugs from the drug bank were selected for molecular docking against the aminodeoxychorismate lyase protein using the AutoDock Vina tool. Binding affinity was the chosen parameter for selecting the best bound drugs with the aminodeoxychorismate lyase protein target. The greater the negative binding affinity, the more influential the binding capability of the complex. For subsequent examination, the top 200 drugs in a descending order of binding affinity were selected. These top 20 drugs have a maximum binding affinity of -10.8 kJ/mol and a minimum binding affinity of -10.1 kJ/mol. **Table 1** shows the names of the selected drugs, along with their binding affinity values in descending order, complexed with aminodeoxychorismate lyase protein.

S.N.	Drug_Id	Binding Affinity (kJ/mol)	Name	S.N.	Drug_Id	Binding Affinity (kJ/mol)	Name
1	DB01078	-10.8	Deslanoside	11	DB00320	-10.3	Dihydroergotamine
2	DB09280	-10.8	Lumacaftor	12	DB06810	-10.3	Plicamycin
3	DB01590	-10.7	Everolimus	13	DB08871	-10.3	Eribulin
4	DB00872	-10.6	Conivaptan	14	DB11574	-10.3	Elbasvir
5	DB01263	-10.6	Posaconazole	15	DB00693	-10.2	Fluorescein
6	DB04868	-10.6	Nilotinib	16	DB09372	-10.2	Tannic acid
7	DB06290	-10.5	Simeprevir	17	DB13345	-10.2	Dihydroergocristine
8	DB00115	-10.4	Cyanocobalamin	18	DB15328	-10.2	Ubrogepant
9	DB00696	-10.4	Ergotamine	19	DB11581	-10.1	Venetoclax
10	DB00619	-10.3	Imatinib	20	DB01395	-10	Colchicine

**Table 1:** selected drugs' names, drug bank IDs, and binding affinities in descending order when complexed with the Aminodeoxychorismate lyase protein.

## Conclusion

In this study, we identified the FDA-approved drugs with the best binding affinity with the aminodeoxychorismate lyase protein, which is a key enzyme of folate biosynthesis and is vital for parasite survival. The interaction analysis reveals that the best binding affinity is shown by the deslanoside (DB01078), which is -10.8 kcal/mol. These results suggest that it could be a promising candidate for antimalarial drug discovery; however, further *in vivo*, *in vitro*, and pharmacological investigations are required to validate its efficacy and safety.

## References –

1. Cosconati, Sandro, Stefano Forli, Alex L. Perryman, Rodney Harris, David S. Goodsell, and Arthur J. Olson. 2010. "Virtual Screening with AutoDock: Theory and Practice." *Expert Opinion on Drug Discovery* 5(6):597-607. doi:10.1517/17460441.2010.484460.
2. Dallakyan, Sargis, and Arthur J. Olson. 2015. "Small-Molecule Library Screening by Docking with PyRx." Pp. 243-50 in *Chemical Biology*. Vol. 1263, *Methods in Molecular Biology*, edited by J. E. Hempel, C. H. Williams, and C. C. Hong. New York, NY: Springer New York.
3. Eberhardt, Jerome, Diogo Santos-Martins, Andreas F. Tillack, and Stefano Forli. 2021. "AutoDock Vina 1.2.0: New Docking Methods, Expanded Force Field, and Python Bindings." *Journal of Chemical Information and Modeling* 61(8):389-198. doi:10.1021/acs.jcim.1c00203.
4. Eswar, Narayanan, Ben Webb, Marc A. Marti-Renom, M. S. Madhusudhan, David Eramian, Min-yi Shen, Ursula Pieper, and Andrej Sali. 2006. "Comparative Protein Structure Modeling Using Modeller." *Current Protocols in Bioinformatics* 15(1). doi:10.1002/0471250953.bi0506s15.
5. Hyde, John E. 2005. "Exploring the Folate Pathway in Plasmodium Falciparum." *Acta Tropica* 94(3):191-206. doi:10.1016/j.actatropica.2005.04.002.
6. Jendele, Lukas, Radoslav Krivak, Petr Skoda, Marian Novotny, and David Hoksza. 2019. "PrankWeb: A Web Server for Ligand Binding Site Prediction and Visualization." *Nucleic Acids Research* 47(W1):W345-49. doi:10.1093/nar/gkz424.
7. Laskowski, R. A., M. W. MacArthur, D. S. Moss, and J. M. Thornton. 1993. "PROCHECK: A Program to Check the Stereochemical Quality of Protein Structures." *Journal of Applied Crystallography* 26(2):283-91. doi:10.1107/S0021889892009944.
8. McConkey, Glenn A. 1999. "Targeting the Shikimate Pathway in the Malaria Parasite Plasmodium Falciparum." *Antimicrobial Agents and Chemotherapy* 43(1):175-77. doi:10.1128/AAC.43.1.175.
9. Salentin, Sebastian, Sven Schreiber, V. Joachim Haupt, Melissa F. Adasme, and Michael Schroeder. 2015. "PLIP: Fully Automated ProteinLigand Interaction Profiler." *Nucleic Acids Research* 43(W1):W443-47. doi:10.1093/nar/gkv315.
10. Soding, J., A. Biegert, and A. N. Lupas. 2005. "The HHpred Interactive Server for Protein Homology Detection and Structure Prediction." *Nucleic Acids Research* 33(Web Server):W244-48. doi:10.1093/nar/gki408.
11. World malaria report 2024: addressing inequity in the global malaria response. n.d.

## GREEN SYNTHESIS OF SILVER NANOPARTICLES USING ALGAE AND THEIR APPLICATIONS

Preeti Maurya and Sanjay Singh\*

Department of Botany, CMP Degree College, Prayagraj, 211002, Uttar Pradesh INDIA  
[pm7963809@gmail.com](mailto:pm7963809@gmail.com); [cmpsanjay@gmail.com](mailto:cmpsangjay@gmail.com)

---

### Abstract

In recent years, green nanotechnology has gained importance for the production of nanoparticles due to its biosafety and affordability. This study synthesized silver nanoparticles utilizing a *Rhizoclonium* sp. extract as a capping and reducing agent. We investigated the synthesised nanoparticles using scanning electron microscopy, Fourier transform infrared spectroscopy, UV-visible spectroscopy, and X-ray diffractive analysis. The SEM image indicated a spherical shape with an average grain size of 40-90 nm. In nanobiotechnology, establishing an environmentally benign approach for generating nanoparticles is a daily advancement. The antibacterial, antifungal, anticancer, antioxidant, and wound-healing characteristics of silver nanoparticles make the present research into their ecologically friendly production and usage important.

---

**Keywords:** *Rhizoclonium* sp., green nanotechnology, SEM, eco-friendly, biological applications

## Introduction

Silver nanoparticles, or AgNPs, are becoming more and more popular due to their many uses in industry, medicine, and agriculture, as well as their exceptional biological and physicochemical characteristics –(Qi et al., 2023; Ravindran et al., 2013; Zheng et al., 2018). AgNPs are now used in food packaging to extend the shelf life of foods as well as in cosmetics and healthcare items –(de Moura et al., 2012; Hamida et al., 2024; Qi et al., 2023). Realizing this fact that the synthesis of AgNPs by physical and chemical methods are environmentally hazardous and have several drawbacks. The superiority of green NPs over their physical and chemical counterparts lies on their organic origin and non-toxic property. Besides this, green synthesis involves a wide range of environmentally acceptable methodology with low-cost production in lesser time. Because of their unique shape-dependent, optical, electrical, and chemical characteristics that have potential uses in nanobiotechnology, the synthesis of nanoparticles utilizing biological entities has piqued the interest of many researchers.

Chemical, biological, and physical processes can all be used to create AgNPs. Each of these techniques uses the reduction of silver ions from salt followed by atom self-assembly to create nanoparticles (Vidyasagar et al., 2023). Silver ions are reduced in green synthesis by microorganisms such fungi, bacteria, algae, and plants (Patil et al., 2022). The inherent reducing and stabilizing agents of organisms, including amino acids, polyphenols, flavonoids, polysaccharides, terpenoids, alkaloids, and others, are utilized in this environmentally benign method —(Michalec et al., 2025; Patil et al., 2022).

Adopting the fundamentals of green chemistry, such as a solvent medium, a reducing agent, and a non-hazardous stabilizing agent, is necessary for the green synthesis of distinctively safer AgNPs. It has been suggested that NP synthesis employing microbes, enzymes, plants, and algae is a feasible and sustainable substitute for physical and chemical methods. Furthermore, algae are excellent candidates for the biosynthesis of NPs due to their capacity to accumulate metals and decrease metal ions; as a result, they are perfect for the production of metallic NPs. Additionally, phenolic compounds and polysaccharides enhance their stability by acting as capping agents. The discovery of strong natural chemicals produced in green macroalgae as secondary metabolites has sparked a current surge in interest in these algae. These secondary metabolites' biological characteristics have been widely investigated, and it is known that they contain antibacterial, antiviral, anticancer, and anti-inflammatory capabilities.(Keerthirathna et al., 2025).

In this paper we have synthesize silver nanoparticles with the help of green algae as a reducing and capping agent. In the present study, aqueous extract of *Rhizoclonium* sp.(macroalgae) and AgNO<sub>3</sub> was utilised for the green synthesis of AgNPs. The *Rhizoclonium* -mediated synthesis of silver nanoparticle denoted as “Rhi-AgNPs” were characterized

for their physical properties like confirmation of quality, texture, porosity, morphology, shape and size of nanoparticles, using UV–Vis spectroscopy (Ultraviolet–visible spectroscopy), Fourier-Transform Infrared Spectroscopy (FTIR), and Scanning Electron Microscopy (SEM) techniques. Their biological functions were evaluated using antioxidant and antibacterial assays to determine potential uses in medicine, environmental remediation, and sustainable biotechnology –(Do et al., 2025).

**Material & Methods:** Algal sample – *Rhizoclonium* sp. Were collected from Phaphamau Prayagraj, Microscope – True Vision BLISCO India; Centrifuge machine -Remi R-4C, Centrifuge tube, Water bath – impact ICON phase -II, New Delhi-110020, Conical flask -100ml, 250ml; Borosil company, Thermometer, Pestle Mortar, Double Distilled Water, Sieve Plate, Butter Paper, Aluminum Foil, Pipette 2ml- Borosil company, Weighing machine, 0.01M AgNO<sub>3</sub> solution – LOBA CHEMIEPVT. Ltd. Company, Magnetic Stirrer – LABQUEST Borosil company, Spectrophotometer – SYSTRONICS AU- 2701 UV- Vis DOUBLE BEAM SPECTROPHOTOMETER, Cuvette, Refrigerated Centrifuge (8000rpm, 30min,30degree)- M-Labs company, Eppendorf tube 2ml (12in no.) -, Micropipette (20-200μl) – LABQUEST Borosil company, Beaker 500ml - Borosil company, Measuring cylinder (10ml) – Borosil company; purchased from – 1101, Crescenzo, G- Block, Opp. MCA Club, Bandra (E), Mumbai – 400051, Maharashtra, India, EPMA – JEOL JXA-8100 Electron Probe Micro Analyzer, Gloves were used.

**Collection of samples:** The green alga was collected by handpicking method as depicted from Phaphamau Prayagraj area, India. The green alga samples which were collected in large amounts were repeatedly surface-sterilized using sterile seawater followed by distilled water to get rid of extraneous materials such as sand, dust, and salt content as well(Maurya et al., 2023).

**Algal extract preparation:** The algal sample was crushed and milled into a fine powder form and then the powder sample was weighed by the weighing machine. The 1 gm of dry weight of algal biomass was added into the 100 ml of DDW (double Distilled Water). The sample was kept in the water bath at 100°C for 20 minutes. Then, the mixture was allowed to cool at room temperature, and then the mixture was filtered through the filter paper. After filtration the yellow-green color supernatant the algal extract was prepared(Maurya et al., 2023).

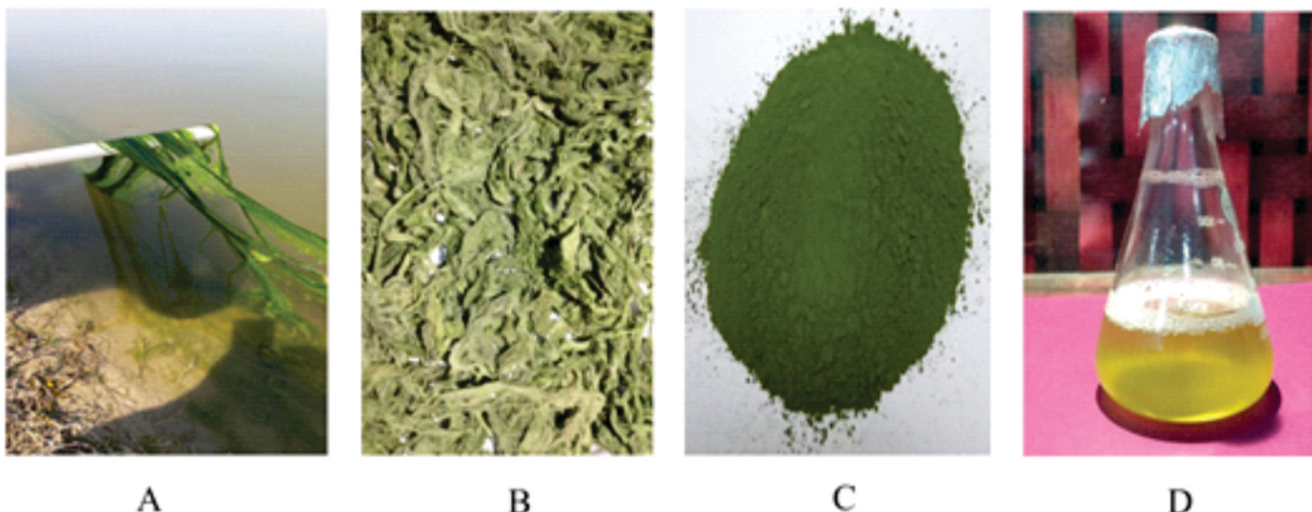


Figure 1: A Collection of samples; B Drying of sample; C Powdered sample; D Extract of sample

**Synthesis of nanoparticles:** The green synthesis of silver nanoparticles, 20 ml of algal extract was added in the 180 ml 0.001M AgNO<sub>3</sub> solution which is prepared using deionized water in a conical flask. To guarantee a full reduction of metal ions, the synthesis medium was heated gradually and indirectly to 30°C and agitated for 48 hours at 400 rpm using a magnetic stirrer. The experiment was set up and the synthesis medium was used in triplicate. In addition, the setup was done in a dark environment to reduce the rate of silver nitrate photoactivation. Additionally, a control setup devoid of the aqueous green alga extract was maintained. The change in color from yellowish-green to a concentrated cherry red color solution was observed as a visible confirmation of the formation of silver nanoparticles before the sample was subjected to further characterization process(Maurya et al., 2023).



Figure 2: Synthesis process of silver nanoparticles

**Characterization of nanoparticles:** The characterization of AgNPs were done by using different methods.

**UV- Vis spectrophotometer:** The primary characterization of silver nanoparticles was done by using UV-Vis spectrophotometer, was used to measure the wavelength between 300 and 700 nm to monitor the synthesis of silver nanoparticles using green algal extract with the intervals of 0 min (before heating), 15 min, 30 min, 1 h, 24 h and then followed by 48 h. The UV-visible reading was analyzed using the Origin Pro tool.

**Scanning Electron Microscope:** SEM analysis reveals both the size and shape of the nanoparticles. After a copper grid was covered with carbon and taken to the microscope, a small drop of powdered nanoparticles was placed on it. The silver nanoparticles' morphology was examined in further information, and high-resolution pictures of them were taken(Maurya et al., 2023).

**FTIR analysis:** FTIR analysis was used to identify the functional groups of the algal compounds responsible in the stabilization of AgNPs and the reduction of Ag<sup>+</sup> ions. The biosynthesized Rhi-AgNPs were combined with potassium bromide (Kbr) to form a pellet, which was then examined using an FTIR spectrophotometer to check for the presence of infrared spectral bands with a resolution of 4 cm<sup>-1</sup> and wavelengths between 4000 and 400 cm<sup>-1</sup> — (Choudhary et al., 2024).

**Result and discussion:** The synthesis of silver nanoparticles using green macroalga extract was validated by the characterization of the particles based on surface plasmon resonance (SPR) vibration detected at 445 nm. Up to 18 hours, the absorbance of the silver SPR band, which was located between 400 and 445 nm, increased steadily. The peak's widening indicated that the particles were widely distributed. Additionally, the longer the samples were treated, the higher the peak intensity.

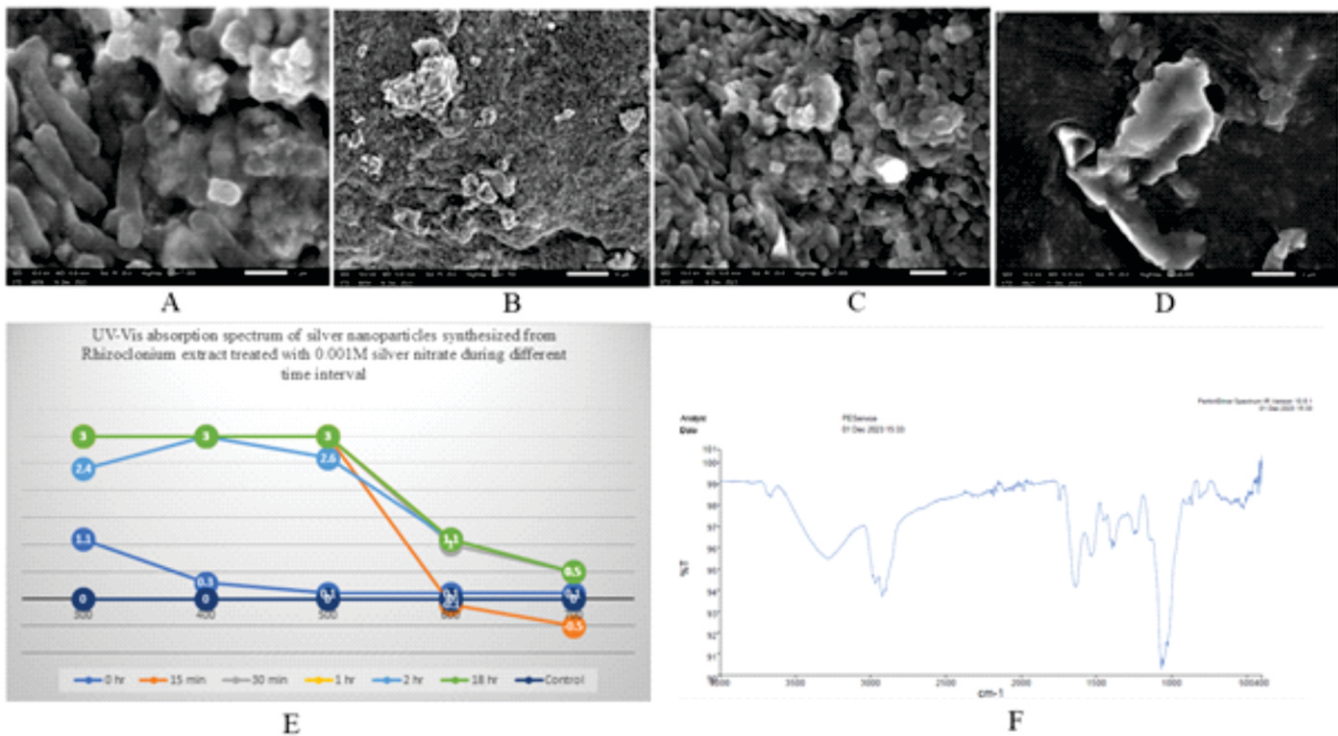


Figure 3: A-D images of scanning electron microscope; E graph of UV-Vis spectroscopy; F graph of Fourier Transform Infrared spectroscopy

The SEM image (figure 3A-D) in showing the high-density silver nanoparticles synthesized by treating *Rhizoclonium* sp. extract further confirmed the development of silver nanostructures. The silver nanoparticles seem to be distributed with an average mean size of 40-90 nm.

FTIR analysis revealed the chemical composition of the AgNPs. FTIR spectra of AgNPs (Figure. 3F) showed that several peaks appeared at 3250cm<sup>-1</sup>, 2980cm<sup>-1</sup>, 2950cm<sup>-1</sup>, 1650cm<sup>-1</sup>, 1535cm<sup>-1</sup>, 1400cm<sup>-1</sup>, 1250cm<sup>-1</sup>, and 1095cm<sup>-1</sup>. A broad band appears at 3250cm<sup>-1</sup> may refers to the stretching vibrations of the O-H group due to the adsorption of AgNPs, as it has a very high surface area. The bands at 2980 cm<sup>-1</sup> and 2950cm<sup>-1</sup> refers to the stretching of the C-H group of alkanes. Band 1650cm<sup>-1</sup> refers to the stretching vibration of C=O group of amides from protein stabilizing the AgNPs. The bands at 1535cm<sup>-1</sup> may refer to the C=O stretching vibration on the AgNPs surface that results from the acetyl group in trisodium acetate employed as the stabilizing agent. The appearance of peaks at 1400, 1250 and 1095 may refer to the O-H bending vibrations. The portion of the infrared spectrum ranging from 1500 to 400 cm<sup>-1</sup> is referred to the fingerprint region, which exhibits the unique characteristics for every compound.

AgNPs are a unique type of silver with a size of less than 100 nm. This small size allows for a high ratio of surface area to volume that exposes different biological activities (Ghannam et al., 2025). FTIR reveals the functional groups on the surface of AgNPs, which include -OH, C=O, and C-O. The acetyl groups that gave the AgNPs their stability during synthesis gave rise to these groups. SEM looked at the AgNPs' exterior morphology and verified that they were formed in a spherical shape with a highly porous surface.

## Conclusion:

AgNPs produced a stable green macroalga extract in this case. Therefore, for the traditional chemical and physical process, the green synthesis technique works effectively. Nanoparticles will be highly effective in the medical profession in the near future. In conclusion, *Rhizoclonium sp.* algae extract was used to create stable silver nanoparticles; hence, this novel green synthesis method could potentially replace traditional chemical synthesis methods due to its affordability, effectiveness, and environmentally friendly. FTIR, SEM analysis, and UV Vis spectroscopy were used to analyze the AgNPs. The nanoparticles produced by biosynthesis were less than 100 nm. The current study shows a biological method that is safe, inexpensive, and effective for a wide range of potential uses, including heavy metal removal, wound healing, cosmetics, antimicrobial, antioxidant, anticancer, drug delivery, and agriculture. Because of its effectiveness in removing heavy metals, the method may also be used to purify water.

## References:

1. Choudhary, S., Kumawat, G., Khandelwal, M., Khangarot, R. K., Saharan, V., Nigam, S., & Harish. (2024). Phyco-synthesis of silver nanoparticles by environmentally safe approach and their applications. *Scientific Reports*, 14(1), 9568. <https://doi.org/10.1038/s41598-024-60195-3>
2. de Moura, M. R., Mattoso, L. H. C., & Zucolotto, V. (2012). Development of cellulose-based bactericidal nanocomposites containing silver nanoparticles and their use as active food packaging. *Journal of Food Engineering*, 109(3), 520524. <https://doi.org/10.1016/j.jfoodeng.2011.10.030>
3. Do, J.-M., Hong, J. W., & Yoon, H.-S. (2025). Microalgae-mediated green synthesis of silver nanoparticles: A sustainable approach using extracellular polymeric substances from *Graesiella emersonii* KNUA204. *Frontiers in Microbiology*, 16. <https://doi.org/10.3389/fmicb.2025.1589285>
4. Ghannam, H. E., Khedr, A. I., El-Sayed, R., Ahmed, N. M., & Salaah, S. M. (2025). Oxidative stress responses and histological changes in the liver of Nile tilapia exposed to silver bulk and nanoparticles. *Scientific Reports*, 15(1), 15390. <https://doi.org/10.1038/s41598-025-97731-8>
5. Hamida, R. S., Ali, M. A., Alkhateeb, M. A., Alfassam, H. E., Momenah, M. A., & Bin-Meferij, M. M. (2024). Harnessing *Desmochloris edaphica* Strain CCAP 6006/5 for the Eco-Friendly Synthesis of Silver Nanoparticles: Insights into the Anticancer and Antibacterial Efficacy. *Molecules*, 29(16), Article 16. <https://doi.org/10.3390/molecules29163750>
6. Keerthirathna, L., Sigera, S., Rathnayake, M., Senarathne, A., Udesika, H., Kodikara, C., Sirimuthu, N. M., Samarakoon, K. W., Boudjelal, M., Ali, R., & Peiris, D. C. (2025). *Chnoospora minima* Polysaccharide-Mediated Green Synthesis of Silver Nanoparticles: Potent Anticancer and Antimicrobial Activities. *Biology*, 14(7), Article 7. <https://doi.org/10.3390/biology14070904>
7. Maurya, P., Soni, K., & Singh, S. (2023). BIOSYNTHESIS OF SILVER NANOPARTICLES USING FRESHWATER GREEN ALGA AND THEIR CHARACTERIZATION. 10(10).
8. Michalec, S., Nieckarz, W., Klimek, W., Lange, A., Matuszewski, A., Piotrowska, K., Hotowy, A., Kunowska-Słosarz, M., & Sosnowska, M. (2025). Green Synthesis of Silver Nanoparticles from *Chlorella vulgaris* Aqueous

- Extract and Their Effect on *Salmonella enterica* and Chicken Embryo Growth. *Molecules*, 30(7), Article 7. <https://doi.org/10.3390/molecules30071521>
9. Patil, S. P., Chaudhari, R. Y., & Nemade, M. S. (2022). Azadirachta indica leaves mediated green synthesis of metal oxide nanoparticles: A review. *Talanta Open*, 5, 100083. <https://doi.org/10.1016/j.talo.2022.100083>
  10. Qi, M., Wang, X., Chen, J., Liu, Y., Liu, Y., Jia, J., Li, L., Yue, T., Gao, L., Yan, B., Zhao, B., & Xu, M. (2023). Transformation, Absorption and Toxicological Mechanisms of Silver Nanoparticles in the Gastrointestinal Tract Following Oral Exposure. *ACS Nano*, 17(10), 88518865. <https://doi.org/10.1021/acsnano.3c00024>
  11. Ravindran, A., Chandran, P., & Khan, S. S. (2013). Biofunctionalized silver nanoparticles: Advances and prospects. *Colloids and Surfaces B: Biointerfaces*, 105, 342352. <https://doi.org/10.1016/j.colsurfb.2012.07.036>
  12. Vidyasagar, RajPatel, R., KumarSingh, S., & Singh, M. (2023). Green synthesis of silver nanoparticles: Methods, biological applications, delivery and toxicity. *Materials Advances*, 4(8), 18311849. <https://doi.org/10.1039/D2MA01105K>
  13. Zheng, K., Setyawati, M. I., Leong, D. T., & Xie, J. (2018). Antimicrobial silver nanomaterials. *Coordination Chemistry Reviews*, 357, 117. <https://doi.org/10.1016/j.ccr.2017.11.019>

# Exploring Conserved Motifs and Novel Functional Elements in Human Olfactory Receptors: A Phylogenetic and Domain-Based Analysis

Nidhi Dubey, Imlimaong Aier, Prabhat Tripathi, Ankish Arya,  
Amaresh Kumar Sahoo, Pritish Kumar Varadwaj\*

*Department of Applied Sciences, Indian Institute of Information Technology Allahabad, Prayagraj, 211015, Uttar Pradesh, India, \*Corresponding author: Email: [pritish@iiita.ac.in](mailto:pritish@iiita.ac.in)*

---

## Abstract

**H**uman olfactory receptors (ORs), part of the G protein-coupled receptor (GPCR) superfamily, detect diverse odorants and initiate olfactory signaling. Despite their sequence diversity, ORs share conserved motifs critical for structural and functional integrity. This study investigates the evolutionary and functional architecture of ORs through an integrated approach combining motif discovery and phylogenetic analysis. Conserved motifs were identified using the MEME Suite, and a phylogenetic tree was constructed via FastTree based on multiple sequence alignments. Motif mapping onto the evolutionary tree using iTOL revealed both highly conserved and potentially novel motifs, particularly within transmembrane domains linked to ligand binding and receptor activation. These results highlight evolutionary constraints on OR structure and function and provide a framework for future studies in sensory biology, artificial olfaction, and biomedical applications.

# Introduction

Olfaction is an ancient and essential sensory system that enables animals to detect chemical cues critical for survival. In humans, this function is mediated by olfactory receptors (ORs), the largest multigene family in the genome, comprising ~400 functional genes and over 600 pseudogenes (Niimura & Nei, 2003). These class A GPCRs feature a canonical seven-transmembrane (7TM) structure involved in signal transduction. Despite their diversity, many ORs retain conserved sequence motifs crucial for ligand binding and activation (Billesbølle et al., 2023; Choi et al., 2023). Conserved motifs serve as structural and functional signatures, maintaining receptor stability and mediating interactions with ligands (Krieger et al., 2022; Li et al., 2023). While some motifs are well-characterized, a systematic evolutionary mapping of conserved and novel motifs in human ORs remains limited. Phylogenetic analysis enables the identification of motif retention, divergence, and subfamily-specific features, shedding light on domain conservation and adaptive shifts.

To address this gap, we present a motif-guided phylogenetic and domain-level analysis of human ORs. Using computational motif discovery, tree construction, and domain annotation, this study aims to uncover conserved sequence elements and interpret their functional and evolutionary significance.

## **1. Materials and methods**

### **1.1. Dataset Collection and Preprocessing**

The dataset used in this study consisting of complete amino acid sequences of human ORs were retrieved from UniProt (Apweiler et al., 2004) and OlfactionBase (Sharma et al., 2022). Only full-length, protein-coding ORs were retained; truncated or low-confidence entries were excluded. Redundant sequences were removed using CD-HIT at 100% identity, resulting in a curated dataset of several hundred representative ORs spanning all major human subfamilies.

### **1.2. Motif Discovery Using MEME**

Conserved motifs within OR protein sequences were identified using MEME Suite v5.4.1 (Bailey & Elkan, 1994; Bailey et al., 2009), which applies expectation-maximization for *de novo* motif discovery. MEME was run in discriminative mode, set to identify up to 10 motifs with widths between 6 and 50 amino acids to capture both short functional and longer structural patterns. Outputs included position-specific scoring matrices (PSSMs), E-values, and site occurrence data, which were used to classify motifs into high, moderate, and low frequency categories based on their distribution across the dataset.

### **1.3. Phylogenetic Construction and Motif-Based Tree Annotation**

Multiple sequence alignment (MSA) of human OR proteins was performed using MUSCLE for accurate homologous alignment. The aligned sequences were analyzed with FastTree v2.1 (Price et al., 2010) to construct an approximately maximum-likelihood phylogenetic tree using the WAG substitution model, optimized via NNI and SPR, with node support estimated by the Shimodaira-Hasegawa (SH)-like test. The resulting Newick-format tree was visualized and annotated in iTOL (Letunic & Bork, 2007; 2019), where MEME-identified motifs were mapped as binary and quantitative features. This allowed visualization of domain-specific conservation and clade-level motif retention, revealing evolutionary patterns in OR structural organization.

## **2. Results and Discussion**

### **2.1. Identification, Frequency Classification, and Characterization of Conserved Motifs**

MEME Suite analysis of human OR sequences identified forty significant motifs varying in conservation, width, and frequency. Most were 15 residues long and mapped to transmembrane helices, while shorter motifs occurred in loop regions. Several motifs had extremely low E-values, with some aligning to canonical GPCR features such as the DRY motif in TM3 and NPxxY in TM7, both crucial for receptor stability and signaling (Billesbølle et al., 2023; Choi et al., 2023). Motifs were categorized by frequency: >80% as highly conserved, 30–60% as subfamily-specific, and <10% as potentially novel or lineage-specific. High-frequency motifs localized to TM3, TM6, and TM7, while rare motifs appeared in extracellular or clade-specific domains. These patterns highlight a layered architecture of conserved and variable elements in ORs, guiding future structural and functional exploration.

### **2.2. Phylogenetic Tree Construction and Clade Differentiation**

The phylogenetic tree constructed using FastTree displayed well-resolved branching patterns, capturing both deep evolutionary splits and recent diversification events. Class I and Class II ORs formed distinct clusters, confirming previously established lineage boundaries (Niimura & Nei, 2003). Subfamilies such as OR1, OR2, and OR10 showed tight internal clustering, indicating functional coherence and sequence conservation. FastTree's use of likelihood-based rearrangements resulted in an optimized topology supported by SH-like confidence values exceeding 0.85 for most nodes. These high support values added credibility to subsequent motif mapping and functional inferences drawn from the tree.

### **2.3. Motif Distribution and Domain-Level Insights**

The most striking observation emerged from the motif mapping onto the phylogenetic tree using iTOL. Highly conserved motifs were concentrated in basal lineages and in large clades like OR2 and OR4, suggesting that these receptors retain ancient functional elements vital for core olfactory processes. For instance, motifs in TM6 and TM7 were consistently observed across all Class II receptors but were absent in Class I receptors, hinting at functional divergence. The spatial localization of these conserved motifs across phylogenetic clades is illustrated in Fig. 1, where motif annotations highlight domain-specific evolutionary constraints and conserved sequence patterns. Conversely, several motifs unique to smaller clades, such as OR51 or OR11, appeared to be innovations correlating with niche adaptations. Some extracellular loop motifs were present only in a few sequences, potentially representing recently acquired features associated with narrow ligand specificity.

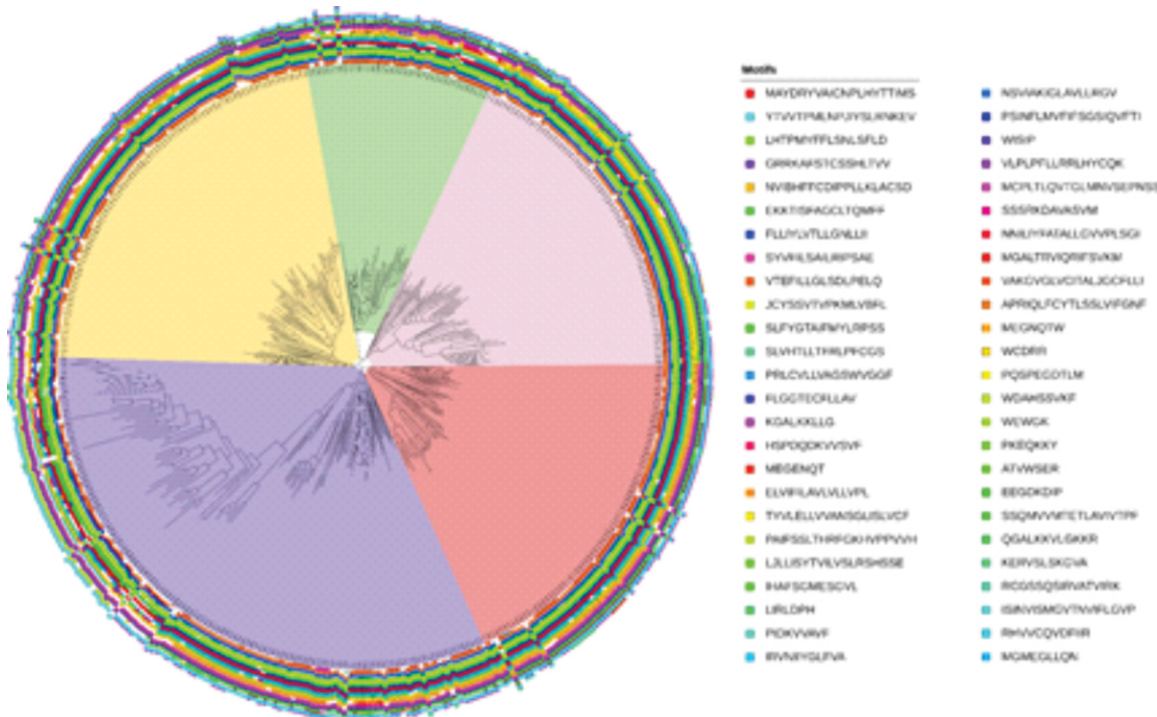


Fig. 1. Motif Mapping on the Phylogenetic Tree

#### 2.4. Functional and Evolutionary Implications

Motif mapping onto the phylogenetic tree revealed conserved domains under strong selective pressure, particularly in TM regions, suggesting their essential role in OR function. In contrast, motif variation in terminal branches may reflect adaptive divergence. Unique motifs in functionally characterized receptors like OR51E2 and OR2W1 imply that motif composition can predict receptor specialization. This connection between evolutionary conservation and receptor function is further supported by structural shifts in TM6 and TM7 during activation, as shown in Fig. 2.

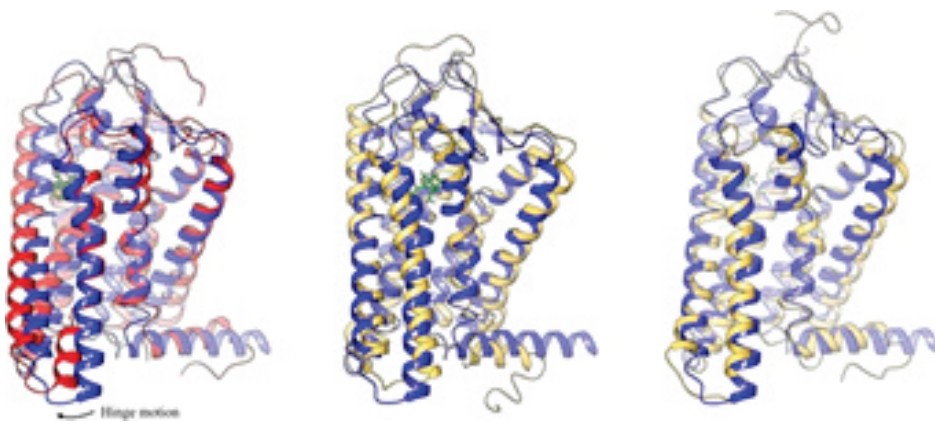


Fig. 2. TM6 and TM7 Structural Motions in ORs (OR11A1, OR51E2, OR2W1)

## Conclusion

This study offers an integrative framework for investigating the molecular evolution of human olfactory receptors by combining computational motif discovery with phylogenetic analysis. Using MEME, FastTree, and iTOL, we identified conserved sequence motifs and mapped them onto evolutionary lineages, revealing domain-specific and lineage-associated patterns particularly within transmembrane regions that likely influence receptor function. These findings contribute to evolutionary genomics by illustrating how large gene families retain core functionalities while diversifying, and have broader implications in biomedical research and synthetic biology. Conserved motifs may serve as biomarkers for olfactory disorders or as design elements in artificial olfaction systems. Future directions include extending this analysis to ORs from other species to uncover evolutionary constraints and validating motif functionality through structural and biochemical studies. Together, this work provides a foundation for future research in olfactory receptor biology and comparative genomics.

## References

1. Apweiler, R., Bairoch, A., Wu, C. H., Barker, W. C., Boeckmann, B., Ferro, S., Gasteiger, E., Huang, H., Lopez, R., Magrane, M., Martin, M. J., Natale, D. A., O'Donovan, C., Redaschi, N., & Yeh, L. S. (2004). UniProt: The universal protein knowledgebase. *Nucleic Acids Research*, 32(Database issue), D115-D119. <https://doi.org/10.1093/nar/gkh131>
2. Bailey, T. L., Boden, M., Buske, F. A., Frith, M., Grant, C. E., Clementi, L., ... & Noble, W. S. (2009). MEME Suite: Tools for motif discovery and searching. *Nucleic Acids Research*, 37(suppl\_2), W202-W208. <https://doi.org/10.1093/nar/gkp335>
3. Bailey, T. L., & Elkan, C. (1994). Fitting a mixture model by expectation maximization to discover motifs in biopolymers. *Proceedings of the Second International Conference on Intelligent Systems for Molecular Biology*, 2, 28-36.
4. Billesbølle, C. B., de March, C. A., van der Velden, W. J., Ma, N., Tewari, J., Del Torrent, C. L., ... & Manglik, A. (2023). Structural basis of odorant recognition by a human odorant receptor. *Nature*, 615(7953), 742-749. <https://doi.org/10.1038/s41586-023-05842-3>
5. Choi, C., Bae, J., Kim, S., Lee, S., Kang, H., Kim, J., ... & Choi, H. J. (2023). Understanding the molecular mechanisms of odorant binding and activation of the human OR52 family. *Nature Communications*, 14(1), 8105. <https://doi.org/10.1038/s41467-023-43896-4>
6. Krieger, G., Lupo, O., Wittkopp, P., & Barkai, N. (2022). Evolution of transcription factor binding through sequence variations and turnover of binding sites. *Genome Research*, 32(6), 1099-1111. <https://doi.org/10.1101/gr.276715.122>
7. Letunic, I., & Bork, P. (2007). Interactive Tree Of Life (iTOL): An online tool for phylogenetic tree display and annotation. *Bioinformatics*, 23(1), 127-128. <https://doi.org/10.1093/bioinformatics/btl529>
8. Letunic, I., & Bork, P. (2019). Interactive Tree Of Life (iTOL) v4: Recent updates and new developments. *Nucleic Acids Research*, 47(W1), W256-W259. <https://doi.org/10.1093/nar/gkz239>
9. Li, S., & Dohlman, H. G. (2023). Evolutionary conservation of sequence motifs at sites of protein modification. *Journal of Biological Chemistry*, 299(5), 104617. <https://doi.org/10.1016/j.jbc.2023.104617>
10. Niimura, Y., & Nei, M. (2003). Evolution of olfactory receptor genes in the human genome. *Proceedings of the National Academy of Sciences*, 100(21), 12235-12240. <https://doi.org/10.1073/pnas.1635157100>
11. Price, M. N., Dehal, P. S., & Arkin, A. P. (2010). FastTree 2-Approximately maximum-likelihood trees for large alignments. *PLOS ONE*, 5(3), e9490. <https://doi.org/10.1371/journal.pone.0009490>
12. Sharma, A., Saha, B. K., Kumar, R., & Varadwaj, P. K. (2022). OlfactionBase: A repository to explore odors, odorants, olfactory receptors and odorant-receptor interactions. *Nucleic Acids Research*, 50(D1), D678-D686. <https://doi.org/10.1093/nar/gkab795>

## Screening of Fresh Water Algal Extracts for their Antioxidant Potential

Khushaboo Soni, and Sanjay Singh\*

Department of Botany, CMP Degree College, Prayagraj, 211002, Uttar Pradesh, INDIA  
[ksmeera786@gmail.com](mailto:ksmeera786@gmail.com), [cmpsanjay@gmail.com](mailto:cmpsangaj@gmail.com)

---

### Abstract

Reactive oxygen species are associated with aging and can exacerbate a number of conditions, including cancer, atherosclerosis, arthritis, Parkinson's disease, and Alzheimer's disease. Antioxidants can help to some extent reduce the harmful effects of reactive oxygen species. Many bioactive metabolites are known to be obtained from algae, and different compounds have been developed using them to develop novel drugs by the pharmaceutical industry further. In this context, the antioxidant properties of *Hydrodictyon reticulatum* and *Rhizoclonium hieroglyphicum* that were isolated from the Ganga water in the Prayagraj district were examined. Three organic solvents (methanol, ethyl acetate, and hexane) were used to make extracts of the algae chosen for the study. The findings showed that *Rhizoclonium hieroglyphicum* extracts in methanol exhibited the highest antioxidant activity (93.6%), whereas hexane extracts exhibited the lowest (65.05%). The inhibitory activity of *Hydrodictyon reticulatum* was low with hexane (75.8%) and high with ethyl acetate (79.1%). Gallic acid has been used to compare the antioxidant activity of all the extracts. The primary goal of the study was to assess the antioxidant capacity of specific Ganga water algae and their potential for use as important pharmaceuticals in the medical field to treat illnesses brought on by reactive oxygen species. The antioxidant activity of the extracts was assessed using the DPPH free radical scavenging method.

---

**Keywords:** Algae, Antioxidant activity, Reactive Oxygen Species, Pharmaceutical industry, DPPH assay

## Introduction

Reactive oxygen species are linked to aging and can worsen various conditions, including cancer, atherosclerosis, arthritis, Parkinson's disease, and Alzheimer's disease. The human body constantly produces radicals and other reactive oxygen species, which are eliminated by the antioxidant defense system's enzymatic and non-enzymatic processes (Halliwell and Gutteridge 2015). Lipids, proteins, carbohydrates, and DNA can all be damaged by the disruption of "redox homeostasis" caused by insufficient antioxidant defense. One approach to reduce tissue damage may be to use medications with multiple protective properties, such as antioxidant activity, properties, such as antioxidant activity(Halliwell 1991).

Numerous studies conducted in recent years have demonstrated that plants with high levels of antioxidant phytochemicals can offer protection against a range of disorders(Urquiaga and Leighton 2000). Alternative medical treatment has grown in popularity in recent years. In India, Ayurveda and other indigenous medical systems frequently suggest dietary changes and traditional plant remedies. Additionally, the World Health Organization has advised assessing the effectiveness of plants in cases where there are insufficiently safe current medications.

Many researchers are interested in freshwater species as sources of bioactive chemicals due to their unique chemical structures, which are complicated and challenging to manufacture chemically, as well as their characteristics and molecular diversity. Bioactive substances such as carotenoids, polysaccharides, proteins, lipids, fatty acids, pigments, vitamins, polyphenols, and microelements are all abundant in green algae —(Borowitzka 2013). Nowadays, cosmeceutical products incorporate biological compounds from algae as additives with bioactive qualities. These cosmetics feature pharmacological or medicinal qualities, which set them apart from traditional cosmetics. Natural active chemicals have gained popularity recently as a substitute for manmade ones. Despite frequently exhibiting reduced activity, these substances are harmless and do not produce residues. Since the potential toxicity and health concerns of the antioxidants found in algal extracts are lower than those of synthetic antioxidants, they are particularly interesting for application in cosmetics and nutraceuticals (oral and topical formulations) -(Thomas and Kim 2013). Oxidative imbalance and pharmacological activity (anti-inflammatory and anti-tumor) have been closely related. By slowing oxidation, the antioxidant qualities of natural algal compounds can extend the shelf life of foods and cosmetics(Ashwini et al. 2013).

Apart from antioxidants, algae also contribute minerals, polysaccharides, and other bioactive substances that are utilized in the manufacturing of cosmetic items. This supports the use of algae as functional foods and/or dietary supplements to improve human health because of the beneficial effects they would have on preventing and/or treating diseases associated with oxidative stress -(Yuan and Walsh 2006). The purpose of this study is to assess the antioxidant activity of algal extracts for their use in bioactive applications.

## 1. Methods

### 1.1. Morphological characterization

The morphological characterisation of the macroalgal species was accomplished by utilizing a compound microscope (Blisco India, an ISO 900 2015) to examine the cells at various magnifications (10x, 20x, 40x, and 100x). Taxonomic reference guides were used to identify algal flora (Bellinger and Sigee 2010; Wehr et al. 2015).

### 1.2. Algal extract preparation

The crude extracts of the macroalgae species were prepared using methanol, ethyl acetate, and hexane, three different solvents with different levels of polarity. 20 ml of each solvent (100%) was mixed with 1 gm of macroalgal powder. The mixture was placed in a water bath (IMPACT ICON Instrument Company) for 20 minutes after being mixed for an hour at room temperature in a shaker (IMPACT ICON Instrument Company). Filter paper (Whatman filter paper grade 1) was used to filter the extract that included the supernatant. To recover the remaining chemicals from the sample, the leftover pellet was extracted twice more. After that, solvents were evaporated in a rotary evaporator (IMPACT ICON Instrument Company) to produce powdered material.

### 1.3. Antioxidant assays

The algal extract's ability to transfer hydrogen atoms or electrons was evaluated by bleaching a purple methanol solution of DPPH, with gallic acid serving as the reference. The reagent for this spectrophotometric assay is the stable radical DPPH. The procedure comprises measuring the decrease in DPPH (0.1mM) absorbance at the absorption maximum of 517 nm.

The stock solutions of the extracts were prepared in methanol, ethyl acetate, and hexane (1 mg/10 ml). Different concentrations (200, 150, 100, 50, 25, and 12.5 µg/ml) of extracts were taken in separate test tubes, and volumes were made up to 2 ml with different solvents. Now, 2ml of DPPH solution was added to each test tube and incubated in the dark for 30 minutes. The same procedure was followed for gallic acid as well. Later, optical absorbance was recorded at 517 nm using UV- Visible spectrophotometer (SYSTRONICS AU-2701). Methanol with DPPH was used as a control. All the samples were tested in triplicate. The formula used for the calculation of DPPH activity is:

$$\text{Inhibition (\%)} = \frac{A_{\text{control}} - A_{\text{test}}}{A_{\text{control}}} \times 100$$

here, A Control =OD of DPPH with methanol; A Test =OD of DPPH with extract

### 1.4. Statistical analysis

The mean of at least three replicates with standard error is used to display the results. The validity of the results was confirmed by evaluating for significant differences in the DPPH assay between the two algae species and three distinct organic solvents using analysis of variance (ANOVA<0.05) and Duncan's multiple range test (DMRT<0.05).

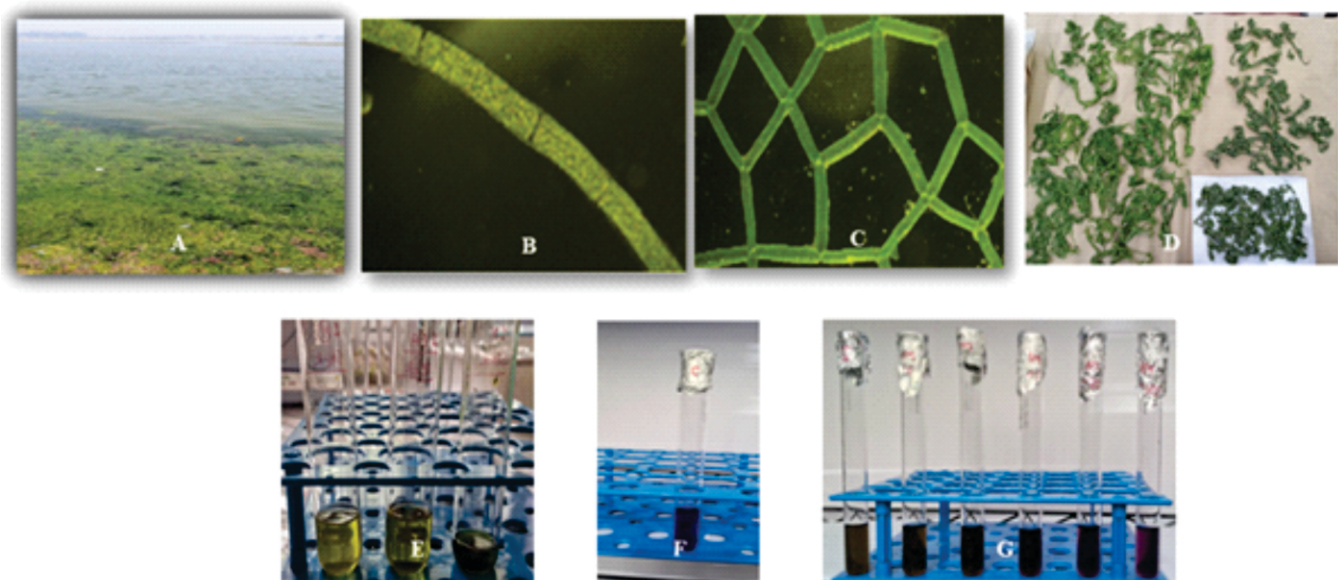


**Figure 1:** A. Collection site, B & C. Microscopic images of *Rhizoclonium hieroglyphicum* and *Hydrodictyon reticulatum*, D. Dried biomass of algae, E. Crude extract of algae, F. DPPH Stock, G. Algae extract with DPPH at different concentrations

## 2. Results

### 2.1. Morphological identification

A compound microscope was used for the methodical verification of the algae, and the samples were classified as *Rhizoclonium hieroglyphicum* and *Hydrodictyon reticulatum*, respectively (fig 1 B&C).

### 2.2. Antioxidant activity of green macroalgae extracts

Algal extracts of various solvents and their bioactive components were tested for antioxidant value using the DPPH assay. Methanolic extract of *Rhizoclonium hieroglyphicum* shows different antioxidant activity 93.40, 92.11, 91.40, 89.40, 88.46, 87.16 with different concentrations of 200, 150, 100, 50, 25 and 12.5 respectively (table 1) whereas methanolic extract of *Hydrodictyon reticulatum* shows different antioxidant activity 77.21, 74.30, 70.03, 69.13, 67.51 and 66.16 with different concentrations 200, 150, 100, 50, 25 and 12.5 respectively (table 2). Ethyl acetate extract of *Rhizoclonium hieroglyphicum* shows different antioxidant activity 82.63, 79.1, 77.63, 75.90, 75.34 and 74.95 with 200, 150, 100, 50, 25 and 12.5 respectively (table 1) whereas ethyl acetate extract of *Hydrodictyon reticulatum* shows 78.98, 78.03, 77.66, 71.04, 63.15 and 60.22 with different concentrations 200, 150, 100, 50, 25 and 12.5 respectively (table 2). Hexane extract of *Rhizoclonium hieroglyphicum* shows different antioxidant activity 65.09, 62.90, 55.30, 50.76, 48.83 and 45.96 with different concentrations of 200, 150, 100, 50, 25 and 12.5 respectively (table 1) whereas hexane extract of *Hydrodictyon reticulatum* shows 75.90, 75.36, 73.98, 73.16, 71.64 and 70.08 with different concentrations 200, 150, 100, 50, 25 and 12.5 respectively (table 2). Gallic acid is used as a standard that shows maximum antioxidant activity of 95.58.

**Table 1.** Antioxidant activity of *Rhizoclonium hieroglyphicum*

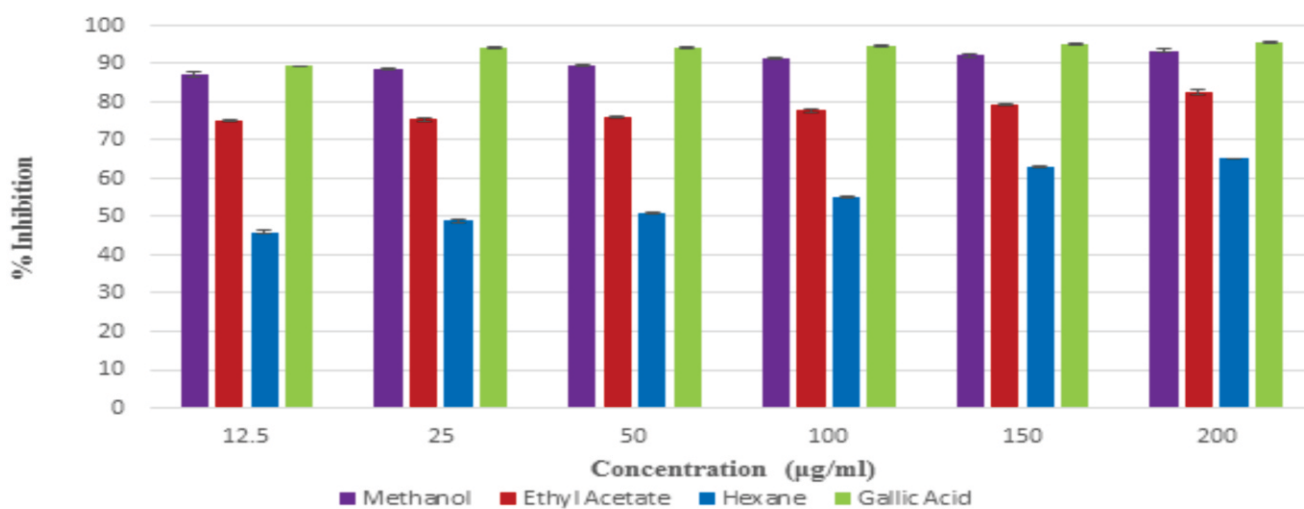
Concentration ( $\mu\text{g/ml}$ )	Methanol (%)	Ethyl Acetate (%)	Hexane (%)	Gallic Acid (%)
12.5	87.16 $\pm$ .612	74.95 $\pm$ .307	45.96 $\pm$ .4258	9.26 $\pm$ .185
25	88.46 $\pm$ .317	75.34 $\pm$ .571	48.83 $\pm$ .284	94.05 $\pm$ .124
50	89.40 $\pm$ .173	75.90 $\pm$ .230	50.76 $\pm$ .234	94.22 $\pm$ .171
100	91.40 $\pm$ .321	77.63 $\pm$ .384	55.30 $\pm$ .230	94.72 $\pm$ .318
150	92.11 $\pm$ .331	79.1 $\pm$ .251	62.90 $\pm$ .251	95.12 $\pm$ .088
200	93.40 $\pm$ .643	82.63 $\pm$ .606	65.09 $\pm$ .124	95.58 $\pm$ .148

The data was statistically tabulated and tested at 0.05 level of significance (ANOVA and Duncan's multiple range test) where n=3

**Table 2.** Antioxidant activity of *Hydrodictyon reticulatum*

Concentration ( $\mu\text{g/ml}$ )	Methanol (%)	Ethyl Acetate (%)	Hexane (%)	Gallic Acid (%)
12.5	66.16 $\pm$ .161	60.22 $\pm$ .179	70.08 $\pm$ .135	89.26 $\pm$ .185
25	67.51 $\pm$ .148	63.15 $\pm$ .239	71.64 $\pm$ .398	94.05 $\pm$ .124
50	69.13 $\pm$ .131	71.04 $\pm$ .193	73.16 $\pm$ .190	94.22 $\pm$ .171
100	70.03 $\pm$ .137	77.66 $\pm$ .233	73.98 $\pm$ .182	94.72 $\pm$ .318
150	74.30 $\pm$ .288	78.03 $\pm$ .101	75.36 $\pm$ .240	95.12 $\pm$ .088
200	77.21 $\pm$ .182	78.98 $\pm$ .171	75.90 $\pm$ .236	95.58 $\pm$ .148

The data was statistically tabulated and tested at 0.05 level of significance (ANOVA and Duncan's multiple range test) where n= 3

**Figure 2.** *Rhizoclonium* species showing antioxidant activity with three different organic solvents. Values are expressed as mean  $\pm$  SE (n=3)

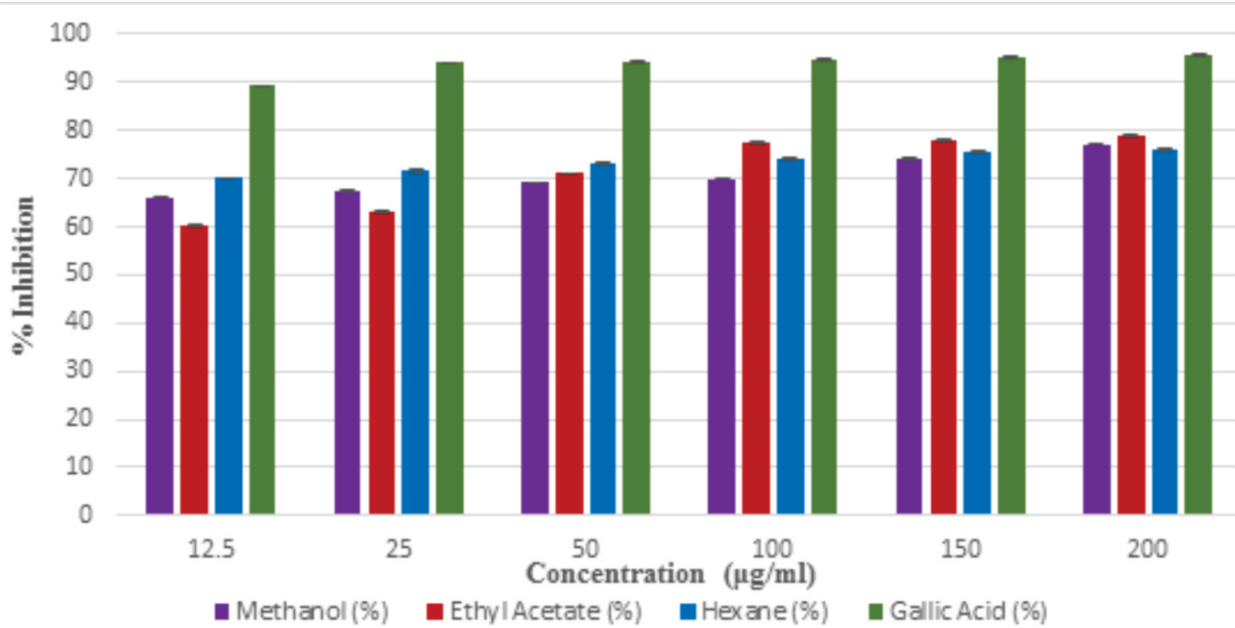


**Figure 3.** *Hydrodictyon reticulatum* showing antioxidant activity with three different organic solvents. Values are expressed as mean  $\pm$  SE ( $n=3$ )

## Discussion

*Rhizoclonium* species' methanolic extract had more antioxidant activity, exhibiting 93.40% inhibition (fig 2), in contrast to *Hydrodictyon* species' methanolic extract, which showed 77.21% inhibition (fig 3). Likewise, the ethyl acetate extract of *Rhizoclonium* species showed more antioxidant activity (82.63% inhibition) (fig 2) compared to *Hydrodictyon* species (78.98% inhibition) (fig 3). *Hydrodictyon* species, on the other hand, demonstrated antioxidant activity in the hexane extract with 75.90% inhibition (fig 3), whereas *Rhizoclonium* species demonstrated 65.09% inhibition (fig 2). Gallic acid was used as the reference and showed the greatest antioxidant activity (95.66% inhibition) (fig 2&3) when all extracts were tested against it.

Both of the green macroalgae include common bioactive compounds, including n-Tetracosanol-1, Hexadecanoic acid methyl ester, Heptadecane, 8-methyl-, Benzenepropanoic acid, 3,5-bis(1,1-dimethylethyl)-4-hydroxy methyl ester, 9-Octadecene, (E)-, Squalene, 1-Hexadecanol, responsible for antioxidant activity (Soni et al. 2023). Methanol, a polar solvent, has been shown to have the highest antioxidant activity in *Rhizoclonium* species, suggesting that this species mostly comprises polar molecules with good inhibitory capability. A good inhibitory capability with ethyl acetate and hexane was also demonstrated by *Rhizoclonium* species, suggesting that this species also includes certain non-polar and less polar chemicals that are responsible for antioxidant action. The finding that the *Hydrodictyon* species with ethyl acetate had the highest inhibitory capability compared to the other two solvents suggests that this species contains more less polar compounds than polar ones.

Green macroalgae are an underutilized source of phenolic compounds that have a lot of promise for use in industry or medicine. In this study, we investigated the bioactive potential of extracts made from two freshwater macroalgae, *Hydrodictyon reticulatum* and *Rhizoclonium hieroglyphicum*, with an emphasis on their antioxidant properties. The variations in antioxidant potential may be explained by the polarity of the phenolic compounds that each species produces. There are several intricate ways that antioxidant molecules can work (Frankel and Meyer 2000).

We suggest that phenolic compounds found in freshwater macroalgae are likely very effective antioxidants against free radicals (peroxyl or hydroxyl radicals) due to their low redox potential, since the reducing power assay relies on the redox potential of the compounds present in a sample (Zhu et al. 2002). Various naturally occurring substances with antioxidant properties have been documented to impact both clinical and biological processes (Karadeniz et al. 2015). To further understand the mechanisms of action of the biologically active compounds found in freshwater macroalgae, future research should isolate, identify, and test each one independently.

## Conclusions

The great nutritional value and wide range of uses in food, energy, medicine, cosmetics, and biotechnology make macroalgae a very promising resource for the future. *Rhizoclonium hieroglyphicum* and *Hydrodictyon reticulatum* extracts were analyzed to assess their antioxidant activity in order to investigate the potential of macroalgae. According to the previously described experimental research, the results of this study are highly significant and might be used as crucial pharmaceutical medications to treat illnesses caused by reactive oxygen species.

## References

1. Ashwini, G.C., Vaishali, S.K., Ram, S.S., Ganesh, O.B., and Digambar, N.N. 2013. Role of nutraceuticals in various diseases: A comprehensive review. Available from <https://www.cabidigitallibrary.org/doi/full/10.5555/20133281651> [accessed 26 July 2025].
2. Bellinger, E.G., and Sigee, D.C. 2010. Freshwater Algae: Identification and Use as Bioindicators John Wiley & Sons. Ltd. 1th edition. pp 284.
3. Borowitzka, M.A. 2013. High-value products from microalgae their development and commercialisation. Journal of applied phycology 25(3): 743756. Springer.
4. Frankel, E.N., and Meyer, A.S. 2000. The problems of using one-dimensional methods to evaluate multifunctional food and biological antioxidants. J. Sci. Food Agric. 80(13): 19251941. doi:10.1002/1097-0010(200010)80:13<1925::AID-JSFA714>3.0.CO;2-4.
5. Halliwell, B. 1991. Drug Antioxidant Effects: A Basis for Drug Selection? Drugs 42(4): 569605. doi:10.2165/00003495-199142040-00003.
6. Halliwell, B., and Gutteridge, J.M.C. 2015. Free Radicals in Biology and Medicine. Oxford University Press.
7. Karadeniz, F., Ahn, B.-N., Kim, J.-A., Seo, Y., Jang, M.-S., Nam, K.-H., Kim, M., Lee, S.-H., and Kong, C.-S. 2015. Phlorotannins suppress adipogenesis in pre-adipocytes while enhancing osteoblastogenesis in pre-osteoblasts. Arch. Pharm. Res. 38(12): 21722182. doi:10.1007/s12272-015-0637-0.
8. Soni, K., Maurya, P., and Singh, S. 2023. Bioactive compounds from fresh water green macro algae of Ganga water. J Pharmacogn Phytochem 12(5): 369385. AkiNik Publications. doi:10.22271/phyto.2023.v12.i5d.14750.
9. Thomas, N.V., and Kim, S.-K. 2013. Beneficial effects of marine algal compounds in cosmeceuticals. Marine drugs 11(1): 146164. MDPI.
10. Urquiaga, I., and Leighton, F. 2000. Plant Polyphenol Antioxidants and Oxidative Stress. Biological Research 33(2): 5564. Sociedad de Biología de Chile. doi:10.4067/S0716-97602000000200004.
11. Wehr, J.D., Sheath, R.G., and Kociolek, J.P. 2015. Freshwater algae of North America: ecology and classification. In 2nd edition. Elsevier/AP, Academic Press is an imprint of Elsevier, Amsterdam Boston.
12. Yuan, Y.V., and Walsh, N.A. 2006. Antioxidant and antiproliferative activities of extracts from a variety of edible seaweeds. Food and chemical toxicology 44(7): 11441150. Elsevier.
13. Zhu, Q.Y., Hackman, R.M., Ensunsa, J.L., Holt, R.R., and Keen, C.L. 2002. Antioxidative Activities of Oolong Tea. J. Agric. Food Chem. 50(23): 69296934. doi:10.1021/jf0206163.

## Genetic Determinants of *Helicobacter pylori* Adaptation and Survival mechanism: Prospects for Therapeutic Targeting

Meghna Agrawal, Diksha Singh, Ashutosh Mani\*

Department of Biotechnology, Motilal Nehru National Institute of Technology Allahabad, Prayagraj -211004, India

**\*Corresponding author**

Dr.Ashutosh Mani, Ph.D

Department of Biotechnology

Motilal Nehru Institute of Technology (Allahabad)

Prayagraj-211004

Phone: +91-945534251

Email: [amani@mnnit.ac.in](mailto:amani@mnnit.ac.in)

**Affiliation:** <sup>1</sup>Department of Biotechnology, Motilal Nehru National Institute of Technology Allahabad, Prayagraj - 211004, India

**Funding:** This research did not receive any specific grant from the funding agencies in the public, commercial and not-for-profit sectors.

**Compliance with ethical standards: NA**

**Conflict of Interest :** The authors declare that they have no known competing financial interests or personal relationships that could have appeared to influence the work reported in this paper

---

### Abstract

The global prevalence of *Helicobacter pylori* infection exceeds more than half of the world's population. It significantly contributes to the development of gastritis, peptic ulcer disease, and gastric carcinoma. Increasing *H. pylori* antibiotic resistance, and its remarkable ability to colonize and thrive in the hostile gastric environment, has made the eradication regimes against the pathogen ineffective. Targeting the survival and adaption proteins might offer advantages over available antimicrobials. This review focuses on the screened *H. pylori* genes (flaA, flab, ureA, ureB, mutY, mutS, recA, dps, hsp60 and dnaK) related to adaptation and survival mechanisms. The genes are associated with flagellar motility, urease activity, DNA repair, oxidative stress and heat shock that can also be considered as therapeutic target against the pathogen.

## Introduction

**H**elicobacter pylori are a micro-aerophilic, spiral-shaped Gram-negative bacterium that lives in the human stomach.<sup>1</sup> *H. pylori* thrive in the stomach's acidic environment by producing large amounts of urease to neutralize acid.<sup>2</sup> It can penetrate and adhere to gastric epithelial cells using flagella and other specialized proteins.<sup>3</sup> It also injects effector proteins like CagA and VacA to influence host signalling.<sup>4</sup> With over half the world's population infected and rising antibiotic resistance, understanding its biology remains critical for developing novel therapies.<sup>5</sup>

Conventional treatments use proton-pump inhibitors along with multiple antibiotics. However, the growing resistance to clarithromycin and metronidazole is now lowering eradication rates worldwide.<sup>6</sup> Studying on treatments focusing on the survival and adaptation methods of bacteria, rather than their viability, the treatments might reduce the pressure for resistance; protect beneficial flora of the stomach, and lower inflammation.<sup>7</sup> Additionally, by disrupting the key proteins needed for colonization and virulence, we might eradicate *H. pylori*, attenuate disease progression, or work effectively with lower doses of antibiotics.

In this knowledge-based study, we explored the UniProt database to systematically screen *H. pylori* genes that code for proteins with known or predicted virulence-related functions. We focused on the gene, involved in acid resistance, epithelial adhesion, and evading host immune responses. Those genes were screened in which literature evidence confirms that the genes are involved in facilitating bacterial adaptation and survival under gastric conditions, driving chronic infection and mucosal damage. Building on this functional understanding, we prioritized candidates that are essential for living of *H. pylori* in the stomach and also have favourable drug-target properties, such as extracellular localization, enzymatic activity, and minimal homology to human proteins. This two-step filtering process provided a focused list of targets for developing new treatments aimed at disrupting the main ways how *H. pylori* survives and causes disease in the stomach. The list of targets is provided in the Box1. The detailed role of genes related to adaption mechanism during *H. pylori* pathogenesis is mentioned below:

### Flagellar Motility: flaA and flaB

The movement of *Helicobacter pylori* rely on flagellin components, FlaA and FlaB. FlaA subunit makes up most of the filament shaft, which is essential for motility. FlaB is the smaller subunit at the tip of the filament; it brings rigidity and helps with torque transmission. Thus, FlaA and FlaB allows the bacterium to move through the thick gastric mucus layer like a corkscrew. It is reported, when either flaA or flaB is genetically removed, motility stops and the bacterium cannot colonize in animal models. This shows that both components are crucial for colonization.<sup>3,8</sup>

The study reports, expression of the flagellar genes gets down-regulated before the bacterium changes to a coccoid form. Both the flagellar genes are transcribed from σ<sup>54</sup>-type (RpoN) promoters, which allows them to be turned up in response to environmental factors like acid stress, temperature changes, and nutrient levels. Post-transcriptional control is managed by regulator CsrA. The repression of the translation of flaA mRNA, lifts when the flagellar assembly factor FliW2 binds to CsrA, ensuring regulated expression of FlaA proteins.

In terms of structure, FlaA and FlaB monomers have conserved N and C-terminal domains that help them polymerize into a helical filament. They also feature a central hypervariable domain (residues ~450–500) that is exposed on the surface and provokes strong immune responses. The immunogenicity of flaA and flaB makes it a key target for diagnostic and therapeutic efforts. By leveraging these structural and regulatory features, several anti-virulence

strategies have emerged against the genes. It is reported, small-molecule inhibitors, like metal chelators and ATP-competitive compounds, can stop polymerization or destabilize the assembled filaments. Moreover, natural products, such as Triphala, can lower flaA and flaB expression, harm flagellar structure, and reduce bacterial movement in *in-vitro* setup. Additionally, ammonium compounds, like cetylpyridinium chloride, can also decrease flaA and flaB transcripts, disrupt flagellar assembly, and hinder *H. pylori* survival.

Furthermore, monoclonal antibodies and synthetic peptides aimed at the central hyper-variable domain or polymerization interfaces can prevent subunit association and filament growth. Vaccine development has focused on the immune-dominant central domain of FlaA. Multi-epitope constructs have triggered strong IgG and IgM responses with over 90% sensitivity and specificity in serodiagnosis. Combination vaccines containing FlaA, FlaB, and other adhesins like HpaA and Omp18 have shown protection against colonization in mouse models.

Lastly, new nucleic acid approaches, such as antisense oligonucleotides and CRISPR interference delivered through lipid nanoparticles, can precisely knock down flaA and flaB transcripts in the gastric mucosa. By focusing on both the structural polymerization machinery and the complex networks that regulate flagellin expression, these strategies hold promise for immobilizing *H. pylori*, improving bacterial clearance through gastric movement, and reducing harmful persistence without the strong selective pressure seen with traditional antibiotics.

### **1. Urease Activity: ureA and ureB**

*Helicobacter pylori* urease is a nickel-dependent metalloenzyme consist of two structural subunits, UreA ( $\alpha$ -subunit, ~61.7 kDa) and UreB ( $\beta$ -subunit, ~26.5 kDa). These subunits together form a dodecameric complex (UreA-UreB), which is anchored in the periplasm and outer membrane. Each active site has a binuclear  $\text{Ni}^{2+}$  center, coordinated by conserved histidines and a carbamylated Lys219. This center catalyzes the hydrolysis of urea into ammonia and carbon dioxide. Thus, it buffers the periplasmic pH and allows the bacteria to survive in the stomach's acidic environment. The expression of ureA and ureB increases under low pH conditions through the ArsRS two-component system. Moreover, urease maturation is a multistep process that requires accessory proteins (UreE, UreF, UreG, UreH), the pH-gated urea channel, and Urel for nickel insertion and proper folding. In addition, post-translational modifications and interactions with chaperones help to maintain enzyme stability. Functionally, urease activity not only neutralizes gastric acid to support initial colonization and biofilm formation but also produces cytotoxic ammonia. This substance disrupts epithelial tight junctions and triggers inflammation, which is linked to disease severity in clinical isolates. Therapeutic strategies to target urease involve active-site chelators like acetohydroxamic acid, flap-region and allosteric inhibitors such as baicalin and ebselen, and methods to disrupt UreG-mediated nickel loading. There are also structure-based virtual screening scaffolds with sub-micromolar potency and siRNA constructs that achieve over 99% urease knockdown *in vitro*. Given its crucial role in acid resistance and its absence in human cells, UreA/UreB urease is a key antivirulence target for developing next-generation *H. pylori* therapies.<sup>2,9</sup>

### **2. DNA Repair and Oxidative Stress Defense: mutY, mutS, recA, and dps**

*Helicobacter pylori* survives the oxidative burst from its host by using four linked DNA-maintenance systems: MutY, MutS, RecA, and Dps. MutY, the 8-oxoG:A glycosylase, it removes adenines that are mispaired with oxidized guanines (8-oxoG), which helps prevent G:C to T:A changes. Compounds that inhibit its active site or those that bind to its essential [4Fe-4S] cluster could lock MutY onto DNA and cause lethal mutagenesis.<sup>10</sup> MutS detects base mismatches and Holliday junctions.<sup>11</sup> It can be knocked out by ATP-binding pocket antagonists, stapled peptides that disrupt its dimer interface or small molecules that block its DNA-binding groove. This inhibition overwhelms the cell

with unresolved errors. RecA forms nucleoprotein filaments on single-stranded DNA, driving homologous recombination and SOS induction.<sup>12</sup> Non-hydrolyzable ATP analogs designed for its P-loop, intercalators that target protomer-protomer contacts, SOS-suppressing stabilizers of its inactive form, or natural-product scaffolds can prevent filament assembly and make bacteria more sensitive to genotoxic antibiotics.<sup>5</sup> Lastly, the ferritin-like Dps dodecamer compacts the genome and oxidizes Fe<sup>2+</sup> to Fe<sup>3+</sup>.<sup>13</sup> High-affinity ferroxidase chelators, ligands that disrupt oligomers, or anionic polymers that cover its DNA-binding surface expose the chromosome to Fenton-mediated radicals. Combining each of these inhibitors with ROS-generating antibiotics, such as β-lactams plus H<sub>2</sub>O<sub>2</sub>, increases oxidative stress, overwhelms repair pathways, and works well with conventional antimicrobials.

### 3. Heat Shock and Chaperone Proteins: hsp60 and dnaK

*Helicobacter pylori* relies on two central chaperones, Hsp60 (a GroEL homolog) and DnaK (an Hsp70 homolog), to handle the extreme stresses of the gastric environment, stabilize virulence factors, and maintain protein balance. Hsp60 forms oligomeric rings that trap unfolded proteins in its central cavity. This process prevents the aggregation of acid-damaged proteins and helps assemble multi-meric complexes like urease and the type IV secretion pilus.—<sup>14</sup> It also appears on the bacterial surface, where it may help the bacteria stick to epithelial cells and influence the host's immune response. DnaK, with its ATP-hydrolyzing and substrate-binding domains, works with co-chaperones DnaJ and GrpE to rescue mis-folded proteins that build up under stress from acid, oxidative damage, or antibiotics.—<sup>15</sup> It also prepares proteins for transport. Together, these chaperones protect *H. pylori* from damaging stresses, improve acid tolerance, and maintain the function of secreted factors that drive inflammation and cancer development. Their essential roles and unique structures compared to human versions make them appealing targets for anti-virulence drugs. Small-molecule inhibitors designed after Hsp90 ligands, like geldanamycin analogs, can be modified to fit into Hsp60's ATP-binding pocket or disrupt its inter-ring connections.—<sup>14</sup> This would keep the chaperone in an inactive state. Similarly, DnaK inhibitors such as myricetin derivatives or di-hydro-pyrimidines can interrupt its ATP-hydrolysis cycle or block the substrate-binding site, collapsing the entire DnaK-DnaJ-GrpE system. By disrupting these folding machines, we can destabilize several stress-response pathways, make *H. pylori* more vulnerable to acid and antibiotics, and lessen its ability to secrete key virulence factors by applying less selective pressure for traditional resistance. Recent advancements in high-resolution structures of *H. pylori* Hsp60 and DnaK, along with in silico docking and fragment-based screening, now allow for the clever design of chaperone inhibitors that specifically target *H. pylori*. This approach holds promise for disarming *H. pylori*'s survival strategies and enhancing current treatments.

## Conclusion

Disarming *H. pylori* by targeting its adaptation and survival machinery represents a promising strategy to overcome rising antibiotic resistance. The article reviewed flagellar motility, acid neutralization, stress response, DNA repairs, adhesins genes that offer multiple intervention points. Rational design of small molecules, biologics, and vaccines against these determinants could usher in a new generation of therapeutics that attenuate pathogenesis with minimal collateral damage to the host microbiota. Delivery of biologics to the gastric mucosa must overcome acidic degradation and mucus diffusion barriers. Advances in single-cell transcriptomics and structural biology will refine target selection. Integration of computational docking, medicinal chemistry, and in vivo infection models can accelerate lead optimization. Collaborative efforts between microbiologists, structural biologists, and pharmacologists are critical to translate these targets into clinical candidates. Continued structural characterization, high-throughput screening, and innovative delivery methods will be pivotal to bringing these prospective targets from bench to bedside.

## References:

1. Malfertheiner P, Camargo MC, El-Omar E, et al. Helicobacter pylori infection. *Nat Rev Dis Primers.* 2023;9(1):1-24. doi:10.1038/s41572-023-00431-82.
2. Debowski AW, Walton SM, Chua EG, et al. Helicobacter pylori gene silencing in vivo demonstrates urease is essential for chronic infection. *PLoS Pathog.* 2017;13(6):e1006464. doi:10.1371/journal.ppat.10064643.
3. Gu H. Role of Flagella in the Pathogenesis of Helicobacter pylori. *Curr Microbiol.* 2017;74(7):863-869. doi:10.1007/s00284-017-1256-44.
4. Costa DM da, Pereira E dos S, Rabenhorst SHB. What exists beyond cagA and vacA? Helicobacter pylori genes in gastric diseases. *World Journal of Gastroenterology : WJG.* 2015;21(37):10563. doi:10.3748/wjg.v21.i37.10563.
5. Bui PH, Cao TNM, Tran TT, Matsumoto T, Akada J, Yamaoka Y. Identification of genetic determinants of antibiotic resistance in Helicobacter pylori isolates in Vietnam by high-throughput sequencing. *BMC Microbiology.* 2025;25(1):264. doi:10.1186/s12866-025-03990-w
6. Zagari RM, Bianchi-Porro G, Fiocca R, Gasbarrini G, Roda E, Bazzoli F. Comparison of 1 and 2 weeks of omeprazole, amoxicillin and clarithromycin treatment for Helicobacter pylori eradication: the HYPER Study. *Gut.* 2007;56(4):475-479. doi:10.1136/gut.2006.102269
7. Yu Y, Zhu S, Li P, Min L, Zhang S. Helicobacter pylori infection and inflammatory bowel disease: a crosstalk between upper and lower digestive tract. *Cell Death Dis.* 2018;9(10):1-12. doi:10.1038/s41419-018-0982-2
8. Tian W, Jia Y, Yuan K, et al. Serum antibody against Helicobacter pylori FlaA and risk of gastric cancer. *Helicobacter.* 2014;19(1):9-16. doi:10.1111/hel.12095
9. Olivera-Severo D, Uberti AF, Marques MS, et al. A New Role for Helicobacter pylori Urease: Contributions to Angiogenesis. *Front Microbiol.* 2017;8. doi:10.3389/fmicb.2017.01883
10. Huang S, Kang J, Blaser MJ. Antimutator Role of the DNA Glycosylase mutY Gene in Helicobacter pylori. *J Bacteriol.* 2006;188(17):6224-6234. doi:10.1128/JB.00477-06
11. Wang G, Alamuri P, Humayun MZ, Taylor DE, Maier RJ. The Helicobacter pylori MutS protein confers protection from oxidative DNA damage. *Molecular Microbiology.* 2005;58(1):166-176. doi:10.1111/j.1365-2958.2005.04833.x
12. Amundsen SK, Fero J, Hansen LM, et al. Helicobacter pylori AddAB helicase-nuclease and RecA promote recombination-related DNA repair and survival during stomach colonization. *Molecular Microbiology.* 2008;69(4):994-1007. doi:10.1111/j.1365-2958.2008.06336.x
13. Ceci P, Mangiarotti L, Rivetti C, Chiancone E. The neutrophil-activating Dps protein of Helicobacter pylori, HP-NAP, adopts a mechanism different from Escherichia coli Dps to bind and condense DNA. *Nucleic Acids Res.* 2007;35(7):2247-2256. doi:10.1093/nar/gkm077
14. Guo L, Yang H, Tang F, et al. Oral Immunization with a Multivalent Epitope-Based Vaccine, Based on NAP, Urease, HSP60, and HpaA, Provides Therapeutic Effect on *H. pylori* Infection in Mongolian gerbils. *Front Cell Infect Microbiol.* 2017;7:349. doi:10.3389/fcimb.2017.00349
15. Donahue JP, Israel DA, Torres VJ, Necheva AS, Miller GG. Inactivation of a Helicobacter pylori DNA methyltransferase alters dnaK operon expression following host-cell adherence. *FEMS Microbiology Letters.* 2002;208(2):295-301. doi:10.1111/j.1574-6968.2002.tb11097.x

## Molecular Cloning and Expression of a Recombinant Laccase Gene in *Escherichia coli*

Manasee Wadgaonkar, Vidya Tale\*, Shamim Shaikh, Shraddha Jaiswal

Rajiv Gandhi Institute of IT and Biotechnology, Bharati Vidyapeeth Deemed to be University,  
Pune, Maharashtra-India 411046

\*Corresponding author: [vidya.tale@bharatividyapeeth.edu](mailto:vidya.tale@bharatividyapeeth.edu)

---

### Abstract

Laccase gene (*lac2*) from *Coriolopsis caperata* was successfully cloned and expressed in *E. coli* BL21. The recombinant enzyme (~55 kDa) was confirmed by SDS-PAGE and LC-MS/MS. It effectively degraded bromophenol blue dye by 76.2% in 36 hours and exhibited catalytic activity using ABTS as substrate. Molecular docking indicated stable binding with ABTS. These results highlight the potential of the recombinant laccase for industrial use and future enzyme optimization.

---

### Introduction

Laccases (EC 1.10.3.2), a class of multicopper oxidases, have acquired significant attention due to their ability to catalyse the oxidation of a wide range of phenolic and non-phenolic substrates using molecular oxygen, producing water as the sole byproduct. (Baldrian, P. 2006) This eco-friendly catalytic mechanism has enabled their application across diverse industries. Laccases are eco-friendly enzymes used across industries: in pulp and paper for chlorine-free bleaching, in textiles for dye removal, in food for flavor and shelf-life improvement, and in bioremediation for degrading pollutants. They also show promise in pharmaceuticals and personal care due to their biocatalytic and antimicrobial properties. (Gursharan Singh & Shailendra Kumar Arya, 2019), (Arora, D. & Sharma, R., 2010).

The increasing demand for high-redox potential laccases has driven advances in heterologous expression systems, including bacterial hosts like *E. coli*, which offer ease of manipulation, cost-effectiveness, and scalability for industrial enzyme production. Genetic manipulation plays a crucial role in optimizing industrial enzyme production. (Madan Kumar, et al. 2018). Through recombinant DNA technology, enzymes like laccase can be engineered for specific applications, improving efficiency and reducing costs (Nicholl, 2008).

## Materials and methods:

### Cloning of Laccase gene in *E coli* BL21

The laccase gene (*lac2*) from *Coriolopsis caperata* was PCR-amplified and digested using *Ncol* and *Xhol* along with the pET28b vector to create compatible sticky ends. After vector dephosphorylation, ligation was performed overnight at 4°C using T4 DNA ligase. Competent *E. coli* BL21 cells were prepared, transformed via heat shock, and plated on kanamycin media. Positive colonies were cultured, and plasmid DNA was extracted, verified on a 1% agarose gel. Cloning was confirmed by PCR with T7 primers and restriction digestion with *Ncol* and *Xhol*, confirming the presence of the laccase gene. (Ghasemi, Y et al., 2014). As *E. coli* lacks the cellular machinery to perform many of these modifications, which can lead to the **aggregation of heterologous proteins as inclusion bodies**.

**Therefore**, recombinant *E. coli* cultures were induced with 1 M IPTG and incubated for 5 hours. Cells were harvested, homogenized, and washed to isolate inclusion bodies, which were resuspended and stored at -40°C. (Singh, R., 2016).

### Molecular weight determination by SDS PAGE

Protein samples (150 µg/75 µL) were loaded onto a prepared SDS-PAGE gel alongside a molecular marker. Electrophoresis was run at 100 V for 1 hour, followed by Coomassie Blue staining. A distinct band at ~57 kDa confirmed the presence of recombinant laccase.

### Peptide analysis by LC MS

The 57 kDa protein band was excised, destained with ammonium bicarbonate and acetonitrile, then digested with trypsin overnight at 37°C. The resulting peptides were collected and stored at -40°C for further analysis. The resulting peptides were freeze-dried, reduced, alkylated and analyzed through reverse-phase nanoflow HPLC-MS/MS for peptide identification. (Shevchenko, A., et al/2006).

### Dye degradation ability of recombinant laccase

Recombinant laccase (100 µL) was incubated with Bromophenol blue for 12, 24, and 36 hours at room temperature. Dye degradation was assessed by measuring absorbance at 590 nm using a UV-Vis spectrophotometer. The percentage of dye decolorization was calculated using the formula:

$$\% \text{ Dye Decolorization} = (\text{Ac} - \text{As}) / \text{Ac} \times 100,$$

Where, Ac is the initial absorbance without enzyme, and As is the absorbance with the enzyme. (Yadav, A. et al, 2021)

### Enzyme activity by using substrate ABTS

Laccase activity was measured by ABTS oxidation in 100 mM citrate buffer (pH 4.5) at 37°C. Absorbance at 420 nm was recorded after 10 min. Enzyme activity was calculated and expressed as units/min.

## Result and Discussion:

### Transformation of laccase gene in *E. coli* BL21

The laccase gene was amplified from cDNA using gene-specific primers, yielding a 1600 bp product confirmed by gel electrophoresis. PCR product (54.2 µg/mL) and pET28b vector (200 ng/mL) were both digested with *Xba*I and *Nco*I, and the vector was dephosphorylated. Ligation with T4 DNA ligase and transformation into *E. coli* BL21 (DE3) was followed by colony selection on kanamycin plates, confirming successful cloning of the laccase gene for further expression studies.

### Confirmation of clones by restriction digestion

Plasmid DNA from recombinant *E. coli* showed clear bands on gel and was quantified at 7.96 µg/mL. PCR and sequencing confirmed the presence of the laccase gene, matching the expected sequence validating successful cloning for further expression studies.

### Confirmation by SDS PAGE

The SDS-PAGE analysis confirmed the successful expression of recombinant laccase in *E. coli*, exhibiting a comparable molecular weight of approximately 55 kDa to the theoretically predicted size of 55 kDa.

### Dye degradation ability of recombinant laccase enzyme

The recombinant laccase enzyme demonstrated efficient dye decolorization, with a significant 76.2% degradation of bromophenol dye observed after 36 hours of incubation.

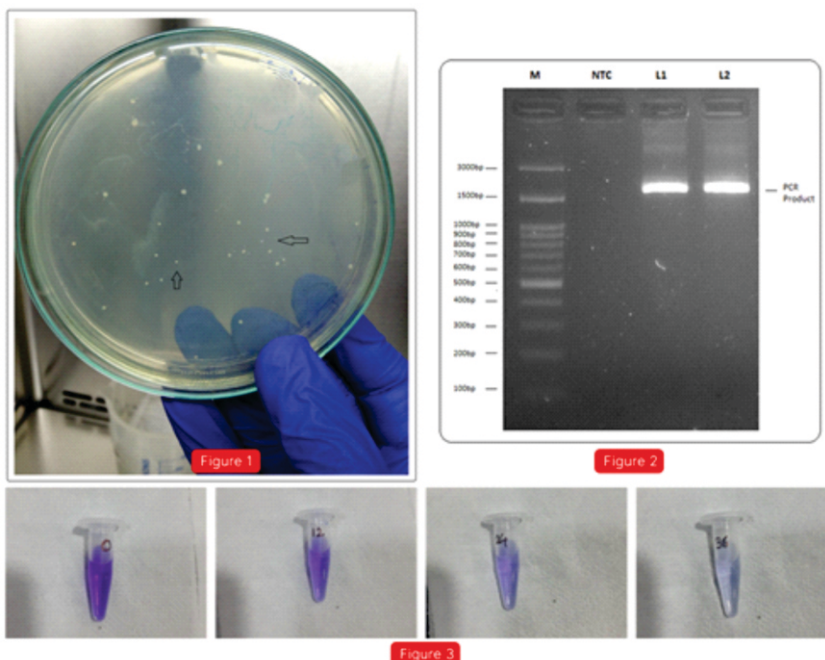


Figure 1: Dye degradation at various time points (0, 12, 24, 36 hours) using the recombinant laccase enzyme.

Figure 2: The laccase gene amplified using PCR and viewed in agarose gel.

Figure 3: Dye degradation at various time points (0, 12, 24, 36 hours) using the recombinant laccase enzyme.

### Peptide analysis by LCMS

Mass spectrometry analysis confirmed the protein identity with 40% sequence coverage with 100% similarity in the matched regions, confirming the presence of identified peptides. The results indicate successful peptide matches and contribute to understanding the laccase protein structure.

### Molecular Docking

Molecular docking of recombinant laccase (PDB ID: 4JHV) with ABTS indicated stable binding with no structural disruption and a favourable binding energy of -5.94 kcal/mol, supported by five hydrogen bonds. ABTS met Lipinski's rule, confirming its drug-likeness. Docking was performed using AutoDock 4.2.6, with ligand prepared in PyMOL and interactions analyzed to explore protein-ligand dynamics at the active site.

### Conclusion:

The cloned laccase gene, containing 1622 bp encoding 517 amino acids, demonstrated successful expression, confirmed through SDS-PAGE, with molecular weight similar to native laccase. The recombinant laccase exhibited significant dye degradation, with a 76% reduction in bromophenol dye after 36 hours, showcasing its enzymatic activity. The study opens avenues for further enzyme engineering techniques to improve stability, specificity and activity.

### References:

1. Arora, D. S., & Sharma, R. K. (2010). Ligninolytic fungal laccases and their biotechnological applications. *Applied Biochemistry and Biotechnology*, 160(6), 1760–1788. DOI: [10.1007/s12010-009-8676-y](https://doi.org/10.1007/s12010-009-8676-y)
2. Baldrian, P. (2006). Fungal laccases – occurrence and properties. *FEMS Microbiology Reviews*, 30(2), 215-242. DOI: [10.1111/j.1574-4976.2005.00010.x](https://doi.org/10.1111/j.1574-4976.2005.00010.x)
3. Ghasemi, Y., Dabbagh, F., & Hosseinkhani, S. (2014). Cloning, expression and purification of laccase enzyme from *Bacillus subtilis* PTCC 1023 in *Escherichia coli* BL21 (DE3). *Minerva Biotechnologica*, 26(4), 295-302.
4. Gursharan Singh, Shailendra Kumar Arya (2019) Utility of laccase in pulp and paper industry: A progressive step towards the green technology, International Journal of Biological Macromolecules, Volume 134, Pages 1070-1084.
5. Madan Kumar, Arti Mishra, Shashi Shekhar Singh, Shaili Srivastava, Indu Shekhar Thakur (2018). Expression and characterization of novel laccase gene from *Pandoraea* sp. ISTKB and its application, International Journal of Biological Macromolecules, 115, 308-316, <https://doi.org/10.1016/j.ijbiomac.2018.04.079>.
6. Nicholl, D. S. T. (2008). *An Introduction to Genetic Engineering* (3rd ed.). Cambridge University Press.
7. Shevchenko, A., Tomas, H., Havlis, J., Olsen, J. V., & Mann, M. (2006). In-gel digestion for mass spectrometric characterization of proteins and proteomes. *Nature Protocols*, 1(6), 2856–2860. <https://doi.org/10.1038/nprot.2006.468>
8. Singh, R., Kumar, M., Mittal , A., & Mehta, P. K. (2016). Microbial enzymes: industrial progress in 21st century. *3 Biotech*, 6(2), 174. <https://doi.org/10.1007/s13205-016-0485-8>
9. Yadav, A., Yadav, P., Kumar Singh, A., kumar, V., Chintaman Sonawane, V., Markandeya, Naresh Bharagava, R., & Raj, A. (2021). Decolourisation of textile dye by laccase: Process evaluation and assessment of its degradation bioproducts. *Bioresource Technology*, 340, 125591. <https://doi.org/10.1016/j.biortech.2021.125591>

## Characteristics of Thermal Power Plant Ash in Slurry form using Treated Waste Water from STP

Sapna Gautam<sup>a</sup>, Anubhav Rawat<sup>b</sup>, Nekram Rawal<sup>c</sup>

<sup>a</sup> Department of Civil Engineering, Motilal Nehru National Institute of Technology Allahabad, Prayagraj-211004

<sup>b</sup> Department of Applied Mechanics, Motilal Nehru National Institute of Technology Allahabad, Prayagraj-211004

<sup>c</sup> Department of Civil Engineering, Motilal Nehru National Institute of Technology Allahabad, Prayagraj-211004

\*Email: [anubhav-r@mnnit.ac.in](mailto:anubhav-r@mnnit.ac.in)

### Abstract

India generates huge amount of ash, and its transportation in slurry form for disposal requires fresh water as per existing design criteria. Due to scarcity of fresh water transportation of ash using treated waste water from STPs in form of Hydro-Sluicing may be an alternate solution. In The current study aims to investigate the relationship between the static settling rate with time and a comparison between the condition when ash water slurry was prepared with fresh water and when with treated waste water at various initial by weight concentration conditions of  $C_w=30\%, 40\% \text{ and } 50\%$ . The study reveals that the settling rate does not change substantially with the treated waste water with respect to the case of when slurry was prepared with fresh water for all initial concertation values.

---

### Introduction

Thermal power plants are backbone of India's energy infrastructure, by fulfilling the significant amount of country's electricity demands. However, these plants generates a huge amount of fly ash—a fine particulate residue resulting from the combustion of coal. Traditionally, this fly ash is mixed with fresh water to form a slurry and is then transported to ash ponds or to the disposal sites. The old practice required a huge amount of freshwater, which is becoming increasingly scarce due to population explosion, rapid increase in industrialization, and climate change. Therefore, current study explores the potential of using treated wastewater from sewage treatment plants (STPs) as a sustainable alternative to freshwater in ash slurry formation and its transportation through pipes. This approach not only addresses water scarcity but also promotes the reuse of wastewater, thereby supporting environmental sustainability for both in solid waste management and water management. Many scientific researches were conducted to address the problem of ash transportation and establishing design strategy for the same in thermal power plants [Chandel, S., 2010; Prakash, et al 2025; Rawat, et al 2020; Rawat et al 2019; Rawat, et al 2022; Singh, 2011; Verma, 2004; Pandian, et al. 1998; Senapati, et al 2005; Biswas, et al 2000; National Research Council of the National Academies 2006; Rawat et al 2017]. But these methods consume substantial amount of water and require constant monitoring.

Using treated wastewater for ash slurry formation presents a few advantages: 1. conserving freshwater and utilizing an underused resource 2. Reduction in dependency on freshwater resources by minimizing environmental impact of wastewater discharge 3. Lower costs associated with sourcing and transporting freshwater. 4. Cost-effective utilization of STP output that might otherwise go unused. Therefore, in current work it was aimed to check whether the treated waste water from STPs can replace the necessity of fresh water for the formation of water-ash slurry for the disposal of ash.

### 1. Materials and Methods:

The combined coal ash samples from the Electro- Static Precipitators (ESP) and bottom ash hoppers have been collected from Prayagraj Power Generation Company Ltd. (PPGCL), Bara, and used for the present study.

The fresh water was collected from the regular supply water from MNNIT Allahabad campus and treated waste water was collected from STP Salori, Prayagraj. Various physical characteristics of the ash, fresh water and treated waste water shall be explained in subsequent sections.

#### 1.1. Physical Properties of ash samples:

The ash was dark grey and stored in airtight sacks. Moisture content is removed by oven drying the ash samples at 105°C according to IS 1727. It was ensured that the Moisture content must not exceed 2% as per IS 3812 standards. The moisture content in ash samples used for current work were found to be limited to 0.142%. For transportation of solids through pipeline, specific gravity is an important design parameter as it decides the settling and transportation characteristics of the slurry. The specific gravity of the solid is determined using Standard Pycnometer Method and is found to be 2.36. The measured values of pH of fly ash slurry prepared with tap water lies in the range of 7.29 to 7.36 and the measured values of pH of fly ash slurry prepared with treated waste water lies in the range of 7.90 to 7.91, which indicates that the suspensions to be non-reactive at all concentrations which falls within the typical range for Class F and Class C fly ash (2.1–2.6). The particle size distribution is determined using sieve analysis and hydrometer analysis. To determine the particle size distribution of fly ash, a sieve analysis was conducted using a representative oven-dried sample weighing approximately 500 grams.

The sieves were arranged in descending order based on mesh size, with the largest opening (1.18 mm) at the top and a collecting pan at the bottom. The fly ash sample was then placed onto the top sieve. The entire stack was mounted on a mechanical sieve shaker and shake-operated for a duration of 10 to 15 minutes to ensure proper separation of particles by size. After the shaking process, the material retained on each sieve was carefully collected, weighed, and the values recorded. From these measurements, the percentage of material retained on each sieve and the cumulative weight retained were calculated.

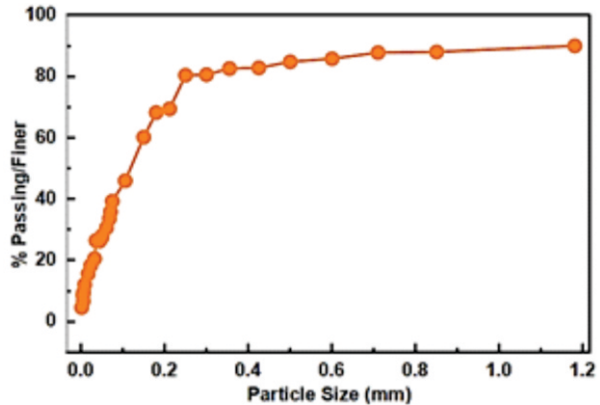


Fig. 1. Particle Size Distribution (PSD) of fly ash

From the above Fig.1, it is clearly seen that the % finer gradually decreases from 90% at 1.18 mm to 4.59% at 1.9 micron. This shows a continuous distribution of particle sizes, indicating well-graded behavior, especially with a significant portion of fine particles.

### **1.2. Physical and chemical Properties of Tap water samples:**

The temperature of tap water collected from MNNIT campus was 21.5 °C, pH value was 7.54, dissolved oxygen was measured as 7.8 mg/L, TDS (Total Dissolved Solids) in sample were found to be as 369 mg/L, Conductivity of tap water was measured as 729 siemens per meter, Nephelometric Turbidity unit was measured 2.2 NTU, Biochemical Oxygen Demand (BOD) was 4 mg/L, Chemical Oxygen Demand was 9 mg/L, turbidity in Tap water sample was found 0.6 NTU and Total Suspended Solid (TSS) were measured as 8 mg/L. All of the parameters considered in the sample of water were found to be under permissible limits.

### **1.3. Physical and chemical Properties of Treated Waste Water samples:**

The temperature of treated waste water collected from STP Salori situated in Prayagraj (U.P.) was 22.95 °C, pH value was 7.42, dissolved oxygen was 5 mg/L, TDS (Total Dissolved Solids) 640 mg/L, Conductivity of tap water was measured 1394 siemens per meter, Nephelometric Turbidity unit was measured 5.0 NTU, Biochemical Oxygen Demand (BOD) was 23 mg/L, Chemical Oxygen Demand was 42 mg/L turbidity in Tap water sample was found 1.0 NTU and Total Suspended Solid (TSS) were measured as 40 mg/L and all the parameters considered in the sample of treated waste water were under permissible limits.

By comparing the various considered parameters of both water and treated waste water it is found that the physical and chemical characteristics were found to be under permissible limits for the safe operation of slurry pipelines and treated waste water can be safely used for slurry preparation of ash in place of fresh water.

## **2. Results and discussions:**

### **2.1. Static Settle Concentration (SSC) of Slurry samples with fresh and treated waste water:**

The SSC is the parameter which decides how much solid particles can be loaded while transportation of its slurry form through pipelines. The SSC of ash slurry both in fresh water and treated waste water are determined using standard methods for three samples having initial concentration by weight of solids as 30%, 40% and 50%. These tests help determine how the ash settles over time, crucial for designing ash ponds and optimizing slurry transport systems. In this process 30% by weight concentration of ash and 70% by weight concentration of fresh water slurry was mixed manually in measuring cylinders of 1 litre and then reading of settling is taken between 0 sec to 86400 seconds for all 6 samples of water and treated waste water and Various graphs Figs. 2 to 4 are drawn to

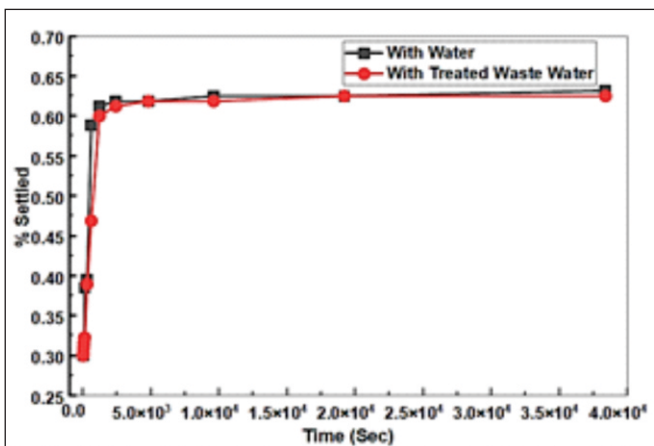


**Fig.2:** Comparison of settling characteristics for the particles of ash with water and waste water at intial  $C_w=30\%$

differentiate the settling rates in two cases of slurry in fresh water and in treated waste water.

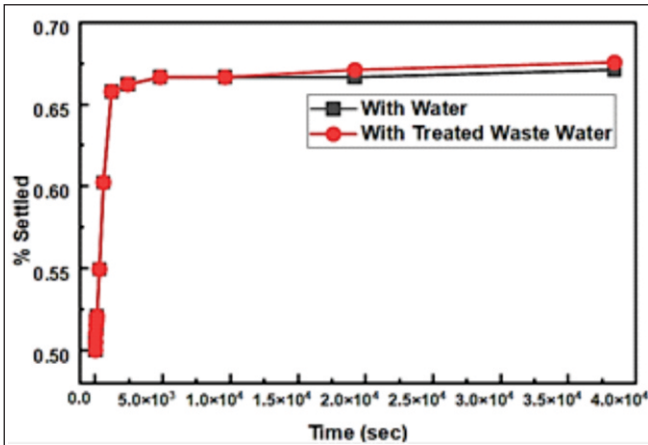


**Fig.3:** Comparison of settling characteristics for the particles of ash with water and waste water at initial  $C_w=40\%$

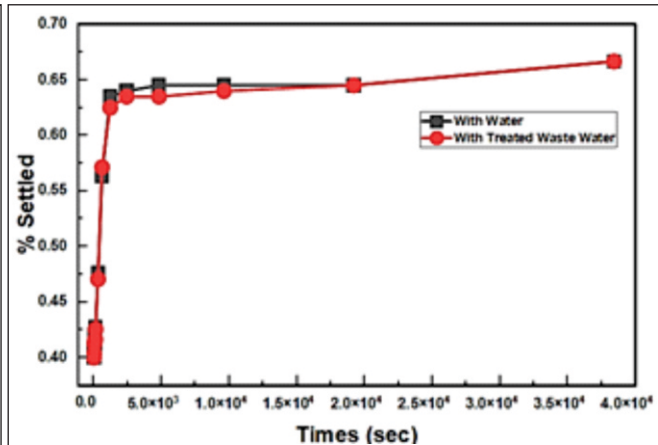


**Fig.4:** Comparison of settling characteristics for the particles of ash with water and waste water at initial  $C_w=50\%$

From Figs.2 to 4 it can be clearly shown that the settling rate is slightly higher in the case of treated wastewater due to the presence of additional Total Dissolved Solids (TDS) and Total Suspended Solids (TSS) in the samples. But the variation is very marginal upto a level that this can be neglected for all concentration and SSC of ash slurry both in fresh water and treated waste water may be treated as same. Thus, based on the current study, it can be concluded that treated wastewater from the sewage treatment plant (STP) can be effectively used as an alternative for fresh water in the preparation of ash slurry in thermal power plants for the transportation of ash to the ash pond or dumping sites.

## Conclusion

The use of treated wastewater in ash slurry management represents a significant advancement toward sustainable water resource management in thermal power plants. This study illustrates the technical feasibility and environmental benefits of replacing freshwater with treated sewage water. However, comprehensive field trials and infrastructure assessments are needed to ensure this solution's long-term viability. Incorporating this practice into standard operations can lead to substantial cost savings, reduced environmental impact, and improved water use efficiency across the energy sector.

## References:

- Chandel, S., 2010. Studies on the flow of high concentration coal ash slurry through pipelines (Doctoral dissertation, IIT Delhi)
- Prakash, Ankit, A. K. Upadhyay, and Anubhav Rawat. "Optimization of specific energy consumption in the high concentration slurry disposal pipelines for coal ash in thermal power plants." *International Journal of Coal Preparation and Utilization* 45, no. 1 (2025): 39-71.

3. Rawat, Anubhav, S. N. Singh, and V. Seshadri. "CFD analysis of the performance of elbow-meter with high concentration coal ash slurries." *Flow Measurement and Instrumentation* 72 (2020): 101724
4. Rawat, Anubhav, S. N. Singh, and V. Seshadri. "Variation of physical and rheological properties of fly ash slurries with particle size and its effect on hydraulic transportation at high concentrations." *Particulate Science and Technology* 37, no. 2 (2019): 151-160.
5. Rawat, A., Singh, S.N. and Seshadri, V., 2022. Computational investigation on the flow of high concentration flies' ash slurries through converging-diverging bends. International Journal of Coal Preparation and Utilization5.
6. Singh, S. N. 2011. Wet disposal of coal ash at higher concentrations. Conference on Fly Ash utilization, New Delhi.
7. Verma, A. K. 2004. Study on high concentration fly ash slurry disposal through pipeline. PhD diss., Department of Applied Mechanics, IIT Delhi.
8. Pandian, et al. (1998): "Studies on the specific gravity of some Indian coal ashes", Journal of Testing and Evaluation, ASTM.
9. Senapati, P.K., Panda, D. and Parida, A. (2005): "Studies on the maximum settled concentration, mixing and rheological properties of high concentration fly ash-bottom ash mixture slurry", Proc. of the International Conference on Fly Ash Utilization, New Delhi.
10. Biswas, A., Gandhi, B.K., Singh, S.N. and Seshadri, V. (2000): "Characteristics of coal ash and their role in hydraulic design of ash disposal pipelines", Indian Journal of Engineering and Material Science.
11. Managing Coal Combustion Residues in Mines, Committee on Mine Placement of Coal Combustion Wastes, National Research Council of the National Academies, 2006.
12. [http://en.wikipedia.org/wiki/Fly\\_ash](http://en.wikipedia.org/wiki/Fly_ash) - Fly ash classification and utilization
13. <http://www.iflyash.com/featuresflyash.htm> - Fly ash features and Introduction
14. [www.uic.edu/classes/Experiment 204-Specific Gravity.pdf](http://www.uic.edu/classes/Experiment%204-Specific%20Gravity.pdf), Reddy, K
15. Rawat, Anubhav, S. N. Singh, and V. Seshadri. "Erosion wear studies on high concentration fly ash slurries." *Wear* 378 (2017): 114-125.

## Computational Design and virtual screening of designed short peptides as potential BACE1 inhibitors for Alzheimer's disease

Kavita Patel, Ashutosh Mani\*

\*Department of Biotechnology, Motilal Nehru National Institute of Technology Allahabad,  
Prayagraj-211004, India.

Email- amani@mnnit.ac.in

---

### Abstract

**A**lzheimer's disease (AD) is a neurological condition caused by the formation of amyloid-beta (A $\beta$ ) plaques, which are primarily generated by the activity of  $\beta$ -site amyloid precursor protein cleaving enzyme 1 (BACE1). BACE1, an enzyme involved in A $\beta$  synthesis, is a possible therapeutic target for Alzheimer's disease management. In this work, we designed peptides with four-length amino acid residues and predicted their tertiary structures to investigate their potential as BACE1 inhibitors. A virtual screening technique was used to assess these peptides' binding affinity to BACE1, followed by molecular docking studies to examine hydrogen bond interactions between the docked peptides and the BACE1 protein. Furthermore, the peptides' pharmacokinetic and toxicity profiles were evaluated using ADMET (Absorption, Distribution, Metabolism, Excretion, and Toxicity) predictions to determine drug-likeness and safety. Finally, a complete dataset was developed, which included structural, binding affinity, and ADMET-related features for all constructed peptides. This work sheds light on the development of peptide-based BACE1 inhibitors and adds vital data to future peptide drug discovery efforts.

---

**Keywords:** Alzheimer's disease(AD), BACE1, Peptide design, Molecular docking, Virtual screening, ADMET prediction, Drug discover

# Introduction

The most prevalent kind of neurodegeneration is Alzheimer's disease (AD), which mostly presents as gradual cognitive deterioration that ultimately results in dementia and memory loss"(Albert et al. 2011; Cole and Vassar 2007). Over 55 million people globally are already affected, and projections suggest that number might rise to 2 trillion in the ensuing decades, making it a significant worry among aging populations. Neurofibrillary tangles, amyloid buildups, and senile plaques in the cerebral cortex are pathological features that set AD apart"(Chen et al. 2017; Bhatia et al. 2022; De Strooper and Karran 2016). The most well-known of the many hypothesized pathways is the Amyloid  $\beta$  (A $\beta$ ) plaque hypothesis(Hardy and Selkoe 2002), which contends that A $\beta$  accumulation disrupts cholinergic transmission(Butterfield and Boyd-Kimball 2005; Cui et al. 2015), speeds up cognitive decline, and modifies behavioral and psychosocial processes. The memory impairments seen in AD are directly related to the buildup that causes neuronal cell death in the brain(Ano et al. 2018; Giacobini 2003).

Complex pathogenic processes, including as tau hyperphosphorylation and the production of amyloid  $\beta$  (A $\beta$ ) plaque, are involved in Alzheimer's disease (AD)(Dhamodharan and Mohan 2022; Goldman et al. 2011). APP is cleaved by  $\alpha$ -secretase to yield soluble APP $\alpha$  and C83 in non-amyloidogenic processing(Sandbrink et al. 1996). These are then processed by  $\gamma$ -secretase to form P3 peptides and AICD. Because of its involvement in plaque formation, synaptic dysfunction through NMDA receptor binding"(Danysz and Parsons 2003; Yaghmaei et al. 2024), and neuroinflammation through microglial and astrocyte activation, BACE1, a crucial enzyme in amyloidogenic processing, is the rate-limiting factor in A $\beta$  synthesis and has become a prospective therapeutic target. The catalytic residues Asp32 and Asp228 as well as Thr72, Gly75, Val89, Thr292, and Phe108 are essential for substrate binding and enzymatic activity in the two-lobed active site of BACE1"(Cole and Vassar 2007; Hampel et al. 2021). Only symptomatic relief is provided by the FDA-approved medications memantine and acetylcholine esterase inhibitors like as donepezil(Birks and Harvey 2018) and rivastigmine,(Birks et al. 2015) underscoring the critical need for new potent treatment approaches(Pandey et al. 2021).

Our goal is to find strong peptide-based BACE1 inhibitors since they efficiently reduce A $\beta$  levels in the brain and prevent its generation. The search for effective BACE1 inhibitors remains on, however. There are two kinds of inhibitors: peptidic and non-peptidic. While typical peptidic drugs usually have high molecular weights and unsatisfactory pharmacological profiles, conventional non-peptidic inhibitors suffer issues including poor selectivity, limited potency, and unwanted side effects. Consequently, the development of low-molecular-weight peptidic inhibitors with substantial therapeutic potential and good selectivity is urgently needed. Peptides are excellent candidates for targeted therapy because of their many benefits, which include anti-inflammatory and antioxidant effects, neuroprotective properties, favorable pharmacokinetics, regulation of neurotransmission and gene expression, and excellent biodegradability and biocompatibility because of their natural amino acid composition(Patel and Mani 2024b).

## 1. Methodology

### 1.1. Generation of peptide sequence

A Python script was used to create every possible combination of tetra-peptides using the 20 standard amino acids denoted by their three-letter codes, such as "Ala," "Arg," ..., and "Val"-(Patel and Mani 2024a). This script calculates the Cartesian product of list of amino acids using an iterator or a recursive function. Each amino

acid is added one after the other until the required length of four residues is achieved, to create peptide chains(Patel et al. 2021). Each peptide is represented as a space-separated string of three-letter amino acid codes in the resultant sequences, which are written to .seq files and the produced tetra-peptides .seq files used as input for structural modeling.

## 1.2. Feature Extraction and Peptide Dataset Generation

### 1.1.1. Binding Affinity Analysis via Molecular Docking

**1.1.1.1. Molecular Docking Protocol:** AutoDock Vina(Eberhardt et al. 2021; Trott and Olson 2010) was used for molecular docking, and a Perl script was used to coordinate and made it easier to analyze interactions, binding positions of docking to assess peptide binding to BACE1.The Lamarckian genetic(Morris et al. 1998) approach was used to dock each peptide separately, to ensure thorough sampling of conformational space.

To prepare the protein, crystallographic water molecules, ions, co-crystallized ligands, and solvents were eliminated in order to reduce interference and improve the BACE1 crystal structure. Polar hydrogens and Kollman charges were added, to neutralize the receptor, and the structure was then saved in PDBQT format (Yadav, Patel, Varghese, et al. 2025).

A  $48 \times 46 \times 36$  point grid box was created using center coordinates ( $x = -4.600$ ,  $y = 11.826$ ,  $z = 28.170$ ) with grid spacing of  $0.575 \text{ \AA}$  to include the catalytic pocket of BACE1. Other parameters were left at their default settings, while exhaustiveness was set to 9 for in-depth investigation.

**1.1.1.2. Binding Affinity Extraction:** A Python script was written to read docking log files of each peptide for their's lowest energy pose and then to extract docking scores, or binding affinities, and output result of lowest binding affinity of all peptides with BACE1 was written to another csv file(Eberhardt et al. 2021).

**1.1.1.3. Hydrogen Bond Analysis:** A python script was written to detect non-covalent interactions and extracted hydrogen bond counts using a bond length threshold of  $2.7 \text{ \AA}$  from PyMOL tool"""(PDF) Using PyMOL as a Platform for Computational Drug Design, n.d.).

### 1.1.2. Physicochemical and Biochemical Descriptor Calculation

Each peptide's features were calculated using cheminformatics and bioinformatics. First, peptide sequences file (.seq) are converted into SMILES format using RDKit as the SMILES format was used in RDKit"""(RDKit, n.d.) to compute molecular characteristics including hydrophobicity, lipophilicity, logP, and molecular weight. And, then sequence-based characteristics like amino acid composition and isoelectric point were calculated using Biopython's ProtParam"""(Expasy - ProtParam, n.d.) module.

The output of all peptides' feaures were saved in a structured table containing computed descriptors, with each row denoting a peptide and the columns describing its computed characteristics and dataset was exported into excel and csv format.

### 1.1.3. Blood-Brain Barrier (BBB) Permeability Prediction

Peptide BBB permeability was predicted using a deep neural network classifier named DeePred-BBB model(Kumar et al. 2022). SMILES format of all peptides were used in this model to predict BBB predictions in binary format (0,1) indicating whether or not each peptide was capable of passing across the blood-brain barrier(Yadav, Patel, Mani, et al. 2025).

## 2. Results

### 2.1. Peptide Sequence Generation and Structure Prediction

A combinatorial library of tetrapeptides was generated using all 20 amino acids and this yielded 160,000 tetrapeptides. Few structures are not possible to generate though steric hindrances of few amino acids structures leading to final count to 136,000 tetrapeptides. Each sequence was then underwent tertiary structure prediction using the Golden Ratio Simulated Annealing algorithm, which identifies low-energy conformations through iterative minimization. And resulting in 3D models of each peptides. The structures were saved in PDB format, having stereochemistry and backbone geometry suitable for docking.

### 2.2. Comprehensive Peptide Dataset

Each peptide was characterized using a comprehensive dataset that included features for molecular, pharmacokinetic, physicochemical, and interaction. In order to provide input characteristics for machine learning classification, twelve descriptors were computed for each peptide.

**2.2.1. Physicochemical Properties:** physicochemical properties were computed using RDKit tool like molecular weight, LogP, and atom count, which revealed information of structural complexity and lipophilicity, amino acid content and molecular structure were used to calculate hydrophobicity and lipophilicity scores.

**2.2.2. Toxicity and Drug-Likeness:** Potential toxicity like cytotoxic, hepatotoxic, or mutagenic hazards were computed using in silico models which also computed the Quantitative Estimate of Drug-likeness (QED), pharmacological appropriateness using ProtParam. This tool was also used to calculate other parameters like the molar absorptivity and isoelectric point.

**2.2.3. Interaction Features:** Interaction features like binding affinity and inter-molecular Hydrogen bond counts records the strength of peptide binding with the active site of BACE1. BBB permeability was predicted using DeePred-BBB model which categorized peptides as either permeable or non-permeable BBB peptides. The resulting dataset was compiled with all 12 computed features where each row denotes a distinct peptide. This dataset is used as to find promising BACE1 inhibitors and also as input for machine learning models and facilitates the display of property distributions.

Peptide	LogP	Molecular Weight	Number Of Atoms	QED SCORE	Hydrophobicity	Lipophilicity	Toxicity	Isoelectric Point	Molar Extinction Coeff	Hydrogen Bond	Affinity	BBB
AAAA	-2.0677	302.331	21	0.36439115	9	7.2	7.2	0.8557001667	0.10	-7.3	1	
AAAR	-2.82433	387.441	27	0.10482261	8	0.9	0.9	1.4	9.79502010	0.12	-8.2	0
AAAN	-3.2122	345.356	24	0.25278310	7	1.9	1.9	0.9557001667	0.12	-7.6	1	
AAAD	-2.6129	346.34	24	0.26160632	1.9	1.9	1.3	4.29949474	0.11	-7.3	1	
AAAC	-2.1578	334.398	22	0.27834842	6	7.9	7.9	0.7	5.56154766	0.14	-7.2	0

**Table 2.3:** Dataset structure of tetra peptides with all 12 structure-based descriptors

## Conclusion

This study integrates molecular modelling, docking analysis and cheminformatics to provide a strong computational framework for discovery and characterization of potential BACE1 inhibitory peptides. All 20 amino acids were used to create a combinatorial library of tetrapeptides. Golden Ratio Simulated Annealing algorithm was used to model the peptides' tertiary structures in order to provide low-energy conformations appropriate for receptor binding investigations. A comprehensive interaction profiles like Binding affinity scores and hydrogen bond counts were obtained for every peptide-BACE1 complex by molecular docking simulations using AutoDock Vina. In addition, a thorough set of physical and biological descriptors having important molecular characteristics like lipophilicity, molecular weight, isoelectric point, and amino acid composition, were computed using RDKit and Biopython.

Further, the DeePred-BBB deep learning model was used to predict blood-brain barrier permeability, this allowed the discovery of peptides that may have central nervous system activity. Additionally, toxicity profiles and drug-likeness scores were computed to ensure pharmacological compatibility and safety.

The resultant dataset facilitates the logical selection of peptides for experimental validation and provides resources for visualizing peptide property distributions. Especially for neurodegenerative targets like BACE1 in Alzheimer's disease, this integrative method shows usefulness of computational tools in expediting peptide-based drug development.

## References

1. Albert, Marilyn S., Steven T. DeKosky, Dennis Dickson, et al. 2011. The Diagnosis of Mild Cognitive Impairment Due to Alzheimers Disease: Recommendations from the National Institute on Aging-Alzheimers Association Workgroups on Diagnostic Guidelines for Alzheimers Disease. *Alzheimers & Dementia: The Journal of the Alzheimers Association* 7 (3): 27079. <https://doi.org/10.1016/j.jalz.2011.03.008>.
2. Ano, Yasuhisa, Tatsuhiro Ayabe, Toshiko Kutsukake, et al. 2018. Novel Lactopeptides in Fermented Dairy Products Improve Memory Function and Cognitive Decline. *Neurobiology of Aging* 72 (December): 2331. <https://doi.org/10.1016/j.neurobiolaging.2018.07.016>.
3. Bhatia, Shiveena, Rishi Rawal, Pratibha Sharma, Tanveer Singh, Manjinder Singh, and Varinder Singh. 2022. Mitochondrial Dysfunction in Alzheimers Disease: Opportunities for Drug Development. *Current Neuropharmacology* 20 (4): 67592. <https://doi.org/10.2174/1570159X19666210517114016>.
4. Birks, Jacqueline S, Lee-Yee Chong, and John Grimley Evans. 2015. Rivastigmine for Alzheimers Disease. *The Cochrane Database of Systematic Reviews 2015 (9) : CD001191*. <https://doi.org/10.1002/14651858.CD001191.pub4>.
5. Birks, Jacqueline S, and Richard J Harvey. 2018. Donepezil for Dementia Due to Alzheimers Disease. *The Cochrane Database of Systematic Reviews 2018 (6) : CD001190*. <https://doi.org/10.1002/14651858.CD001190.pub3>.
6. Butterfield, D. Allan, and Debra Boyd-Kimball. 2005. The Critical Role of Methionine 35 in Alzheimers Amyloid Beta-Peptide (1-42)-Induced Oxidative Stress and Neurotoxicity. *Biochimica Et Biophysica Acta* 1703 (2): 14956. <https://doi.org/10.1016/j.bbapap.2004.10.014>.

7. Chen, Guo-Fang, Ting-Hai Xu, Yan Yan, et al. 2017. Amyloid Beta: Structure, Biology and Structure-Based Therapeutic Development. *Acta Pharmacologica Sinica* 38 (9): 120535. <https://doi.org/10.1038/aps.2017.28>.
8. Cole, S.L, and R Vassar. 2007. The Basic Biology of BACE1: A Key Therapeutic Target for Alzheimers Disease. *Current Genomics* 8 (8): 50930. <https://doi.org/10.2174/138920207783769512>.
9. Cui, Jin, Xiaoyin Wang, Xiaohang Li, et al. 2015. Targeting the  $\gamma$ - $\beta$ -Secretase Interaction Reduces  $\beta$ -Amyloid Generation and Ameliorates Alzheimers Disease-Related Pathogenesis. *Cell Discovery* 1: 15021. <https://doi.org/10.1038/celldisc.2015.21>.
10. Danysz, Wojciech, and Chris G. Parsons. 2003. The NMDA Receptor Antagonist Memantine as a Symptomatological and Neuroprotective Treatment for Alzheimers Disease: Preclinical Evidence. *International Journal of Geriatric Psychiatry* 18 (Suppl 1): S23-32. <https://doi.org/10.1002/gps.938>.
11. De Strooper, Bart, and Eric Karran. 2016. The Cellular Phase of Alzheimers Disease. *Cell* 164 (4): 60315. <https://doi.org/10.1016/j.cell.2015.12.056>.
12. Dhamodharan, G., and C. Gopi Mohan. 2022. Machine Learning Models for Predicting the Activity of AChE and BACE1 Dual Inhibitors for the Treatment of Alzheimers Disease. *Molecular Diversity* 26 (3): 150117. <https://doi.org/10.1007/s11030-021-10282-8>.
13. Eberhardt, Jerome, Diogo Santos-Martins, Andreas F. Tillack, and Stefano Forli. 2021. AutoDock Vina 1.2.0: New Docking Methods, Expanded Force Field, and Python Bindings. *Journal of Chemical Information and Modeling* 61 (8): 389198. <https://doi.org/10.1021/acs.jcim.1c00203>.
14. Expasy - ProtParam. n.d. Accessed 2 June 2025. <https://web.expasy.org/protparam/>.
15. Giacobini, Ezio. 2003. Cholinesterases: New Roles in Brain Function and in Alzheimers Disease. *Neurochemical Research* 28 (34): 51522. <https://doi.org/10.1023/a:1022869222652>.
16. Goldman, Jill S., Susan E. Hahn, Jennifer Williamson Catania, et al. 2011. Genetic Counseling and Testing for Alzheimer Disease: Joint Practice Guidelines of the American College of Medical Genetics and the National Society of Genetic Counselors. *Genetics in Medicine: Official Journal of the American College of Medical Genetics* 13 (6): 597605. <https://doi.org/10.1097/GIM.0b013e31821d69b8>.
17. Hampel, Harald, Robert Vassar, Bart De Strooper, et al. 2021. The  $\beta$ -Secretase BACE1 in Alzheimers Disease. *Biological Psychiatry* 89 (8): 74556. <https://doi.org/10.1016/j.biopsych.2020.02.001>.
18. Hardy, John, and Dennis J. Selkoe. 2002. The Amyloid Hypothesis of Alzheimers Disease: Progress and Problems on the Road to Therapeutics. *Science (New York, N.Y.)* 297 (5580): 35356. <https://doi.org/10.1126/science.1072994>.
19. Kumar, Rajnish, Anju Sharma, Athanasios Alexiou, Anwar L. Bilgrami, Mohammad Amjad Kamal, and Ghulam Md Ashraf. 2022. DeePred-BBB: A Blood Brain Barrier Permeability Prediction Model With Improved Accuracy. *Frontiers in Neuroscience* 16. <https://www.frontiersin.org/articles/10.3389/fnins.2022.858126>.
20. Morris, Garrett M., David S. Goodsell, Robert S. Halliday, et al. 1998. Automated Docking Using a Lamarckian Genetic Algorithm and an Empirical Binding Free Energy Function. *Journal of Computational Chemistry* 19 (14): 163962. [https://doi.org/10.1002/\(SICI\)1096-987X\(19981115\)19:14<1639::AID-JCC10>3.0.CO;2-B](https://doi.org/10.1002/(SICI)1096-987X(19981115)19:14<1639::AID-JCC10>3.0.CO;2-B).

21. Pandey, Surya Nath, Naresh Kumar Rangra, Sima Singh, Saahil Arora, and Varun Gupta. 2021. Evolving Role of Natural Products from Traditional Medicinal Herbs in the Treatment of Alzheimers Disease. *ACS Chemical Neuroscience* 12 (15): 271828. <https://doi.org/10.1021/acschemneuro.1c00206>.
22. Patel, Kavita, and Ashutosh Mani. 2024a. Structural Bioinformatics and Protein Structure Prediction. [https://doi.org/10.1007/978-981-97-7123-3\\_8](https://doi.org/10.1007/978-981-97-7123-3_8).
23. Patel, Kavita, and Ashutosh Mani. 2024b. Food-Derived Peptides as Promising Neuroprotective Agents: Mechanism and Therapeutic Potential. *Current Topics in Medicinal Chemistry* 24 (March). <https://doi.org/10.2174/0115680266289248240322061723>.
24. Patel, Kavita, Siwangi Srivastava, Shikha Kushwah, and Ashutosh Mani. 2021. Perspectives on the Role of APOE4 as a Therapeutic Target for Alzheimers Disease. *Journal of Alzheimers Disease Reports* 5 (1): 899910. <https://doi.org/10.3233/ADR-210027>.
25. (PDF) Using PyMOL as a Platform for Computational Drug Design. n.d. Accessed 2 June 2025. [https://www.researchgate.net/publication/312107501\\_Using\\_PyMOL\\_as\\_a\\_platform\\_for\\_computational\\_drug\\_design](https://www.researchgate.net/publication/312107501_Using_PyMOL_as_a_platform_for_computational_drug_design).
26. RDKit. n.d. Accessed 2 January 2024. <https://www.rdkit.org/>.
27. Sandbrink, R., C. L. Masters, and K. Beyreuther. 1996. APP Gene Family. Alternative Splicing Generates Functionally Related Isoforms. *Annals of the New York Academy of Sciences* 777 (January): 28187. <https://doi.org/10.1111/j.1749-6632.1996.tb34433.x>.
28. Trott, Oleg, and Arthur J. Olson. 2010. AutoDock Vina: Improving the Speed and Accuracy of Docking with a New Scoring Function, Efficient Optimization and Multithreading. *Journal of Computational Chemistry* 31 (2): 45561. <https://doi.org/10.1002/jcc.21334>.
29. Yadav, Kanchan, Kavita Patel, Ashutosh Mani, Sangeeta Yadav, and Dinesh Yadav. 2025. Elucidating the Potential of Bioactive of Trichoderma Sp.. in Combating Pathogenesis by Fusarium Sp.. by Targeting Pectin Lyases: A Bioinformatics Approach. *Biochemical and Biophysical Research Communications* 742 (January): 151111. <https://doi.org/10.1016/j.bbrc.2024.151111>.
30. Yadav, Kanchan, Kavita Patel, Mohan Varghese, Ashutosh Mani, Sangeeta Yadav, and Dinesh Yadav. 2025. Molecular Modelling and Docking of Cloned Pectin Lyases from Fusarium Species. *Biologia*, ahead of print, March 11. <https://doi.org/10.1007/s11756-025-01915-6>.
31. Yaghmaei, Ehsan, Hongxia Lu, Louis Ehwerhemuepha, et al. 2024. Combined Use of Donepezil and Memantine Increases the Probability of Five-Year Survival of Alzheimers Disease Patients. *Communications Medicine* 4 (1): 18. <https://doi.org/10.1038/s43856-024-00527-6>.

## Exploring the Gut Resistome: Insights into Antimicrobial Resistance Genes in the Indian Population

Ankish Arya, Sankalp Patil, Prabhat Tripathi, Imlimaong Aier, Nidhi Dubey, Pritish Kumar Varadwaj\*

Department of Applied Sciences, Indian Institute of Information Technology Allahabad,  
Prayagraj 211015, India, \*Corresponding author: Email: [pritish@iiita.ac.in](mailto:pritish@iiita.ac.in)

---

### Abstract

The human gut microbiome is a vast reservoir of antimicrobial resistance genes (ARGs), collectively referred to as the *resistome*. Mapping regional patterns of ARG diversity is essential for targeted stewardship. We analysed publicly available shotgun metagenomes from healthy volunteers residing in two geographically and culturally distinct Indian districts—Bhopal (Central India) and Kasaragod (South-West India)—using a uniform bioinformatic pipeline (FASTQC/FASTP → BOWTIE2 → MEGAHIT → PROKKA → AMRFinderPlus). A total of 380 non-redundant ARGs were identified. Bhopal samples exhibited higher overall alpha-diversity and were enriched in *blaCTX-M* and *tetM*. In contrast, Kasaragod samples showed a greater prevalence of *blaTEM* and *blaOXA*. Core-gene analysis revealed 150 ARGs common to both cohorts, with 50 and 30 region-specific ARGs in Bhopal and Kasaragod, respectively. These findings highlight distinct regional selective pressures and underscore the need for location-tailored AMR surveillance programmes.

---

**Keywords:** Antimicrobial resistance (AMR), Anmicrobial resistant genes (ARGs), human gut microbiome.

# Introduction

**A**ntimicrobial resistance (AMR) is one of the leading threats globally, occurring when microorganisms can withstand the drugs which are once effective. In India, the deaths related to AMR were around one million in 2019 (Global Burden of Disease Consortium, 2023). The human gut microbiome is found as the reservoir of Antimicrobial resistant genes (ARGs), which can act as a hub for ARG transfer, accelerating the dissemination of resistant determinants (Theophilus & Taft, 2023). However, the region-based exploration of ARG profiles in gut microbiome from the Indian population is still underexplored. This study characterises and compares ARG profiles in healthy individuals from Bhopal and Kasaragoda, providing baseline data. It underlines the ARG diversity in human gut samples and the relative abundance of keyARGs. Finally, their is a identification of ARGs which is shared by both regions and the unique ARGs specific to both geographic locations.

## 1. Materials and Methods

This study utilised the public dataset of gut metagenomic data sourced from healthy individuals. This is publicly available at BioProject 397112, which analysed two different geographical locations: Bhopal and Kasaragoda. The participants were healthy adults with no antibiotic exposure in the preceding six months. A standard pipeline is followed for analysing the ARG data from the gut metagenome, which is as follows:

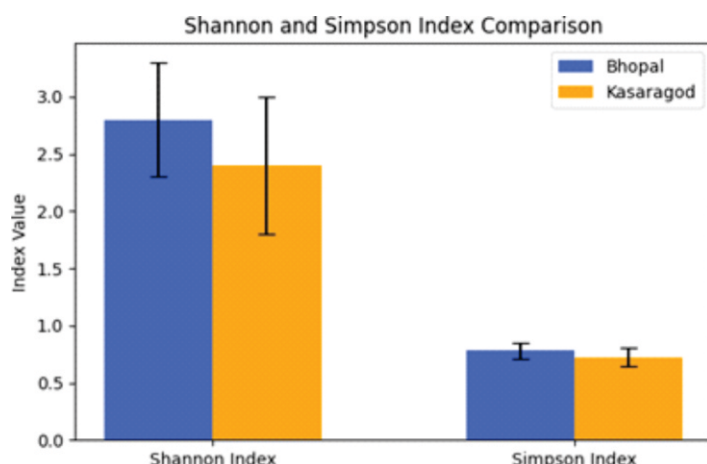
We ran an initial quality check using FASTQC. Following this, we cleaned the sequences with FASTP. We needed to filter out any DNA from the human host. To do this, we used BOWTIE2 to map our sequences against the human genome. Any reads that didn't align were considered microbial and were retained for the next steps. We then used MEGAHIT to assemble the short reads into longe5 Once we had these contigs, we ran them through PROKKA, which identified and annotated the potential genes within them. The core of our investigation was to identify antimicrobial resistance genes (ARGs). Using AMRFinderPlus and the NCBI database, we screened our annotated genes. A gene was classified as an ARG only if it matched a known resistance gene with at least 90% identity across 60% of its length. Finally, the diversity of the resistome in our samples, we calculated the Shannon and Simpson indices, which are standard metrics for measuring the variety and evenness of genes within a community.

## 2. Results

### 2.1 ARG diversity

Bhopal displayed significantly higher alpha-diversity (Figure 1). Greater evenness suggests a more balanced resistome, potentially reflecting broader antibiotic selection pressures from heterogeneous healthcare practices.

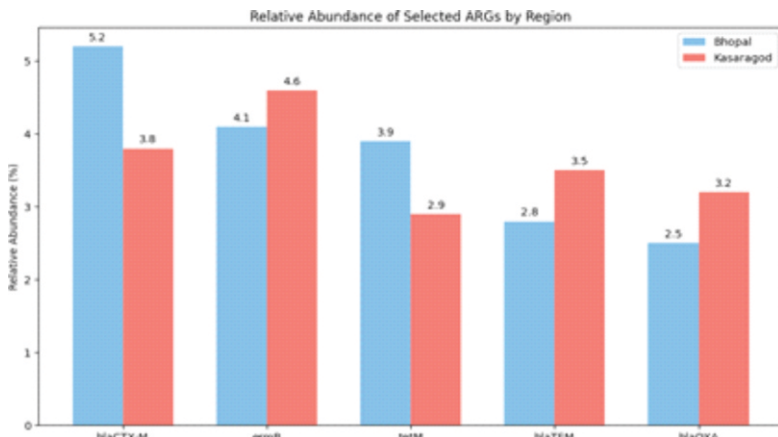
Figure 1: Alpha diversity and Shannon and Simpson index comparison.



## 2.2 Relative abundance of key ARGs

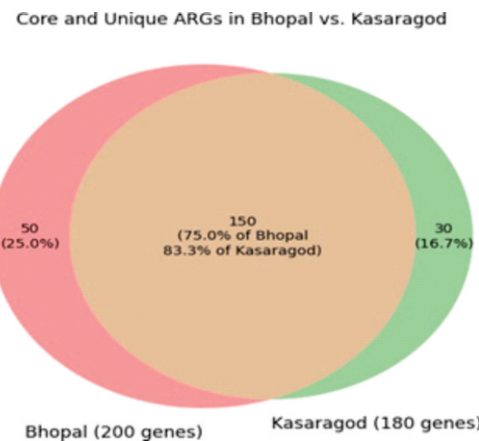
Five clinically relevant ARGs accounted for >25% of total resistome reads (Figure 2). Consistent with prior hospital surveillance, *blaCTX-M* and *tetM* were dominant in Central India, whereas *blaTEM* and *blaOXA* prevailed on the south-western coast (Indian Priority Pathogen List, 2022).

Figure 2: Relative abundance of selected ARGs.



## 2.3 Core vs. unique resistome

Of 380 non-redundant ARGs, 150 were shared, indicating a sizeable national ARG core (Figure 3). Region-specific ARGs—chiefly aminoglycoside- and macrolide-resistance determinants suggest local antibiotic usage patterns (Matzaras et al., 2022).



## Discussion

This study identifies geographical differences in the gut resistome of Indian populations. The higher diversity found in the Bhopal individuals suggests these individuals were exposed to a wide variety of antibiotics. The dominance of specific genes, such as *blaCTX-M* and *tetM* in Bhopal and *blaTEM* and *blaOXA* in Kasaragod, reflects distinct regional antimicrobial usage. While a core set of 150 ARGs was common to both groups, each region also possessed unique resistance genes. These findings strongly advocate for the development of regionally customized AMR monitoring and stewardship programs to combat resistance effectively.

## Conclusion

The Indian gut resistome exhibits pronounced geographical heterogeneity. Bhopal harbors a richer yet more homogeneous ARGs, while Kasaragod shows lower diversity but region-specific dominance of β-lactamase genes.

These insights advocate for regionally customised AMR monitoring and stewardship, complementing national guidelines. Future work should integrate longitudinal sampling and functional metatranscriptomics to elucidate ARG expression dynamics.

## References

1. Centers for Disease Control and Prevention (CDC). 2024. *About Antimicrobial Resistance*. <https://www.cdc.gov/drugresistance/about.html>
2. Global Burden of Disease Consortium. 2023. *Global bacterial antimicrobial resistance burden estimates 2019*. Institute for Health Metrics and Evaluation.
3. Indian Department of Biotechnology. 2022. *Indian Priority Pathogen List*. New Delhi.
4. Matzaras, R., Nikopoulou, A., Protonotariou, E., & Christaki, E. 2022. Gut microbiota modulation and dysbiosis prevention as an alternative to antimicrobial resistance: a narrative review. *Yale Journal of Biology and Medicine*, 95(4), 479–494.
5. Theophilus, R. J., & Taft, D. H. 2023. Antimicrobial resistance genes, the gut microbiome, and infant nutrition. *Nutrients*, 15(14), 3177.
6. World Health Organization. 2024. *Antimicrobial Resistance Fact Sheet*. <https://www.who.int/news-room/fact-sheets/detail/antimicrobial-resistance>

## Metagenomics in the era of deep learning: Addressing the limitations of traditional analysis methods

Diksha Singh, Dr. Ashutosh Mani\*

\*Department of Biotechnology, Motilal Nehru National Institute of Technology Allahabad,  
Prayagraj-211004

\*Corresponding author email id: amani@mnnit.ac.in

---

### Abstract

**M**etagenomics, the study of microbial communities from environmental samples, is broadly categorized into amplicon (e.g., 16S rRNA) and shotgun sequencing approaches. While amplicon sequencing targets specific gene markers, shotgun sequencing offers a comprehensive view of microbial species and their associated genes. Traditional methods are used to analyze metagenomic data suffer from limitations such as low resolution, computational complexity, and dependence on curated reference databases. This review outlines these challenges and highlights how deep learning techniques can overcome them, offering improved accuracy, scalability, and robustness in metagenomic analysis.

---

#### **Keywords:**

Metagenomics, Microbial communities, Amplicon sequencing, Shotgun sequencing, Deep learning, Taxonomic classification, Functional profiling, Computational methods

---

### Introduction

Metagenomics refers to the direct genetic analysis of microbial genomes within samples; it is an advanced method that bypasses culture-based limitations by directly extracting DNA from environmental samples for microbial analysis[1, 2]. Advances in next-generation sequencing (NGS) and bioinformatics, have expanded its capability to explore microbial diversity, function, and host interactions[3]. Metagenomic approaches are broadly categorized into amplicon-based and shotgun sequencing, each with unique strengths and limitations[4].

## 1. Sequencing Strategies in Metagenomics

### 1.1 Amplicon Sequencing

Amplicon sequencing targets specific marker genes like 16S rRNA (bacteria), 18S rRNA (eukaryotes), or ITS (fungi) for taxonomic profiling. The V3-V4 region of 16S rRNA is widely used with the Illumina for its optimal length and resolution[, ]. Tools like QIIME 2, DADA2, and Mothur enable cost-effective microbial diversity analysis[] but offer limited taxonomic resolution and no direct functional insights, as only single gene is targeted.

### Shotgun Metagenomic Sequencing

Shotgun metagenomics is an untargeted approach that sequences the entire genomic content of a microbial sample, providing detailed insights into taxonomic composition and functional profiling beyond specific marker genes[, ]. It allows species-level resolution and gene prediction using tools like Kraken2, MetaPhlAn, and MG-RAST [, ]. However, it faces challenges such as host DNA contamination, large data volumes, and high computational demands[].

## 2. Traditional Analytical Methods

### 2.1 Amplicon Data Analysis

Traditional analysis methods can be broadly grouped into four categories: (a) de-novo clustering, (b) reference-based alignment[], (c) machine learning classification[], and (d) ASV-based inference. These methods were selected based on their prevalence in microbiome literature, historical evolution, and integration into widely used pipelines such as QIIME (QIIME 1 and QIIME 2), Mothur, USEARCH, DADA2, and Deblur[].

- a) **De novo clustering:** De novo clustering groups sequences into OTUs based on similarity thresholds (commonly 97%), enabling detection of both known and novel taxa[, ]. This approach widely used in earlier versions of QIIME and Mothur[].
- b) **Reference-based alignment:** Reference-based alignment methods, such as PathoScope, USEARCH, and Mothur assign taxonomic identities to sequences by comparing them to a reference database[, ].
- c) **Machine learning classification:** This approach uses machine learning models, such as the naïve Bayes classifier (e.g., RDP classifier), trained on taxonomic databases to rapidly assign taxonomic labels to sequencing reads[].
- d) **ASV-based inference:** The ASV approach use denoising algorithms like DADA2 [] and Deblur [] to correct sequencing errors and identify exact biological sequences, differing by even a single nucleotide. Unlike 97% OTU clustering, ASVs offer higher resolution and accuracy in detecting microbial diversity[].

### 2.2 Shotgun Metagenomic Data Analysis

Shotgun metagenomic data analysis involves both taxonomic and functional profiling, using computational approaches broadly categorized as assembly-based, mapping-based, and marker-based methods[].

- a. **Assembly-based methods:** This method assembles reads into contigs, and then predicts ORFs for taxonomic and functional annotation []. Abundance is estimated via read mapping, and binning tools like MetaBAT2 [], MaxBin2 [], and CONCOCT [] generate metagenome-assembled genomes (MAGs). Functional annotation is commonly performed using Prokka[], and EggNOG-mapper[].

- b. **Mapping-based methods:** This method directly aligns reads to reference genomes or curated gene databases (e.g., KEGG, UniRef90) for taxonomic and functional profiling []. Tools like Kraken2 [], Centrifuge [] , and PathoScope[] enable taxonomic classification using k-mer or alignment-based methods, while HUMAnN2[] is widely used for functional profiling and pathway analysis.
- c. **Marker-based methods:** This method detects taxonomy based on conserved, clade-specific genes unique to specific microbial groups. Tools like MetaPhlAn3, which use curated marker gene sets, allow high-resolution taxonomic classification but lack direct functional annotation capability [ , ]. Similarly, mOTUs2 tool targets universal single-copy marker genes for accurate taxonomic profiling []. MetaPhlAn3 is often paired with HUMAnN3 to infer gene and pathway abundances[].

### 3. Limitations of Traditional Methods

#### a. Amplicon-Based Metagenomic Data Analysis – Limitations

Amplicon sequencing methods like 16S rRNA analysis offer limited taxonomic resolution and often fail to distinguish closely related species due to short reads and conserved regions []. Long-read platforms such as ONT and PacBio enable full-length sequencing and improved resolution but are hindered by high error rates, complicating de novo OTU clustering []. Reference-based alignment methods rely on the accuracy of databases, which may contain errors introduced during sequencing or PCR amplification and misannotations, leading to incorrect taxonomic assignments []. Machine-learning classifiers require extensive parameter optimization and are often tested on simulated datasets that lack real sequencing errors and biases, potentially may overestimate their performance []. ASV-based tools like DADA2 and Deblur offer high-resolution taxonomic profiling but have drawbacks. Deblur may cause high read loss and miss novel taxa, while DADA2 can fragment data excessively and vary across replicates. Both rely on error models and databases, risking bias and loss of true diversity[].

#### b. Shotgun Metagenomic Data Analysis – Limitations

Shotgun metagenomics offers comprehensive microbial profiling but poses challenges across analytical approaches. Assembly-based analysis methods face limitations due to uneven coverage, strain variation, and k-mer complexity, often resulting in fragmented contigs []. Mapping-based methods are effective for profiling but have limitations. Tools like PathoScope depend on exact strain genome in the reference database, limiting novel species detection []. Centrifuge, on the other hand, often misclassifies reads due to taxonomic inconsistencies and closely related genomes in RefSeq[], while Kraken 2similarly struggles with distinguishing species when high genomic similarity exists among taxa []. Marker-based methods are limited by their reliance on a restricted set of reference genes. Tools such as MetaPhlAn2 and mOTUs2, which utilize limited marker-based databases, may exhibit reduced taxonomic resolution and overall performance[].

### 4. Deep Learning in Metagenomics

Deep learning (DL) has emerged as a powerful approach in metagenomics, addressing key limitations of traditional methods such as low resolution, reliance on reference databases, and error sensitivity. DL offers effective tools for learning complex patterns directly from high-dimensional, noisy data, providing a scalable and accurate approach for microbial analysis []. Based on applications, DL models are widely used in taxonomic classification, functional annotation, and host-phenotype prediction []. For taxonomic classification, models like convolutional neural networks (CNNs) and recurrent neural networks (RNNs)—particularly Long Short-Term

Memory (LSTM) networks—have been employed to classify short DNA reads directly from raw sequence data [, ]. Among CNN-based models, DL-TODA uses a modified AlexNet architecture to classify short metagenomic reads at the species level. Unlike k-mer-based approaches, DL-TODA learns informative sequence features directly from raw sequences and provides a probabilistic confidence score for each prediction. This not only enhances classification accuracy but also offers a robust mechanism for quality control[ ]. GeNet is another CNN-based deep learning model trained on raw metagenomic reads. It outperforms traditional tools like Kraken and Centrifuge by learning robust, transferable representations directly from raw sequences, enabling better performance on noisy data and downstream task like pathogen detection. Unlike traditional methods, GeNet is also effective with limited labeled data and requires less memory, making it suitable for portable sequencing applications[ ].

In contrast, DeepMicrobes employs a bidirectional LSTM with a self-attention mechanism to achieve near species-level classification of human gut metagenomes, outperforming traditional classifiers like Kraken 2 [ ]. However, its LSTM-based architecture introduces certain limitations. To address these, MetaTransformer, a transformer-based architecture, has been introduced for genus- and species-level classification. MetaTransformer matches DeepMicrobes in genus-level accuracy and surpasses it at the species level, while offering faster training and up to five-fold speed improvements during inference[ ].

Moreover, DL architectures are not limited to sequence classification alone. FGBERT, a pre-trained transformer-based model, utilizes protein-based tokenization to generate functionally meaningful and context-aware representation of gene from metagenomic sequences. This approach effectively overcomes the limitations of traditional k-mer-based methods and maintains high annotation accuracy even in the presence of sequence mutations[ ]. Another DL-based tool, ARGNet, is specifically designed for the identification and classification of antibiotic resistance gene (ARGs) from metagenomic data. Unlike traditional alignment-based methods, ARGNet employs a 1D convolutional network (CNN) combined with a denoising autoencoder architecture, making it alignment-free and capable of detecting novel or distantly related ARGs. It demonstrates superior performance in terms of accuracy, recall, and F1-score when compared to other DL-based tools such as DeepARG and HMD-ARG[ ].

In the domain of host-phenotype prediction, PopPhy-CNN represents a notable advancement. It is a convolutional neural network framework developed to predict host disease status from metagenomic data. The model integrates microbial abundance profiles with phylogenetic tree information, which is transformed into a matrix format using a custom propagation method. This encoding enables the network to learn both abundance patterns and evolutionary relationships among microbial taxa simultaneously [ ]. DeepMicro is another deep learning framework designed for host phenotype prediction using microbiome data. It employs various autoencoders—shallow, deep, variational, and convolutional—to extract low-dimensional features from microbiome profiles [ ]. MetaNN utilizes a neural network coupled with a novel data augmentation strategy to reduce bias toward training data and improve phenotype prediction accuracy[ ].

## Conclusion

While metagenomics has significantly advanced our understanding of microbial communities, conventional analytical methods continue to face major challenges such as limited taxonomic resolution, high computational

complexity, and dependence on curated reference databases. Deep learning (DL) methods address these limitations by learning complex patterns directly from raw sequencing data, offering superior accuracy, scalability, and robustness. Unlike traditional methods that depend heavily on predefined features and databases, DL models generalize well to novel taxa and noisy data while enabling end-to-end tasks such as classification, annotation, and phenotype prediction. With their ability to operate directly on raw sequences, deliver fast inference, and function with minimal computational resources, DL approaches are fundamentally transforming microbiome research. Future work should focus on improving interpretability and integration DL with multi-omics data for holistic insights [1].

## References

1. Oulas, A., et al., Metagenomics: tools and insights for analyzing next-generation sequencing data derived from biodiversity studies. *Bioinform Biol Insights*, 2015. 9: p. 75-88.
2. Nam, N.N., et al., Metagenomics: An Effective Approach for Exploring Microbial Diversity and Functions. *Foods*, 2023. 12(11).
3. Yang, S.Y., et al., Advancing Gut Microbiome Research: The Shift from Metagenomics to Multi-Omics and Future Perspectives. *J Microbiol Biotechnol*, 2025. 26(35): p. 12001.
4. Rausch, P., et al., Comparative analysis of amplicon and metagenomic sequencing methods reveals key features in the evolution of animal metaorganisms. *Microbiome*, 2019. 7(1): p. 019-0743.
5. Matsuo, Y., et al., Full-length 16S rRNA gene amplicon analysis of human gut microbiota using MinION™ nanopore sequencing confers species-level resolution. *BMC Microbiol*, 2021. 21(1): p. 021-02094.
6. Zhang, H., et al., Comparison of the full-length sequence and sub-regions of 16S rRNA gene for skin microbiome profiling. *mSystems*, 2024. 9(7): p. 00399-24.
7. Odom, A.R., et al., Metagenomic profiling pipelines improve taxonomic classification for 16S amplicon sequencing data. *Scientific Reports*, 2023. 13(1): p. 13957.
8. Quince, C., et al., Shotgun metagenomics, from sampling to analysis. *Nat Biotechnol*, 2017. 35(9): p. 833-844.
9. Ranjan, R., et al., Analysis of the microbiome: Advantages of whole genome shotgun versus 16S amplicon sequencing. *Biochem Biophys Res Commun*, 2016. 469(4): p. 967-77.
10. Kibegwa, F.M., et al., A Comparison of Two DNA Metagenomic Bioinformatic Pipelines While Evaluating the Microbial Diversity in Feces of Tanzanian Small Holder Dairy Cattle. *Biomed Res Int*, 2020. 22(2348560).
11. Segata, N., et al., Metagenomic microbial community profiling using unique clade-specific marker genes. *Nat Methods*, 2012. 9(8): p. 811-4.
12. Sharpton, T.J., An introduction to the analysis of shotgun metagenomic data. *Front Plant Sci*, 2014. 5(209).
13. Combrink, L., et al., Best practice for wildlife gut microbiome research: A comprehensive review of methodology for 16S rRNA gene investigations. *Front Microbiol*, 2023. 14(1092216).
14. Wang, Q., et al., Naïve Bayesian Classifier for Rapid Assignment of rRNA Sequences into the New Bacterial Taxonomy. *Applied and Environmental Microbiology*, 2007. 73(16): p. 5261-5267.
15. Prodan, A., et al., Comparing bioinformatic pipelines for microbial 16S rRNA amplicon sequencing. *PLoS One*, 2020. 15(1).

16. Wei, Z.G., et al., Comparison of Methods for Picking the Operational Taxonomic Units From Amplicon Sequences. *Front Microbiol*, 2021. 12(644012).
17. Westcott, S.L. and P.D. Schloss, De novo clustering methods outperform reference-based methods for assigning 16S rRNA gene sequences to operational taxonomic units. *PeerJ*, 2015. 8(3).
18. Callahan, B.J., et al., DADA2: High-resolution sample inference from Illumina amplicon data. *Nature Methods*, 2016. 13(7): p. 581-583.
19. Pérez-Cobas, A.E., L. Gomez-Valero, and C. Buchrieser, Metagenomic approaches in microbial ecology: an update on whole-genome and marker gene sequencing analyses. *Microb Genom*, 2020. 6(8): p. 24.
20. Chiarello, M., et al., Ranking the biases: The choice of OTUs vs. ASVs in 16S rRNA amplicon data analysis has stronger effects on diversity measures than rarefaction and OTU identity threshold. *PLoS One*, 2022. 17(2).
21. Puente-Sánchez, F., N. García-García, and J. Tamames, SQMtools: automated processing and visual analysis of 'omics data with R and anvi'o. *BMC Bioinformatics*, 2020. 21(1): p. 020-03703.
22. Kang, D.D., et al., MetaBAT 2: an adaptive binning algorithm for robust and efficient genome reconstruction from metagenome assemblies. *PeerJ*, 2019. 26(7).
23. Wu, Y.W., B.A. Simmons, and S.W. Singer, MaxBin 2.0: an automated binning algorithm to recover genomes from multiple metagenomic datasets. *Bioinformatics*, 2016. 32(4): p. 605-7.
24. Alneberg, J., et al., Binning metagenomic contigs by coverage and composition. *Nat Methods*, 2014. 11(11): p. 1144-6.
25. Seemann, T., Prokka: rapid prokaryotic genome annotation. *Bioinformatics*, 2014. 30(14): p. 2068-9.
26. Cantalapiedra, C.P., et al., eggNOG-mapper v2: Functional Annotation, Orthology Assignments, and Domain Prediction at the Metagenomic Scale: *Mol Biol Evol*. 2021 Dec 9;38(12):5825-5829. doi: 10.1093/molbev/msab293.
27. Eng, A., A.J. Verster, and E. Borenstein, MetaLAFFA: a flexible, end-to-end, distributed computing-compatible metagenomic functional annotation pipeline. *BMC Bioinformatics*, 2020. 21(1): p. 471.
28. Wood, D.E., J. Lu, and B. Langmead, Improved metagenomic analysis with Kraken 2. *Genome Biology*, 2019. 20(1): p. 257.
29. Kim, D., et al., Centrifuge: rapid and sensitive classification of metagenomic sequences. *Genome Res*, 2016. 26(12): p. 1721-1729.
30. Hong, C., et al., PathoScope 2.0: a complete computational framework for strain identification in environmental or clinical sequencing samples. *Microbiome*, 2014. 2(33): p. 2049-2618.
31. Franzosa, E.A., et al., Species-level functional profiling of metagenomes and metatranscriptomes. *Nat Methods*, 2018. 15(11): p. 962-968.
32. Miossec, M.J., et al., Evaluation of computational methods for human microbiome analysis using simulated data. *PeerJ*, 2020. 11(8).
33. Beghini, F., et al., Integrating taxonomic, functional, and strain-level profiling of diverse microbial communities with bioBakery 3. *Elife*, 2021. 4(10): p. 65088.
34. Milanese, A., et al., Microbial abundance, activity and population genomic profiling with mOTUs2. *Nat Commun*, 2019. 10(1): p. 019-08844.

35. Johnson, J.S., et al., Evaluation of 16S rRNA gene sequencing for species and strain-level microbiome analysis. *Nat Commun*, 2019. 10(1): p. 019-13036.
36. Hui, Y., D. Sandris Nielsen, and L. Krych, De novo clustering of long-read amplicons improves phylogenetic insight into microbiome data. *Gut Microbes*, 2025. 17(1): p. 11.
37. Pollock, J., et al., The Madness of Microbiome: Attempting To Find Consensus "Best Practice" for 16S Microbiome Studies. *Appl Environ Microbiol*, 2018. 84(7): p. 02627-17.
38. Bokulich, N.A., et al., Optimizing taxonomic classification of marker-gene amplicon sequences with QIIME 2's q2-feature-classifier plugin. *Microbiome*, 2018. 6(1): p. 018-0470.
39. Nilsen, T., et al., Swarm and UNOISE outperform DADA2 and Deblur for denoising high-diversity marine seafloor samples. *ISME Commun*, 2024. 4(1).
40. Ghurye, J.S., V. Cepeda-Espinoza, and M. Pop, Metagenomic Assembly: Overview, Challenges and Applications. *Yale J Biol Med*, 2016. 89(3): p. 353-362.
41. Sun, Z., et al., Challenges in benchmarking metagenomic profilers. *Nat Methods*, 2021. 18(6): p. 618-626.
42. Przymus, P., et al., Deep learning in microbiome analysis: a comprehensive review of neural network models. *Front Microbiol*, 2025. 15(1516667).
43. Roy, G., et al., Deep learning methods in metagenomics: a review. *Microb Genom*, 2024. 10(4): p. 001231.
44. Fiannaca, A., et al., Deep learning models for bacteria taxonomic classification of metagenomic data. *BMC Bioinformatics*, 2018. 19(Suppl 7): p. 018-2182.
45. Liang, Q., et al., DeepMicrobes: taxonomic classification for metagenomics with deep learning. *NAR Genom Bioinform*, 2020. 2(1).
46. Cres, C.M., et al., DL-TODA: A Deep Learning Tool for Omics Data Analysis. *Biomolecules*, 2023. 13(4).
47. Rojas-Carulla, M., et al., Genet: Deep representations for metagenomics. *arXiv preprint arXiv:1901.11015*, 2019.
48. Wichmann, A., et al., MetaTransformer: deep metagenomic sequencing read classification using self-attention models. *NAR Genom Bioinform*, 2023. 5(3).
49. Duan, C., et al., FGeneBERT: function-driven pre-trained gene language model for metagenomics. *Brief Bioinform*, 2025. 26(2).
50. Pei, Y., et al., ARGNet: using deep neural networks for robust identification and classification of antibiotic resistance genes from sequences. *Microbiome*, 2024. 12(1): p. 024-01805.
51. Reiman, D., et al., PopPhy-CNN: A Phylogenetic Tree Embedded Architecture for Convolutional Neural Networks to Predict Host Phenotype From Metagenomic Data. *IEEE J Biomed Health Inform*, 2020. 24(10): p. 2993-3001.
52. Oh, M. and L. Zhang, DeepMicro: deep representation learning for disease prediction based on microbiome data. *Scientific Reports*, 2020. 10(1): p. 6026.
53. Lo, C. and R. Marculescu, MetaNN: accurate classification of host phenotypes from metagenomic data using neural networks. *BMC Bioinformatics*, 2019. 20(12): p. 314.
54. Zheng, Z., et al., CasANGCL: pre-training and fine-tuning model based on cascaded attention network and graph contrastive learning for molecular property prediction. *Briefings in Bioinformatics*, 2023. 24(1).



## विज्ञान एवं प्रौद्योगिकी परिषद,उ.प्र.

(विज्ञान एवं प्रौद्योगिकी विभाग, उ.प्र.)

### विज्ञान भवन

9, नवी उल्लाह रोड, सूरज कुण्ड पार्क, लखनऊ-226018

#### परिषद के प्रमुख कार्यक्रम

- 1— प्रदेश की आवश्यकता के अनुसार शोध एवं विकास ।
- 2— प्रौद्योगिकी हस्तांतरण व प्रदेश की आवश्यकतानुसार विकास और उपयोग ।
- 3— जैव-प्रौद्योगिकी की उन्नति एवं विकास ।
- 4— विज्ञान लोकप्रियकरण एवं संचार ।
- 5— नक्षत्रशालाओं के द्वारा खगोलीय दर्शन तथा विज्ञान पार्क ।
- 6— असंगठित क्षेत्रों के कारीगरों, किसानों, युवाओं तथा माध्यमिक स्तर के विद्यार्थियों के लिये नवाचार ।
- 7— बौद्धिक सम्पदा संरण एवं पेटेण्ट सुविधा ।
- 8— विज्ञान सम्मान ।
- 9— राष्ट्रीय व अन्तर्राष्ट्रीय स्तर के सेमिनार, सिम्पोजियम, कान्फ्रेन्स व वर्कशॉप से सम्बन्धित कार्यक्रम ।



विज्ञान भवन

#### विशेष आकर्षण

- 75 जनपदों में गठित जिला विज्ञान क्लबों तथा 04 क्षेत्रीय विज्ञान एवं प्रौद्योगिकी केन्द्र (गोरखपुर, मुरादाबाद, आगरा एवं गाजियाबाद) के द्वारा विज्ञान लोकप्रियकरण एवं संचार ।
- विद्यार्थियों के लिये वैज्ञानिक व्याख्यान व भ्रमण कार्यक्रम ।
- समाज के विभिन्न वर्गों एवं लक्षित समुदायों में व्याप्त सामाजिक अंधविश्वासों व चमत्कारों के लिये वैज्ञानिक जागरूकता और विज्ञान प्रतियोगितायें ।
- लखनऊ, गोरखपुर तथा रामपुर में संचालित 03 स्थायी नक्षत्रशालायें ।
- मेधावी एमएससी विद्यार्थियों के लिये समर रिसर्च फेलोसिप ।
- इंजीनियरिंग स्टूडेण्ट प्रोजेक्ट ग्राण्ट स्कीम ।
- जनपद, मण्डल व राज्य स्तरीय विज्ञान मॉडल प्रतियोगिता कार्यक्रम ।



श्री वीर बहादुर सिंह नक्षत्रशाला  
रामगढ़ ताल रोड, गोरखपुर



बिद्धाननंदी नक्षत्रशाला  
सूरजकुण्ड पार्क, लखनऊ



आर्यभट्ट नक्षत्रशाला  
जिला जैल रोड, रामपुर

## विज्ञान एवं प्रौद्योगिकी परिषद,उ.प्र.

Email—cstup@gov.in; cstup1975@gmail.com

Website:dstup.gov.in | Ph. No. 0522-2202452,2974685